Interconnection Protection of Distributed Energy Resources Using Intelligent Schemes

Qiushi Cui

Department of Electrical & Computer Engineering
McGill University
Montréal, Canada

December 2017

A thesis submitted to McGill University in partial fulfillment of the requirements for the degree of Doctorate of Philosophy in Electrical Engineering.

Abstract

Increased levels of distributed energy resource penetration in distribution systems, including renewable generation, introduce several challenges that hinder safe and efficient system operation. Among them are the protection issues of distributed energy resource interconnection, including unintentional islanding detection, protection of distribution feeders, coordinating distributed energy resource protection relays with inverter fault ride through capability and protection coordination among them. It is generally understood that traditional protection philosophy in distribution networks requires reconsideration. This idea determines the scope of this thesis, which focuses on the above issues of distributed energy resource interconnection protection with the presence of renewable energy sources.

This work utilizes established pattern recognition methods to put forward intelligent protection schemes. A data-mining-based multifunction intelligent relay method is firstly proposed. It includes different protection aspects of distributed energy resource interconnection. To enhance the data utilization, a comprehensive intelligent relay training and testing strategy is developed. The generated relay logic demonstrates enhanced performance in terms of dependability, security and speed in inverter-interfaced systems.

Secondly, the detection of unscheduled islanding, i.e. separation of the distribution network from the main substation, under the condition of small power mismatch at the point of disconnection is efficiently resolved by the proposed non-detection zone reduction methodology. This methodology takes into account different distributed energy resource technologies and controls, topological changes of distribution networks and fault ride through functions. The utilization, assimilation and recognition of simulation data are effectively improved.

Thirdly, in addition to regular fault scenarios, the thesis addresses the high impedance fault detection issue by introducing a feature selection technique and contributing an effective feature set that is suitable for both batch and online machine learning. A detection logic based on those effective features and simple logic circuits are also proposed.

Lastly, part of the intelligent relay functions is validated through hardware-in-the-loop technique. The generated detection logic is programmed into a microprocessor-based relay, which is then connected to a real-time simulator through their analog interfaces. It is shown that the detection time and non-detection zone areas of the intelligent relay decrease significantly in each target location comparing to standard relay elements.

Résumé

Les niveaux accrus de pénétration des ressources énergétiques distribuées dans les systèmes de distribution, y compris la production d'énergie renouvelable, présentent plusieurs défis qui entravent un fonctionnement sûr et efficace. Il est généralement convenu que la philosophie de protection traditionnelle dans les réseaux de distribution nécessite un réexamen. Cette idée détermine la portée de cette thèse, qui met l'accent sur les problèmes cité ci-dessus et notamment la protection de l'interconnexion des ressources énergétiques distribuées en présence de sources d'énergie renouvelable.

Ce travail utilise des méthodes de reconnaissance de tendances établies pour proposer des schémas de protection intelligents. Une méthode de relais intelligent multifonction basée sur l'analyse de données est d'abord proposée. Pour améliorer l'utilisation des données, une stratégie complète de formation et de test pour les relais intelligent est développée. La logique de relais générée démontre des performances améliorées en termes de fiabilité, de sécurité et de vitesse pour les systèmes à base d'onduleurs.

Deuxièmement, la détection de l'îlotage non planifié, c'est-à-dire la séparation du réseau de distribution de la sous-station principale, sous la condition d'un faible déséquilibre de puissance au point de connexion, est résolue efficacement par la méthodologie proposée pour la réduction de la zone de non-détection. Cette méthodologie tient compte des différentes technologies et contrôles de ressources énergétiques distribuées, des changements topologiques des réseaux de distribution et des fonctions de détection des défauts. L'utilisation, l'assimilation et la reconnaissance des données de simulation sont effectivement améliorées.

Troisièmement, en plus des scénarios de défauts réguliers, la thèse aborde le problème de détection des défauts à haute impédance, en introduisant une technique de sélection des fonctionnalités et en offrant un ensemble de fonctionnalités adapté à l'apprentissage par machine en service et hors service. Une logique de détection basée sur ces fonctions et les circuits logiques simples sont également proposés.

Enfin, une partie des fonctions des relais intelligents est validée à l'aide de la technique de hardware-in-the-loop. La logique de détection générée est programmée dans le microprocesseur du relais, qui est ensuite connecté à un simulateur en temps réel via leurs interfaces analogiques. Il est démontré que le temps de détection et les zones de non-détection du relais intelligent diminuent de manière significative comparativement à un relais standard.

Acknowledgements

First of all, I would like to express my deepest gratitude to my supervisor Professor Géza Joós, whose support, guidance, wisdom and stringent requirements have reshaped me not only in knowledge but also in personal qualities. His insightful, valuable and meticulous comments are always thought-provoking. He is a believer and practitioner of "no one can be successful without industriousness", which has always been an inspiration to me.

Meanwhile, a profound note of appreciation must go to my co-supervisor Dr. Khalil El-Arroudi. My thesis could not be accomplished without his help. His immense knowledge in power system field and rich experience in industry nourish me with knowledge beyond books. His kindness, constructive feedbacks and practical suggestions on writing are of enormous benefits to my future career.

Furthermore, I am very grateful to my manager Mrs. Shijia Li and Mr. Jean-Nicolas Paquin during my internship in OPAL-RT Technologies Inc. It is my honour to work in their team, where I realize how is industry different from academia. Thanks a lot for the opportunity as well as the insights, patience and helpful discussions. I feel so lucky to be part of the MITACS research internship program in OPAL-RT in my last year of Ph.D. My gratitude goes as well to all the colleagues from OPAL-RT.

Special thanks to Professor Anthony Rodolakis who guided me in the first stage of my Ph.D. I would also like to thank my labmates at McGill Power Lab for the great time that we shared: Shamwilu Ahmed, Sayed Qaseem Ali, Farah Awan, Subhadeep Bhattacharya, Harmeet Cheema, Martine Chlela, Juan Clavier, Qiyun Dang, Navdeep Dhaliwal, Aboutaleb Haddadi, Quanrui Hao, Yuchong Huo, Haihao Jiang, Amir Kalantari, Xinyun Lu, Samah Mansour, Sijie Qin, Dmitry Rimorov, Michael Ross, Omar Saadeh, Sourabh Sharma, Ali Shojaei, Alexey Sokolov, Chu Sun, Mike Quashie, Can Wang, Fei Zhang and Zhiqi Zhao.

I would like to dedicate the dissertation to my family. I can never repay them for what they did for me. Their perpetual love always gives me the impetus to move forward. Last but not the least, to my wife Jie Gao. Your company, tolerance, encouragement and support have percolated through this thesis. The gratitude to you is beyond words.

Contents

List of Figures

List of Tables

List of Acronyms

AFD	Active frequency drift
ANSI	American National Standards Institute
API	Python Application Programming Interface
APS	Auto phase-shift
CB	Circuit breaker
CHP	Combined heat and power
DER	Distributed energy resource
DFIG	Doubly fed induction generator
DFT	Discrete Fourier transform
DG	Distributed Generation or Distributed Generator
DI	Dependability index
DT	Decision tree
DWT	Discrete wavelet transform
EFS	Effective feature set
EPS	Electrical power system
FCWT	Full-converter wind turbine
FRT	Fault ride through
GOOSE	Generic Object Orientated Substation Events
HIF	High impedance fault
ICD	IED Capability Description
IDM	Islanding detection method
IEC	International Electrotechnical Commission
IED	Intelligent Electronic Device
IIR	Intelligent islanding relay

IR	Intelligent relay
KF	Kalman filter
LAN	Local area network
L/HVRT	Low/High voltage ride through
LLL	Three-line fault
LL	Double-line fault
LLG	Double-line-to-ground fault
MDL	Minimum description length
MM	Mathematical morphology
NDZ	Non-detection zone
O/UF	Over/under frequency
O/UV	Over/under voltage
PCC	Point of common coupling
PLL	Phase-Locked-Loop
PMV	Protection Math Variable
PSV	Protection SELogic Variable
PV	Photovoltaic
RF	Random forest
ROCOF	Rate-of-change-of-frequency
SEL	Schweitzer Engineering Laboratories.
SFS	Sandia Frequency Shift
SG	Synchronous generator
SI	Security index
SLG	Single-line-to-ground fault
SVM	support vector machine
TACS	Transient analysis of control systems
WF	Wind farm
WTG	Wind turbine generator

List of Symbols

I	Current, p.u.
V	Voltage, p.u.
t	Time, sec
P	Active power, p.u.
Q	Reactive power, p.u.
f	Frequency, Hz
R	Resistance, Ω
θ	Angle, rad
pf	Power factor, 1
H	Inertia constant, sec

Chapter 1

Introduction

Power system protection is of paramount importance for power system operation since it protects the personnel safety and power equipment. While trying to provide reliable and continuous power supply, protection devices are seeking for improvement with respect to speed, sensitivity, security and selectivity (the 4S). Since the 1990s, there has been an increasing number of generation units being connected to the distribution systems. These units, often referred as distributed generators (DGs) or distributed energy resources (DERs), play a more significant role than before in modern power systems. Consequently, DG interconnection protection is becoming an indispensable part of distribution protection with deep renewable energy penetration.

Fault protection and islanding protection are two major challenges of DG interconnection protection. According to IEEE 1547 Interconnection Standards [1], as well as other grid codes [2], [3], rotating-machine-based DGs and inverter-interfaced DGs shall be aware of both faults and islanding events and cease to energize the distribution feeder. Therefore the fault and islanding detection in distributed generation is imperative. Currently, different types of conventional relays such as over/under-voltage, over/under-frequency, vector shift, over-current, etc. [4], [5], are utilized for fault detection and islanding detection. However, these conventional methods are not sufficient and reliable in the context of high renewable energy penetration level. This thesis is seeking for an innovative technique on solving DG interconnection problems. Before formulating the problems and proposing an advanced technique, some background information on DGs, islanding and fault detection is presented in this chapter.

1.1 Background

1.1.1 Distributed Energy Resources

Distributed Energy Resources (DERs) have experienced rise and fall for the past few decades. In 1978, in response to the 1973 energy crisis, the Public Utility Regulatory Policies Act (PURPA) in the US made its first attempt in utility deregulation and provided favorable terms to companies that produced electricity from renewable resources. However, DER owners became inactive as the act expired in the mid-1980s. DERs became popular again at the mid-1990s in areas of US where the power cost was high, but it did not last long because of the soaring natural gas prices in the late 1990s. The mid-2000s were marked by an increased interest in renewables and DER research due to policies, fossil fuel prices and the concerns of global warming. By 2014, wind power saw an increase moving from a total installed capacity of 48 GW in 2004 to 318 GW, and solar photovoltaic power generation grew by a factor of 70, from 2.6 GW in 2004 to 139 GW [6].

DERs include the application of small generators, typically ranging in capacity from 15 to 10,000 kW, providing electric power to customers [7]. Ordinarily, these distributed generators are scattered throughout a power system, and can be either located in the grid or at an isolated site not connected to the grid. Traditional DER technology involves reciprocating piston engine and gas turbine engine. Energy resources that utilize this type of technology usually consume fossil fuels such as diesel and gas, which contribute significantly to greenhouse gas emission. Other energy resources – such as fuel cell, small-scale hydro and biomass – are much cleaner energy but have limitations that hinder their large-scale installations. Among conventional DER technologies, conventional DER technologies mostly include:

- Diesel generators.
- Combined heat and power (CHP) plants.

The main electrical part of both applications is the synchronous generator (SG). The operating characteristics and fault behaviours of SG are fully modelled and investigated [8].

On the other hand, since the integration of some renewable energy resources requires converters prior to connecting to an electric grid, these DERs are called inverter-interfaced DERs. Inverter-interfaced DERs utilizing clean energy such as photovoltaic and wind turbines have gained popularity in distribution networks in recent years. Among inverter-

interfaced DERs, two typical technologies have witnessed a remarkable cost drop and installation increase over the past decade:

- Wind turbine generators (WTGs).
- Photovoltaic (PV) systems.

The inverter is the key element of grid-connected WTG or PV power systems. The main function is to convert the AC power obtained from WTGs or the DC power generated by PV panels into grid-synchronized AC power.

1.1.2 Challenges with High DER Penetration Level

Challenges with high DER penetration level in active distribution systems include but are not limited to the following:

- Limited fault current contribution — 130%-150% of inverters nominal current. With conventional power generation, synchronous machines can output approximately 6 times of nominal current during a three-phase fault, and the fault contribution is related to the machine voltage regulation, for example, high contribution to the fault current is directly related to the performance of high-ceiling exciters of SGs. Since the fault contribution is more deterministic therefore it is easier to set the corresponding protective elements. On the other hand, with inverter-interfaced DERs, a limited fault current level is injected upon fault occurrence, which varies with wind/solar available units, and the duration of contribution varies with the fault ride-through characteristic as well as the voltage dip during the given fault. The timing and the possibly low fault contributions can make the issue of coordination of protections more complex, meanwhile, the superior selectivity of protective devices becomes more difficult to achieve.
- Bidirectional power flow in distribution feeders – due to the introduction of DERs. Bi-directional power flow and the use of inverter-based DER brings the following challenges:
  - Concerns about the voltage quality (voltage regulation patterns along the feeders [9] as well as harmonic content).
  - Limitations of the maximum hosting capability of the existing distribution infrastructure/thermal characteristics.
  - Power system stability/frequency regulation can be at risk if DER penetra-

tion is deep. There will be needs to develop adaptive schemes that allow proper frequency ride-through characteristics, power modulation or droop to avoid cascaded trips and eventual blackouts.

  - Since some DERs can contribute to faults upstream of the PCC (point of common coupling) breaker, coordination of the protections can affect the continuity of service if the feeder needs to be tripped.

- Intermittent availability of renewable energy – nature of wind, solar resources. The stochastic nature of solar and wind energies adds more complexity to modern distribution systems. For example, the voltage-current curve of photovoltaic panels depends on the solar irradiance level. The output current and power of PV arrays also depend on solar irradiance.
- Low system inertia during islanded mode – inertia of the machine is isolated by its inverters. The high penetration level of inverter-based DER may decrease the system inertia. Take type-4 wind turbines for example, the inertia dynamic is isolated by back-to-back converters. Frequency deviation in the system will be influenced by the total available inertia that can damp the destabilizing effects of fast frequency response. Questions such as how to set frequency relay in order to allow frequency ride through might be asked.
- Advanced DER function modes and grid code requirements. Advanced DER functions are required. These control modes pose more challenges on system modelling, testing, control and protection. For instance, Hydro Quebec grid code has the low voltage ride through/high voltage ride through (LVRT/HVRT) requirement since 2009 [10]: if there is a fault in the distribution system, in order to avoid cascading outages of generators, wind turbines are required to remain connected as long as its terminal voltage is within the prohibited disconnection zone. Even though a severe short-circuit happens next to the wind turbine PCC, the wind turbine is required to be connected to the grid for at least 0.1 second. In addition, other advanced DER function modes such as volt-var mode and frequency-watt mode are also included in grid codes.

1.1.3 Protection Requirements Associated with DER Integration

The integration of DERs to distribution networks is altering and reshaping the design and operation of the protection schemes. Given the challenges discussed in the previous section, it is justifiable that 1) the limited fault current contribution from inverter-interfaced DERs blinds the overcurrent relay during a fault, 2) the bidirectional power flow in distribution lines affects the torque-based approach implemented in the directional element and 3) the fact that the angle of fault current is independent of the pre-fault voltage desensitizes distance relay [11]. The aforementioned issues require developing new approaches to protection design.

Prior to demonstrating the existing solutions, it is necessary to identify the protection requirements regarding DER interconnection:

- Unintentional or intentional islanding detection that prevents DER units from islanding operation without utility's regulation.
- Protection of the distribution networks to avoid fault current contribution from the DERs.
- Coordinating DER protection relays with DER controllers' "ride through" capability that circumvents cascading generator outages and supports grid stability during external disturbances.
- Protection coordination among islanding detection, protection of faulty networks, fault ride through capability and existing protection strategy.

These protection requirements intend to address protection issues imposed by the increasing employment of renewable DERs. Meanwhile, it is aligned with the IEEE 1547 Standard [12]. However, in order to validate the relay selection and the proposed protection scheme, a clear identification on protection requirements is not sufficient; a preliminary study should be undertaken by the distribution system operator to model the steady-state and dynamic system performance [13]. Considerations from system perspective should be included:

- System topological change.
- DER type and control.
- System loading conditions.
- DER interconnection transformer configuration.
- System grounding.

- Coordination requirements with utility protections.
- DER dynamic response to faults and disturbances.

Some proposed solutions in the literature are demonstrated in the following sections from different aspects of DER interconnection protection.

Islanding Detection

Islanding is an electrical phenomenon that occurs when part of the electric power system is isolated from the main power grid. Islanding phenomenon can be explained as shown in Fig. 1.1. When CB-1 is open, the local electric power system (local EPS) becomes islanded immediately. The protective relay of the islanded relay should detect the islanding event and trip the DER within a certain time.

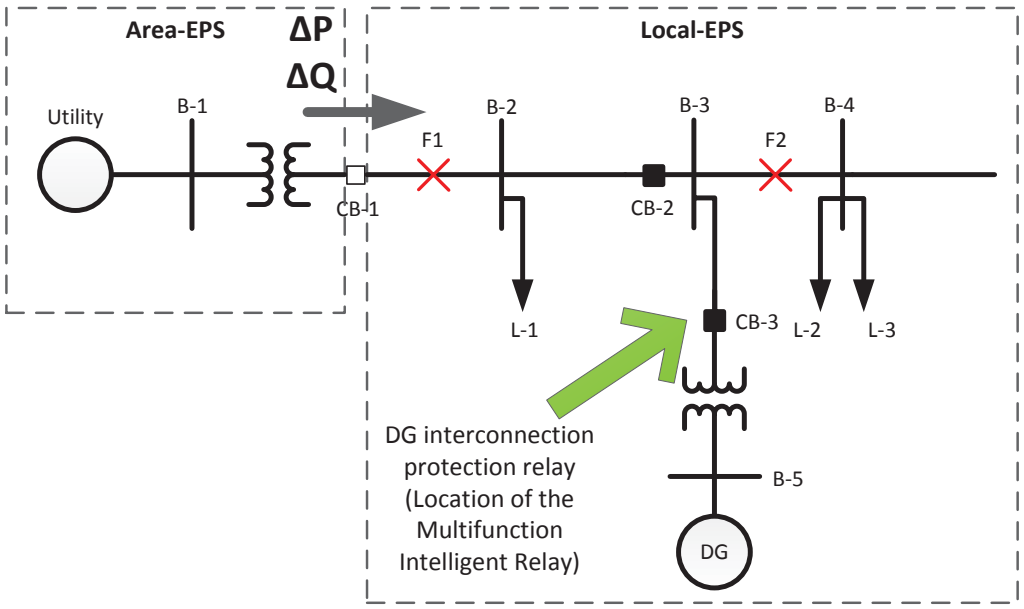

Fig. 1.1 Single line diagram of a typical distribution system with embedded DER.

When one or more DERs are in the isolated electric power system, they are called islanded DERs. According to IEEE standards [12], [14], islanded DERs are required to be detected within two seconds. Therefore, DERs are required to be equipped with islanding

detection functions.

In distribution systems, the protection for synchronous machine based system has been extensively studied in the past years. However, it has been found that, in the absence of the synchronous generator (SG), the resulting frequency and voltage at the terminals of all DERs will follow, upon main grid disconnection or faults, different variation patterns as compared to the ones exhibited with SG present. The reason is that the synchronous distributed generator (DG) possesses rotor mechanical inertia, even in the absence of secondary frequency regulation, which tends to arrest frequency decline depending upon the active/reactive island mismatch. This is, however, not true for the virtually inertia-less inverter interfaced DERs (assuming no inertia-emulator) given that the wind turbine rotor is isolated from the fully-rated power electronic converter.

Islanding Detection Methods (IDMs) have been studied by researchers in both synchronous generator (SG) and inverter-interfaced DER systems. IDMs can be grouped into the following categories [15] according to the detection techniques: communication-based, passive and active. A schematic classification of IDMs is illustrated in Fig. 1.2.

Telecommunication-based techniques, such as transfer trip [16], power line carrier [17], require additional infrastructures, especially in vast distribution networks with multiple feeders, laterals and DERs. Even though the cost and speed of communication might not be an issue to this technique in the future, the development of communication capabilities has opened up new possibilities and vulnerabilities in power systems [18]. In addition, it is reported in [16] that implementation of a transfer trip scheme is complex if the feeder is reconfigurable.

Among active IDMs, impedance measurement method [19], active frequency drift (AFD) [20], Sandia Frequency Shift (SFS) [21], auto phase-shift (APS) [22] and their variations have been utilized for SG-based systems, as well as inverter-based systems [23], [24]. In addition, due to the existence of inverter and the easy access to its controller, islanding detection can be realized by modifying the inverter control schemes. This type of methods either injects different inverter current [25], [26] or introduces enhanced real power reference [27], reactive power reference [28], inverter DC-link voltage [29]. Besides, positive feedback of voltage or frequency is used in inverter-based DER islanding detection as well [30], [31]. However, the drawbacks of the active detection methods are 1) complex control loop modifications on the inverter-based DERs; 2) system instability and undesirable transient behavior; 3) islanding detection performance deteriorates with multiple inverter-

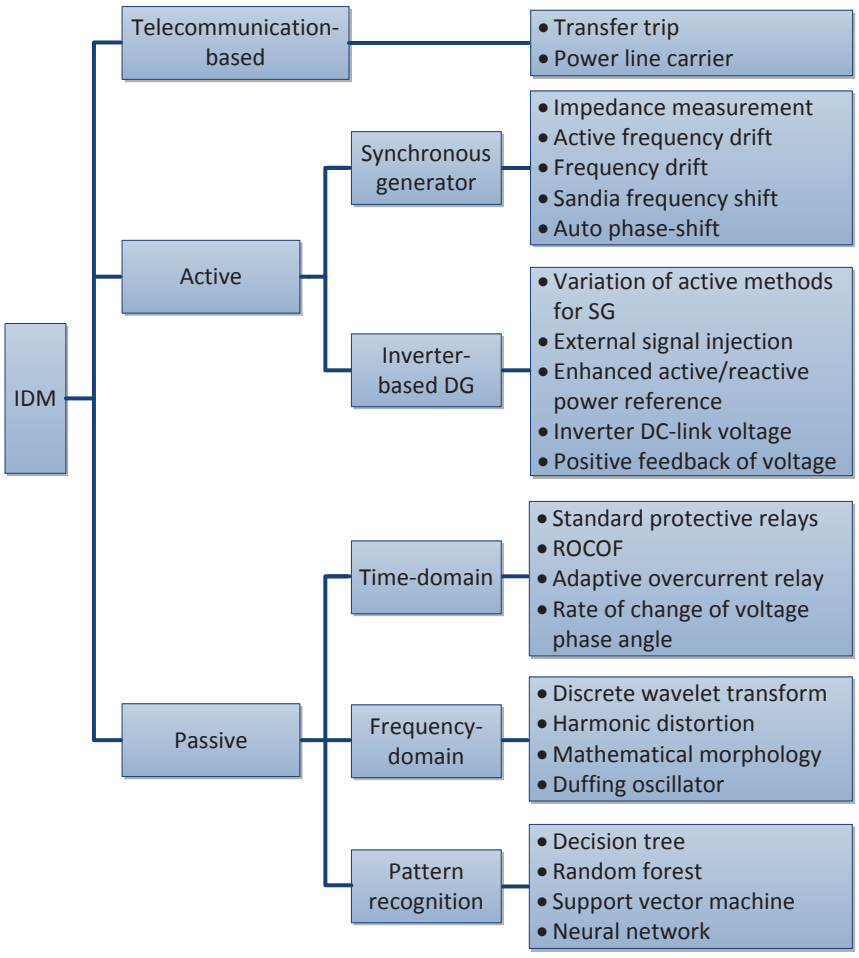

Fig. 1.2 A schematic classification of IDMs.

based DERs [21], [32]; 4) reduced power quality; 5) the NDZ in SFS method highly depends on its design parameters, improper tuning of these parameters may result in failure of this method [33].

Passive IDMs can be classified into time-domain, frequency-domain and pattern recognition based detection methods. In time-domain detection, standard passive islanding detection relays (such as under/over voltage and frequency functions, also called Standard Protective Relays [34]) are widely employed in the industry. Moreover, rate-of-change-of-frequency (ROCOF) relay [35], adaptive overcurrent relay [36] and rate of change of voltage phase angle [37] are proposed. However, they may suffer from a relatively large NDZ when the amounts of generation and load power are close to each other in the islanded area.

Frequency-domain analysis of anti-islanding patterns is attracting researchers' attention in recent years. Different analysis tools or methods have been successfully applied to extract frequency domain islanding patterns, such as discrete wavelet transform [38], harmonic distortion [39], mathematical morphology [40] and duffing oscillators [41]. Passive methods have remarkable performance when the power imbalance between load and generation of the islanded system is noticeable. However, if this imbalance is small, the superiority of passive IDMs diminishes [42]. Fortunately, with the rapid development of signal processing and artificial intelligence, pattern recognition can help solve these issues. Pattern recognition technology relies on different time/frequency domain analysis and extracts data of voltage, current or frequency at the DER location then identifies desirable signatures for detection and classification. Different data mining classifiers are utilized, for example decision tree (DT) [43], random forest (RF) [44], support vector machine (SVM) [45] and neural network [46].

Moreover, real-time simulation and HIL technique are widely adopted in different fields of power system [47], [48], [49], [50]. In islanding detection, a variety of methods are proposed using HIL technique. The study results of [51] proposed a model of frequency-based protection functions, which presents a similar behavior as the commercial relays in islanding detection of synchronous DGs. The work in [52] validated the effectiveness of power HIL based islanding detection approach using discrete hardware-based test configurations. Whereas in [53], the idea of testing islanding by using real-time HIL was brought up in search of a more rigorous and realistic functionality level. A hybrid synchrophasor and GOOSE (Generic Object Orientated Substation Events)-based passive islanding scheme is implemented using real-time HIL in [54]. It is reported that NDZ is reduced to half or two-third if the proposed scheme is used. However, the sensitivity of the proposed scheme is not evaluated to demonstrate the associated security performance. Meanwhile, the plotted NDZs seem more conceptual than realistic [55]. A hardware prototype and real-time validation of a satellite communication based loss-of-mains protection method are proposed and tested in [56], where both sensitivity and stability are considered. However, relying on the satellite communication, this method could be expensive and insecure due to the reliability of satellite. In sum, after reviewing different proposed methods on islanding detection in literature, HIL is utilized more than before to validate the feasibility of the proposed IDMs [57], [58].

Protection of Faulty Distribution Feeders

Protection of faulty networks is another important branch of DER interconnection detection. Standing DER interconnection guidelines require immediate disconnection of DERs upon the inception of any fault since it is required to avoid distribution feeder from injecting current to the fault. In fact, fault features in conventional synchronous machine distribution system differ from those in inverter-based system.

Similarly, if there is a fault along the distribution feeder, no matter at upstream (F1 in Fig. 1.1) or downstream (F2 in Fig. 1.1), DER interconnection protection relay should also detect it and be able to coordinate with other protection devices in order to isolate the faulty section selectively as required in IEEE Standard 1547. However other issues arise since inverter-based DERs normally have limited fault current contribution to the fault, therefore conventional relays have limitations in detecting such kind of cases.

In the synchronous-machine-based distribution system, fault detection is relatively easy and widely known in conventional protection practice. Due to the machine flux dynamics, fault situation is prolonged and exacerbated by the machine and its exciter control system. In distribution generation with purely inverter-based DERs, symmetrical component elements of both current and voltage are no longer as significant as in conventional systems because of the following reasons: 1) limited fault current contribution by the resident inverter controls [59]; 2) inverters, at least for type 4 wind turbines, are designed to generate balanced current regardless of the type of fault in the industry [60]. However, the total contributions of many small units may alter the fault current level enough to cause overcurrent protection mis-coordination and nuisance fuse operation or hamper fault detection [61].

In distribution systems, high impedance fault (HIF) occurs when a conductor breaks down and falls to the ground or some other object such as trees and grass. This phenomenon is hazardous to public safety and utilities. Since normally the impedance at the fault point is high, an excessive change in current is not noticeable. Consequently, conventional overcurrent relays are not able to detect such type of faults. While it is likely that only a few percentages of all faults are high impedance fault [62], it is estimated that one-third to one-half of downed conductor faults are HIFs [63].

The studies on HIF have been conducted since the 1970s with the hope of finding reliable and practical indicators to detect HIF [64]. However, it is still a challenge in distribution systems, especially in rural distributions feeders. HIFs are associated with

downed conductors or unwanted electrical contact with tree limbs, road surfaces, grass and so on. Upon occurrence, HIFs may cause fire hazards or jeopardize public safety.

HIF is characterized by its low, non-linear, asymmetrical and random fault current. The conventional over-current relay is unlikely to detect most of HIFs. A number of HIF detection methods are proposed to address this issue. The first category of HIF detection is related to the time domain analysis. It includes many different methods such as proportional relaying [65], ratio ground relay [66], fractal techniques [67], signal superposition [68], and residual variation analysis of line and phase asymmetries [69]. Methods involving the enhancement of conventional relays are proposed at the early stage, including proportional relaying algorithm [65], impedance-based method [70] and PC-based fault locating and diagnosis algorithm [71]. However, these methods are not effective in detection HIFs when the fault current is low.

Frequency domain analysis is another important area of HIF detection. Third harmonic and its angle [72], third and fifth harmonics [73], burst noise signal [74] and interharmonic [75] based methods are proposed in the past decades. The wavelet-transform-based methods are a significant branch of frequency domain analysis. Selection of mother wavelet affects the HIF detection effectiveness [76], [77]. Other improved versions of wavelet transform analysis such as energy spectrum of wavelet coefficient [78] and the border distortion of wavelet coefficient energy [79] are also proposed. On the other hand, harmonics patterns are utilized to capture the characteristics of HIFs. For example, there are key detection features such as magnitudes and angles of 3^{rd} and 5^{th} harmonics [73], even order harmonic power [80], interharmonic currents [75] utilize the harmonics pattern to detect HIFs. Besides, the work in [81] proposed a Kalman-filter-based method to monitor harmonics so as to detect HIFs. The high frequency spectrum is employed as well to detect HIFs. This type of methods actively injects higher than fundamental frequency signals like positive/zero voltage signals [69] into the grid to detect HIFs. Furthermore, another frequency domain analysis method of detecting HIF called mathematical morphology [82], [83] is attracting researchers' attention.

Thirdly, time-frequency domain analysis of HIF pattern concentrates on both domains simultaneously. Time-frequency analysis with statistical joint moment calculation is proposed in [84]. Moreover, wavelet transform [77], [85], [76], fuzzy logic [86], genetic algorithm [87], mathematical morphology [83] and power line communication [88] are proposed to detect HIFs.

With the advancement of artificial intelligence, methods on expert systems [89], [90], neural networks [91], [92] and machine learning are gaining popularity in recent years. Decision tree learning method is proposed in [93]. The paper [94] uses wavelet transform to extract data and Bayes classifier to differentiate fault cases. The wavelet transform is also used in [95] and the classification method used is nearest neighhourhood rule. The wavelet transform is also combined with fuzzy inference to detect HIFs in [87], [96]. Originating from the analysis and processing of geometrical structures, mathematical morphology (MM) method is presently gaining popularity in data extracting upon the inception of fault, [83] proposed a method based on MM alone to detect HIFs, while [82] combined MM with the neural network, and [97] combined MM with the classifier of support vector machine (SVM). Principal component analysis and SVM are proposed in [84]. The analysis in either time or frequency domain focuses on the extraction of key features associated with HIF, whereas pattern recognition based methods address the issue of classification. This category comprises neural network [82], expert system [89], decision tree [93], Bayes [94], support vector machine (SVM) [97], etc.

Protective relays are usually tested and validated by real-time simulation and HIL. The work in [98] proposes a real-time low-latency hardware digital distance protective relay on the field programmable gate array (FPGA), taking advantage of inherent hard-wired architecture of the FPGA. In [99], a multi-function power system protective relay is designed and implemented in HIL. Detailed emulation of several relay elements and the signal processing functions are presented in this proposed relay that is fed with instantaneous fault data. On the other hand, HIL has become a powerful tool in distribution network protection with the presence of DERs. Different protective schemes and method validation are based on HIL [5], [100], [101], [102].

1.2 Problem Definition

Due to the cost reduction of renewable energy and incentives from government policies, the deep penetration of DERs, especially inverter-interfaced DERs (wind and PV), is changing the dynamic response of distribution networks upon external disturbances, and therefore, altering the design of protective schemes. Unlike synchronous-machine-based DERs that have good frequency regulation because of the inertia of a synchronous machine, inverter-based DERs reflect low or no inertia on the grid due to the interfaced power electronics.

This might be beneficial to islanding detection due to the large frequency deviation. Nevertheless, the role of frequency and voltage features needs to be re-defined in islanding detection. Moreover, when the power mismatch at the point of disconnection is small, it becomes difficult for frequency and voltage relays to detect the subtle variable changes. Thus, detecting islanding conditions solely based on over/under voltage and frequency relays becomes impractical, especially in the context of increased penetration levels of inverter-interfaced generation.

On the other hand, as a result of the limited fault current contribution from the inverter-based DERs, conventional fault detection relays like over-current relay might not be effective to detect faults energized by both the utility and the DERs. The exploration of supplementary detection features to existing protection elements imposes tremendous challenges. Situations are even worse for HIFs, where fault current is low and may be very close to heavy load currents. For this reason, the investigation on the logic combination of effective features in modern distribution networks becomes indispensable in order to protect distribution feeders. In addition, as mentioned in the protection requirements associated with DER integration, a protection scheme considering the coordination among islanding detection, protection of faulty networks and fault ride through capability is also one of the tasks in this thesis.

1.2.1 Thesis Statement

The thesis recognizes the limitations of the conventional protection elements to tackle difficult conditions, and argues that many of them can be effectively addressed using pattern recognition based intelligent approaches. This premise is further developed into a concept of the multi-functional intelligent relay. Some of the proposed functions that constitute an intelligent relay are validated to be implementable using commercial off-the-shelf relays.

1.2.2 Research Objectives

The research objectives of this thesis contain three aspects of DER interconnection protection:

- Design a machine-learning-based multifunction protection scheme that aims at addressing major protection issues associated with DER interconnection and enhancing the utilization of big data from various scenarios. The protection scheme is expected

to detect fault and islanding phenomenon in distribution systems to protect DERs. However, the performance of, for example, the fault detection can be improved if the proposed solution can provide fault type classification, which helps protection engineers on fault identification and fast clearance of the faults. Furthermore, in order to support the stability of the grid with a deep renewable DER penetration level, the possibility of including coordination with fault ride through capability is under study.

- Develop an islanding detection method that is effective under small power mismatch at the isolated location. It is well known that conventional islanding detection relays have difficulties in detecting islanding when there is a reduced power mismatch at the point of common coupling (PCC). If plotted in the active and reactive power coordinate, the malfunctioning area is called non-detection zone (NDZ). An enhanced protective relay that is able to cover entire NDZ is fully investigated in this thesis. Additionally, in order to guarantee relay security, designing an islanding detection relay that is immune to different operational changes, such as load switching, parallel feeder islanding, network topological change, and fault ride through requirement, becomes imperative for the future distribution grids.
- Solution to detect HIF in distributed networks with the integration of renewable energies. Besides regular faults, high impedance fault is threatening the operation of distribution networks and a technical challenge to solve. From the pattern recognition based aspect, the exploration of reliable features that can capture the meaningful pattern of HIF in a modern distribution network is one of the key tasks in this research objective. Afterwards, the approach of detecting HIF utilizing the discovered features is expected to be established. This approach needs to be a feasible solution in the synchronous machine based and inverter-based systems and for different types of faults.

1.2.3 Methodology

This thesis fully adopts the pattern recognition approach to address the challenges mentioned in the previous part. Meanwhile, real-time simulator and hardware-in-the-loop techniques are employed in order to obtain the added value from the combination of pattern recognition technique and real-time simulation. This is carried out through theoretical

methodology and model-based simulations. Practical scenarios in the present and future distribution networks are simulated to establish sufficient data sets (including training and testing data sets) for data mining. Connecting with a real-time simulator, microprocessor-based commercial relays are utilized to provide conventional relay's elements. Moreover, the commercial relays employed are able to be programmed with customer-defined relay logics. Experimental results from the hardware-in-the-loop simulation are therefore expected.

1.2.4 Research Tools

The software packages used to perform the aforementioned researches are as follows:

1. Matlab Statistics and Machine Learning Toolbox^{TM} [103]: data mining analysis and decision tree acquisition.
2. Matlab/Simulink: distribution feeder modelling and data processing.
3. Hypersim/RT-Lab[1]: power plant modelling, power hardware-In-the-Loop validation of the proposed approach.
4. SEL software AcSELerator Quick Set and Architect: setup SEL relay and configure its IEC 61850 setting.

The hardware used to perform the aforementioned researches are as follows:

1. OPAL-RT OP5600 real-time simulator.
2. SEL 421 relay.

1.2.5 Experimental Validation

The proposed fault and islanding detection functions are validated in HIL simulations. The OPAL-RT simulator is employed to model the 25 kV three-phase distribution network in real time, and the microprocessor-based intertie protection device SEL-351S relay from Schweitzer Engineering Laboratories Inc. is programmed with custom-developed logic to represent an intelligent relay for DER interconnection protection. The conventional relay elements are available in the commercial relay, therefore, their performances can be extracted. An Analog I/O card OP5110 from OPAL-RT Technologies, Inc. is used to connect the relay and the real-time simulator.

[1]Real-time simulation software of OPAL-RT Technologies Inc.

1.3 Claims of Originality

The contribution of this dissertation provides the original solutions in DER interconnection protection field in distribution networks with the integration of renewable energies. The originality, as shown in the referenced peer-reviewed papers, consists of the following three perspectives:

- A comprehensive intelligent relay training strategy that improves data utilization and a pattern recognition based multifunction intelligent relay that incorporates islanding detection, fault detection, fault classification and coordination with fault ride through capability [104].
- A methodology for reducing the boundary limits of Non-detection Zone (NDZ) in pattern recognition based islanding detection scheme [105], [106]. This methodology 1) improves the utilization, assimilation and recognition of simulation data and helps in efficient decision making, and 2) considers different DER technologies, topological changes of distribution networks and fault ride through functions.
- A feature selection technique that generates the effective feature set (EFS) suitable for both batch and online machine learning [107] as well as a high impedance fault (HIF) detection method. The feature selection technique screens the features according to variable importance, while the HIF detection method is based on those effective features and simple logic circuits.

1.4 Dissertation Outline

Chapter 1: Introduction

The background of this thesis is discussed in this chapter. DERs are defined in the beginning. The challenges brought by the DER penetration are then demonstrated in five aspects. Next, the protection requirements associated with DER interconnection are identified. Meanwhile, the system level considerations are listed to narrow down the scope of this research. Then some proposed solutions from the literature are demonstrated according to the identified DER interconnection protection requirements. In problem definition, the problems under study are clarified. The scope of the research is further emphasized in thesis statement, followed by the research objectives, methodology, research tools and experimental validation. The contribution of this research work is illustrated in claims of

originality. In the end, it shows dissertation outline of each chapter.

Chapter 2: Architecture of the Proposed Intelligent Protection Schemes

The data mining based intelligent relay method is explained firstly in this chapter in four procedures. Its mathematical formulation and the classification principle are presented. The following functions are incorporated in this proposed multifunction IR architecture: islanding detection, fault detection, fault type recognition, FRT selective blocking and HIF detection. To enhance the data utilization in the context of big data, a comprehensive IR training and testing strategy is proposed. The generated IR logics of the multifunction are exhibited in one wind farm and two wind farms systems. The performance of multifunction relays is compared with standard relays. Moreover, the IR's performance under small power mismatch is studied in different types of distribution systems. A thorough discussion is included and the physical limitations of passive islanding detection schemes are emphasized when the substation bus power mismatch is small.

Chapter 3: Islanding Detection Function

Following the discussion in the previous chapter, this chapter presents a solution under small power mismatch at the point of network disconnection. Typical boundary limits of system operating conditions are depicted and the physical and mathematical formulations of the boundaries of NDZ in synchronous generator and inverter based systems are analysed. A new methodology is proposed for reducing the boundary limits of islanding detection schemes using an NDZ-based training/testing strategy to generate DT logics. The proposed NDZ reduction methodology is presented and explained in three steps: establishing NDZ, reducing NDZ band and generating intelligent relay logics. Case studies consider the advanced inverter control of fault-ride-through, distribution networks' topological change and parallel feeder islanding scenarios. Simulation results and analysis are provided, meanwhile, the case that fails to respect the recommended methodology is added with the subsection title of under-trained DT logic. Prior to the conclusions, the comparison analysis with other methods from literature as well as the DER technologies and controls is discussed.

Chapter 4: High Impedance Fault Detection Function

This chapter incorporates a HIF detection approach into the concept of the multifunction intelligent relay and extends its functionality. The variable-importance in feature evaluation is introduced for HIF study. This concept is established on the theories of information gain and minimum description length algorithm. A large pool of candidate features, which comprises 246 elements from conventional features to some self-defined features based on engineering experience is created. In the meantime, a comprehensive system and event study is conducted to incorporate as many cases as possible. Consequently, through the attribute screening method, the author acquires an effective feature set (EFS) of HIF detection. In addition to the presented typical waveforms, fault scenario analysis is studied. The analysis contains the variable-importance scores of each proposed features in three scenarios: varying fault impedances, varying fault inception angles and varying fault locations. The effect of these scenarios on the variable-importance scores gets better understood. With the EFS, a pattern recognition based HIF detection method is proposed. The author explores the possibility of both the batch learning technique and the online machine learning one. The comparison is made between the performance using full feature set and the effective feature set. Different classifiers in batch learning and online learning are investigated. Moreover, a simple and practical HIF detection logic is developed. The function of each block is explained in this chapter.

Chapter 5: Real-time Hardware-in-the-loop Validation

This chapter firstly details the real-time simulation setup using the research tools mentioned in Section 1.2.4. The HIL connection is presented. Additionally, the procedures of setting standard relay elements and the obtained logics from data mining method are explained, followed by the elucidation of performance acquisition using IEC 61850 communication protocol. Inspired by Chapter 3, an HIL-based NDZ reduction method is proposed. In the meanwhile, this method provides a validation to the proposed NDZ reduction technique in islanding detection. In the case study and result analysis, the HIL experimental NDZ of standard relay functions, the NDZ of Simulink modeled IIR and the HIL experimental NDZ of IIR are presented through software/hardware tests. The practical detection time of the standard relay functions and the proposed IIR programmed in SEL relay with HIL is measured and compared.

Chapter 6: Summary and Conclusions

This chapter summarizes the whole thesis from the research motivation to the originality and the contribution of each proposed method/scheme. Furthermore, potential directions for future work are discussed.

Appendix A: Benchmark systems

The section of Appendix includes the benchmark system 1 and 2, synchronous generator modeling, wind turbine modeling, training and selected testing events of the multifunction IR, the selected intelligent relay features and the minimum description length based algorithm.

Chapter 2

Architecture of Multifunction Intelligent Protection Schemes

2.1 Introduction

Inverter-based DERs such as wind turbines, photovoltaics are widely implemented in modern distribution networks. Although widely used, standard islanding schemes become insensitive when power mismatch at the isolated location is small. On the other hand, standard fault detection functions such as over-current, over/under-voltage and directional element, have also limitations in fault detection because of the limited fault current contribution in various system configurations.

In addition to Section 1.1.3, which illustrates the islanding detection methods (IDMs) in general, lots of research has been done for inverter-interfaced DERs. Typical active IDMs including impedance measurement method, slide-mode frequency shift, AFD, SFS, APS and so on are applicable in inverter-based systems as well, where the small power mismatch problem disappears but power quality of the electric grid is jeopardized due to the introduction of perturbation at predefined intervals. Moreover, active IDMs cannot avoid the problem that when there are multiple inverter-based DERs, positive perturbations can interfere with each other and eventually lead to islanding detection failure [108]. The passive IDMs have remarkable performance when the mismatch between load and generation of the islanded system is noticeable. However, if this mismatch is small, the superiority of passive IDMs diminishes [42]. Fault features in conventional synchronous-machine-based

distribution system differ from those in inverter-based system. In distribution generation with purely inverter-based DERs, symmetrical component elements of both current and voltage are no longer as significant as in conventional systems because of the following reasons: 1) limited fault current contribution by the resident inverter controls [59]; 2) inverters, for example, type 4 wind turbines, are designed to generate balanced current regardless of the type of fault in the industry [60]. However, the total contributions of many small units may alter the fault current level enough to cause overcurrent protection incoordination and nuisance fuse operation [109] or hamper fault detection [61].

Since deep DER penetration level is presenting an altered system performance therefore requiring some different DER interconnection protection schemes from the conventional ones, this chapter proposes a multifunction IR scheme for DER interconnection protection in the inverter-based distributed generation. The proposed IR scheme originally combines islanding detection, fault detection, fault type recognition and fault ride through (FRT) selective blocking functions in data-mining-based protection schemes. Comprehensive IR training and testing event set is, therefore, proposed making the data utilization in an efficient way. The novel FRT selective blocking functions coordinate with the islanding and fault detection logics in order to avoid overriding these logics in the context of FRT in inverter-interfaced systems. Section 2.2 explains the data mining based intelligent relay method. The multifunction intelligent relay scheme is proposed in Section 2.3, which includes islanding detection function, fault detection and fault type recognition functions, FRT selective blocking function and comprehensive IR training and testing strategy. The performance of the multifunction intelligent relay is illustrated in Section 2.4 Results, followed by Section 2.5 Conclusions.

2.2 Data Mining Based Intelligent Relay Method

Data-mining based IR has shown its effectiveness in islanding and fault detection for synchronous DGs [110, 111]. There are four procedures to setup the IR as shown in Fig. 2.1.

The data mining based intelligent relay method uses decision tree (DT) learning algorithm to obtain the IR logic and threshold settings. Comparing with other pattern recognition methods like SVM, neural networks and etc., the DT relies on well-known detection features, simple decision logics and simple if-then classification rules (open systems)

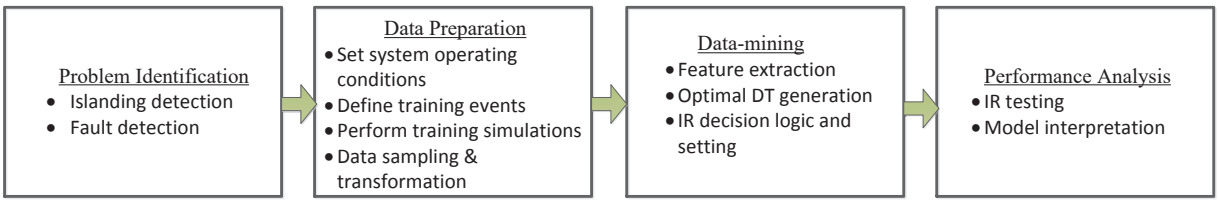

Fig. 2.1 Data-mining based intelligent relay setup procedures.

that can be implemented very easily using the modern numerical relay. Hence, protection engineers can quickly learn, configure and debug. Furthermore, DT is more reliable and implementable using modern microprocessor-based digital relays.

A DT is a hierarchical model for supervised learning whereby the local region is identified in a sequence of recursive splits in a smaller number of steps [112]. Let i, j and t_k represent DG number, event number and time index, then the row vector $\bar{X}$ represents the monitored n features for the i^{th} DG at the j^{th} event of time t_k:

$$\bar{X}_i^j(t_k) = [x_{i1}^j(t_k), x_{i2}^j(t_k), ..., x_{in}^j(t_k)] \tag{2.1}$$

Therefore a time-domain matrix can be structured according to the following format:

$$[T_i^j] = [\bar{X}_i^j(t_1)^T, \bar{X}_i^j(t_2)^T, ..., \bar{X}_i^j(t_n)^T] \tag{2.2}$$

Besides time domain matrix, each vector $\bar{X}$ is also arranged in an event-driven way therefore the database expands over each time cycle. Assuming there are l system events, the event-driven matrix becomes:

$$[E_i^j] = [\bar{X}_i^1(t_k)^T, \bar{X}_i^2(t_k)^T, ..., \bar{X}_i^l(t_k)^T] \tag{2.3}$$

Once the data matrix is established in terms of features, time index and simulated events, it is processed by the CART algorithm that uses Gini index to build the DTs. Gini index [113] is used as the impurity measure to quantify a good split in the DT-based classification technique. In this particular case under study, DT node at each layer originates from the 12 features (refer to Appendix A.7) in the vector $\bar{X}$ and the split provides two paths during decision-making at this node. Those islanding or fault events are marked as "1" and non-islanding or non-fault events as "-1". The ultimate goal of DT

is to classify as many "1s" from "-1s" as possible.

The employed algorithm searches the complete hypothesis space. Let there be J classes numbered $1, ..., J$ and denote the proportions of the classes at a given node m by $\mathbf{p} = p_1, ..., p_J$. The prior Gini-index is defined as follows:

$$GINI(m) = 1 - \sum_j [p(j|m)]^2 \tag{2.4}$$

Note that $p(j|m)$ is the relative frequency of class j at node m. The splitting criterion here is to minimize Gini index of the split. When a node p is split into k partitions (children), the quality of split is computed as:

$$GINI_{split} = \sum_{i=1}^{k} \frac{n_i}{n} GINI(i) \tag{2.5}$$

where n_i and n are the numbers of records at child i and node p. With Gini splitting criterion, the DT firstly grows to its entirety. It is then trimmed in a bottom-up fashion to avoid over-fitting and pruned using a 5-folder cross-validation function.

The time-dependent DI and SI [110] are adopted to quantify the performance of relays:

$$DI_i(t_k) = \frac{DIE}{NIE}, SI_i(t_k) = \frac{DNIE}{NNIE} \tag{2.6}$$

where DIE is the number of detected islanding or fault events that are correctly identified as such, NIE is the total number of islanding or fault events, DNIE is the number of detected non-islanding or fault events that are correctly identified as such, NNIE is the total number of non-islanding or fault events and t_k is the time index of the time-dependent DT.

Then the optimal DT is selected according to the following equation:

$$DT^*(t_m) = maxSI_i(maxDI_i), \forall t_k \tag{2.7}$$

Equation (2.7) guarantees that the islanding or fault detection is reliable and achieves the least possible nuisance tripping.

2.3 Multifunction Intelligent Relay Scheme

The proposed multifunction IR scheme utilizes data mining based pattern recognition method to generate functional prediction and classification models as its relay logic. The installation location of the IR is shown in Fig. 2.2, which is the functional block as well.

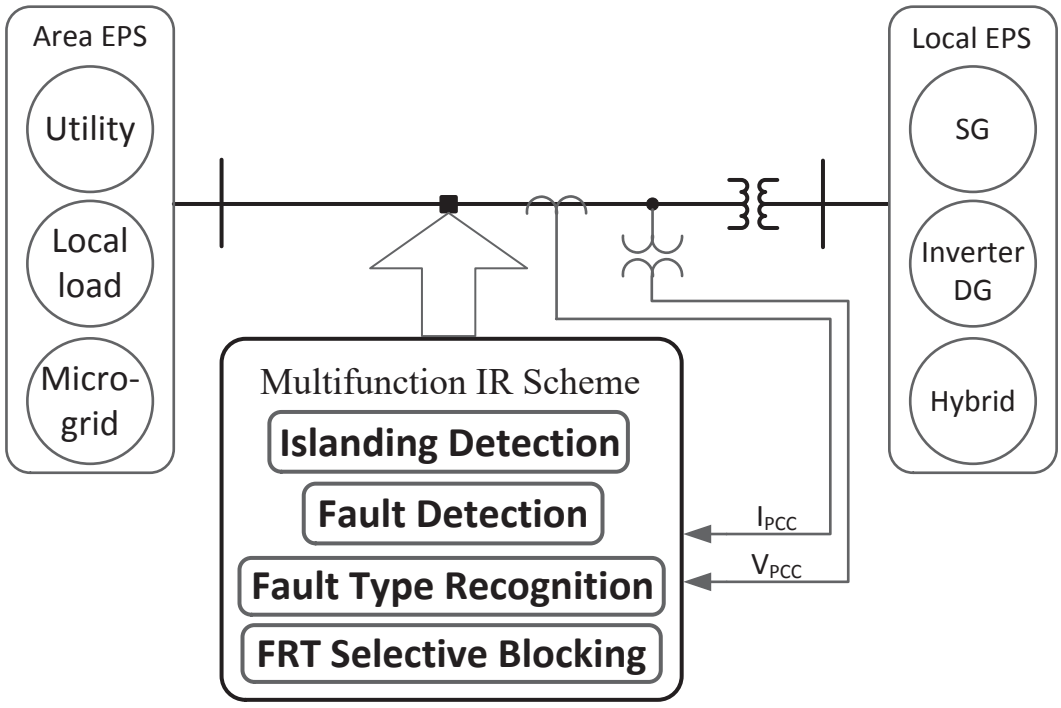

Fig. 2.2 Multifunction Intelligent Relay Scheme.

Two lists of islanding and fault events (refer to Appendix A.4 and A.5) are simulated in order to obtain the classification patterns. Selected key features (see Appendix A.7), such as the rate of change of frequency, voltage, and the rate of change of active power, at the DG PCC are measured and utilized to form the decision making models. Therefore two complementary detection logics for islanding and fault detection can be obtained using the aforementioned method. This section firstly elaborates on each function in the proposed scheme, then a comprehensive IR training and testing strategy is proposed and discussed.

2.3.1 Islanding Detection Function

In islanding detection function, the relay logic is trained from myriad types of system loading scenarios in order to cover different system conditions and to minimize its non-detection zone. Fault and circuit breaker open events can also be recognized by the islanding function. Furthermore, the islanding detection function can as well prevent nuisance tripping since all possible non-islanding events like load shedding, load adding, capacitor switching are part of the training scenarios. Therefore the islanding detection logic is built with sufficient information to distinguish islanding conditions from non-islanding ones.

2.3.2 Fault Detection and Fault Type Recognition Functions

The fault detection function is designed for the inverter-based DERs in order to overcome the problem of limited fault current magnitude. It detects all types of faults (symmetrical and asymmetrical faults) within its zones of protection. Unlike standard fault detection functions, the IR fault detection function employs different combinations of DER features to detect fault event for the inverter-based DERs.

With the classification capability of data-mining method, fault type recognition function is able to identify the following four types of faults: single-line-to-ground fault (SLG), line-to-line-fault (LL), three-phase-fault (LLL) and line-to line-to-ground fault (LLG). Besides, for ground fault, variable fault impedances are considered in the IR training period to enhance the adaptivity of the fault detection function.

2.3.3 FRT selective blocking function

This function fulfills the advanced grid code requirement of fault ride through (FRT), particularly for inverter-based wind turbines. The proposed FRT selective blocking function is designed to coordinate with the FRT requirement [114, 115] in distribution systems with radial feeders. The communication-based technique of blocking the uncoordinated fault tripping has been proposed for the purpose of FRT [116]. However, communication measure is not required in the proposed function.

In order to avoid overriding the FRT capability in the system, fault detection function is supervised by FRT selective blocking logic with certain time delay according to the grid code. This logic is also obtained through data-mining method by differentiating “blocking” from “non-blocking” scenarios. For example, the faults occur upstream the DG and on the

main branch of the radial feeder are supposed to be cleared by the upstream main branch circuit breaker and therefore FRT is not necessary for the islanded DG. Furthermore, FRT capability should be coordinated if the fault occurs at either downstream of the DG or on the load branch which does not involve islanding operation of the DG. Different fault scenarios are shown in Table 2.1.

Table 2.1 FRT Selective Blocking Scenarios in Radial Feeder.

FRT selective blocking	Faults on main branch	Faults on load branch
Upstream Fault	Non-blocking	Blocking
Downstream Fault	Blocking	Blocking

2.3.4 Comprehensive IR training and testing strategy

To acquire a high security performance, the islanding detection function should be able to distinguish non-islanding events and the fault detection function to recognize non-fault events. Since a common non-tripping event set (as shown in Fig. 2.3) is shared by both functions, a comprehensive IR training and testing strategy is proposed with the following three advantages: 1) reduced offline computational resource consumption; 2) easier multi-function integration; 3) better inter-function coordination. By far in the implementation of this chapter, non-tripping events contain normal operating condition, load adding, load shedding and capacitor switching operations.

Only one-time training within the event set in Fig. 2.3 is required in the proposed strategy. Based on the simulation data from the comprehensive IR training set, logics of all functions can be obtained at the same time. Fig. 2.4 illustrates the functional diagram of the proposed multifunction IR scheme. The islanding IR logic is asserted when the islanding decision tree criteria is satisfied with 100 ms time delay. Fault IR logic indicates the fault (output 1) and non-fault (output 0) events with instantaneous/time delay tripping. Meanwhile, the fault IR logic is supervised by the FRT selective blocking logic through an AND logic. In non-FRT scenarios, also known as “non-blocking” cases in this chapter, the output of the FRT selective blocking logic is 1, while it is outputting 0 when the blocking decision logic is triggered and latched for 9 cycles according to Hydro-Quebec grid code [114]. Moreover, the fault identifier reports fault types as its output.

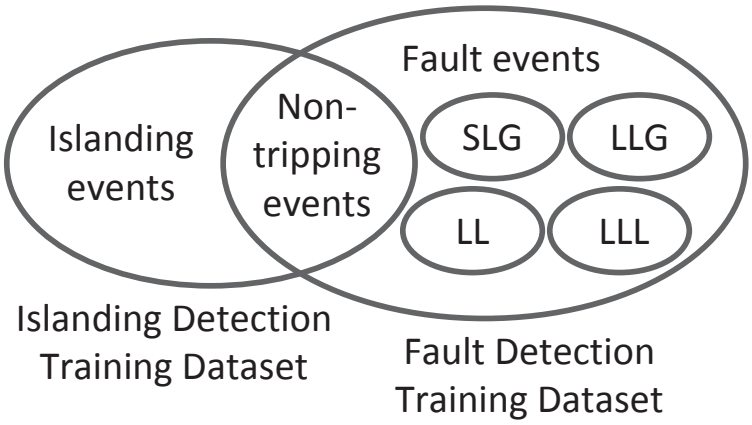

Fig. 2.3 Comprehensive IR training event set.

2.4 Results

This section firstly demonstrates the results of the multifunction relay, then the performance analysis of IR and a conventional relay in small power mismatch is conducted.

2.4.1 Performance of Multifunction Relays

Based on the proposed methods, results are shown in this section. The benchmark distribution system comes from a real distribution feeder (refer to Appendix A.1 for more details) in a remote Canadian community. Firstly, IR logics are presented below for each function in the benchmark system, where two inverter-interfaced systems are presented: one-WF (wind farm) and two-WF systems. The WF locations can be found in Table 2.2. The IR logics of fault and islanding detection functions, fault detection and fault type recognition functions at different DG locations are compared. Secondly, the comparison is made between 1) the proposed IR islanding and fault detection functions and 2) the standard islanding and fault protective elements through HIL real-time simulation.

Islanding and fault detection function IR logics in the one-WF system are shown in Fig. 2.5, where V_2 stands for the negative sequence voltage, P is the active power at the PCC, and df/dt is the rate of change of frequency. Decision logics of fault and fault type recognition functions for the two-WF system are presented in Fig. 2.6 and Fig. 2.7, where V_a is the phase A voltage, V_0 is the zero-sequence voltage, V_1 is the positive-sequence

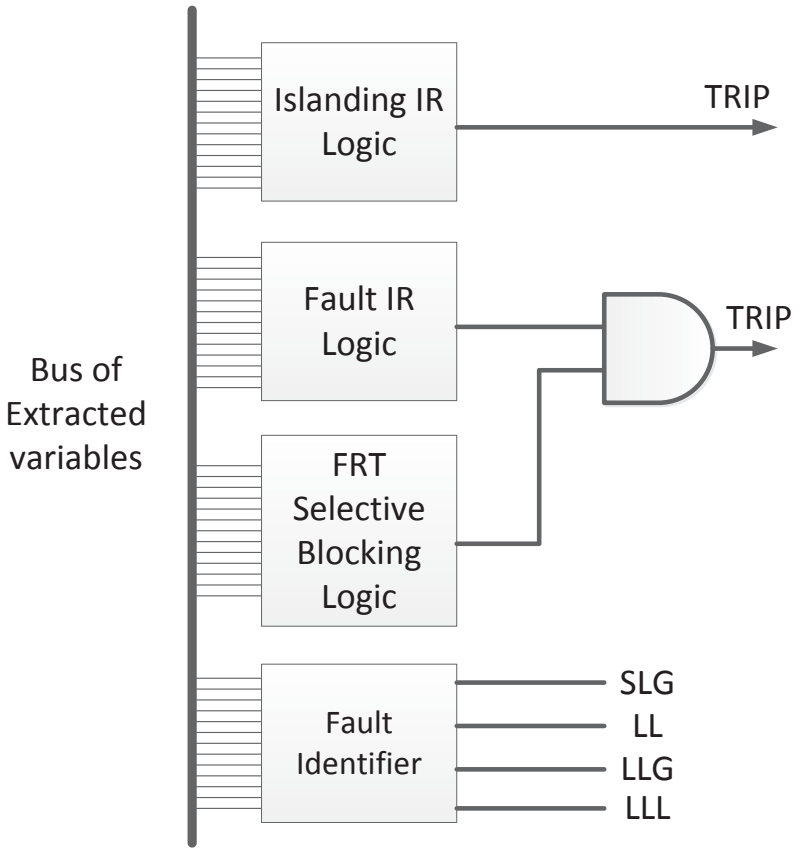

Fig. 2.4 Functional diagram of multifunction IR scheme.

Table 2.2 DG locations in different systems under study.

System	Location A	Location B
1WF	WF	N/A
2WF	WF1	WF2

voltage and dP/dt is the rate of change of active power. The FRT selective blocking logic of WF1 in the two-WF system is of 41 decision nodes and the extra difference of this logic from other IR logics is the classification type "blocking" and "non-blocking" as explained in section 2.3.3.

HIL validation setup can be found in Section 5.2. IR logics in Fig. 2.5 are programmed

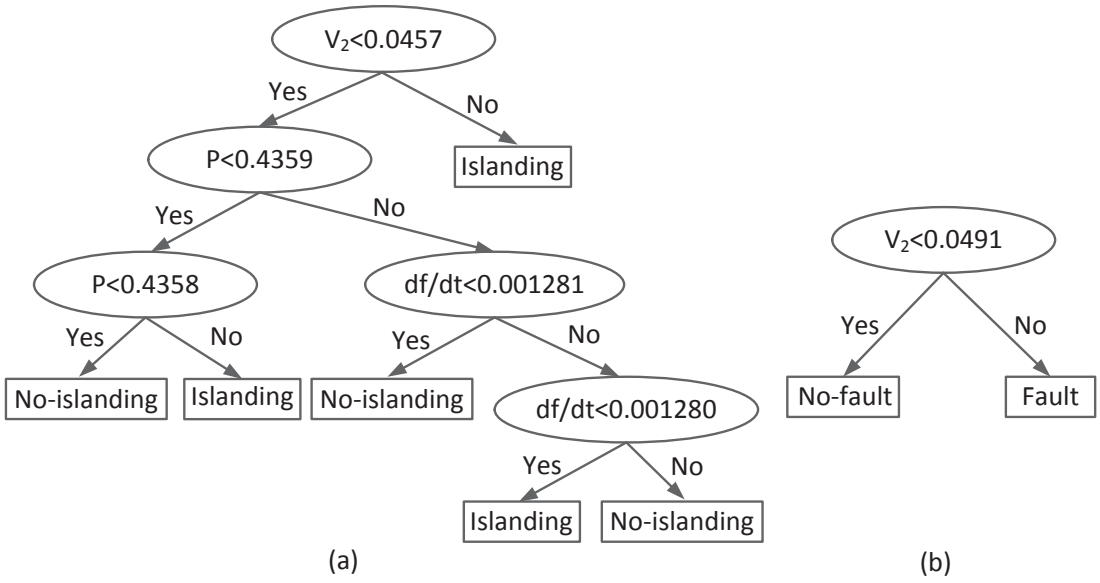

Fig. 2.5 IR logics of (a) islanding and (b) fault detection functions in the one-WF system.

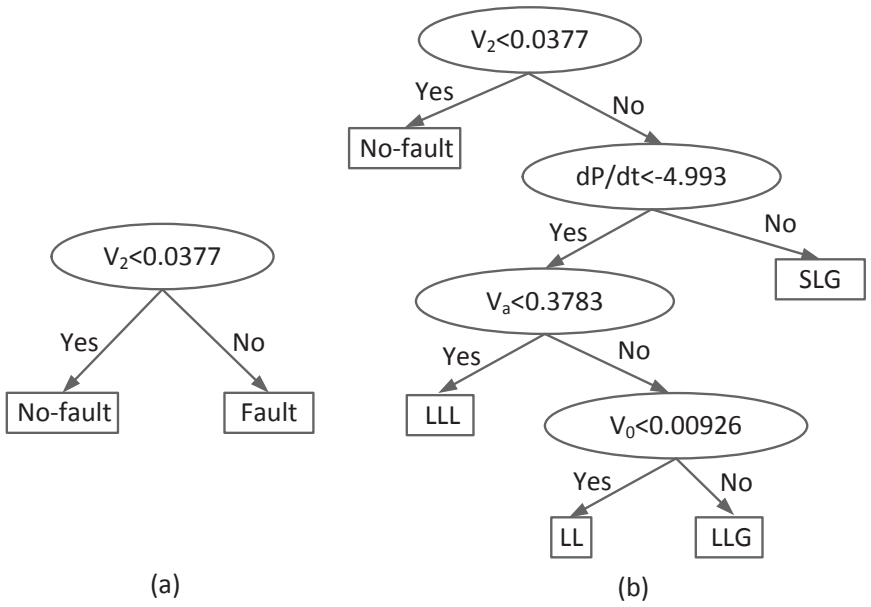

Fig. 2.6 IR logics of (a) fault detection and (b) fault type recognition functions at WF1 in the two-WF system.

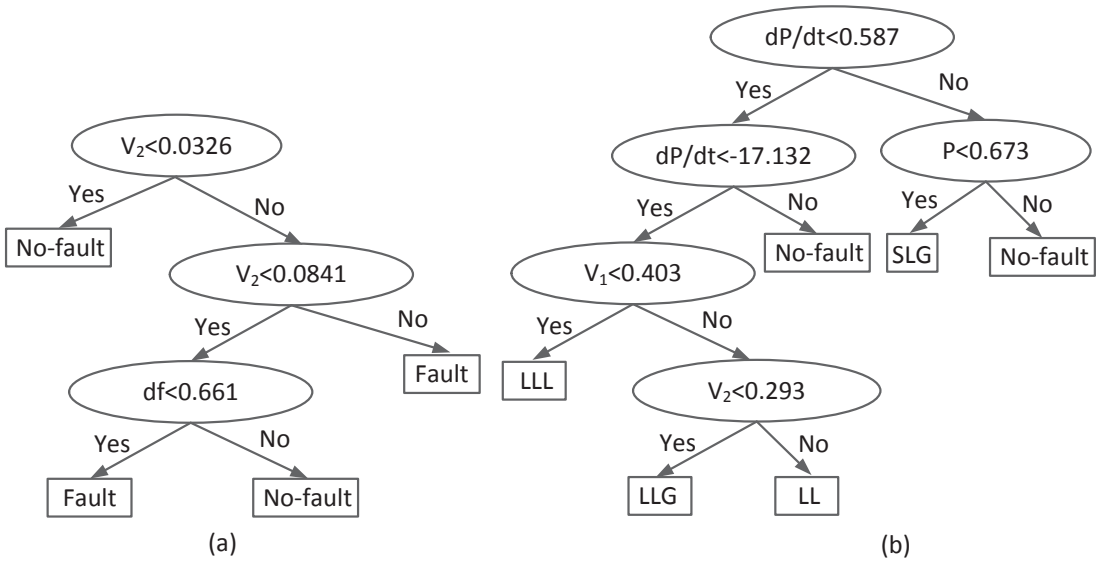

Fig. 2.7 IR logics of (a) fault detection and (b) fault type recognition functions at WF2 in the two-WF system.

into the digital relay as its islanding and fault detection logics in the one-WF system. Relay settings of standard islanding and fault detection elements are shown in Table 2.3 as advised by IEEE standard [1]. Similar to standard elements, the time delay for IR islanding detection function is 100 ms and for fault detection function is instantaneous.

Table 2.3 Standard relay settings.

Device		Setting (time delay)
Islanding detection	Over freq.	60.5 Hz (100 ms)
	Under freq.	59.7 Hz (100 ms)
	Over volt. I	V > 1.2 (100 ms)
	Over volt. II	1.1 < V < 1.2 (500 ms)
	Under volt.	V < 0.8 (100 ms)
Fault detection	Inst. Overcurrent	I_{pickup_ph}=1.2×$I_{nom.}$
	Inst. Ground Overcurrent	I_{pickup_gnd}=0.25×$I_{nom.}$

26 non-tripping events, 8 islanding events and 21 fault events are implemented and tested. Detection results are obtained through GOOSE messages and they are summarized in Table 2.4. The performances of the IR and the standard protection elements are

analyzed in terms of dependability index (DI, the ratio between the number of detected islanding/fault events and the number of total islanding/fault events) and security index (SI, the ratio between the number of not detected non-islanding/non-fault events and the number of total non-islanding or non-fault events). Average detection times of islanding and fault for each device are also provided, considering the dynamics of the DERs.

Table 2.4 HIL validation results.

Device		DI	SI	Avg. detection time (s)
Islanding detection	IR	99%	92.30%	0.23
	Standard	98%	88.50%	0.257
Fault detection	IR	99%	88.50%	0.0215
	Standard	99%	88.50%	0.0389

2.4.2 Intelligent Relay in Small Power Mismatch

The benchmark distribution system can also be found in Appendix A.1. Three types of systems are investigated in this section. According to the DG locations at A and B, three systems are presented in Table 2.5, namely, hybrid, 1WF and 2WF systems.

Table 2.5 DG locations in different systems under study.

System	Location A	Location B
Hybrid	SG	WF
1WF	WF	N/A
2WF	WF1	WF2

All of the relays for DER interconnection protection are mounted on the high voltage side of the step-up transformer between DG and the distribution feeder, as indicated at buses B-9 and B-20 in Appendix A.1. The protective relays are set up to meet the DER interconnection requirements in IEEE Standard 1547 [12], and their parameters can be found in Table 2.3. In addition, ROCOF relays with a time delay of 50 ms are tested as well, under the thresholds of 0.1, 0.25, 0.5, 0.75, 1.0 and 1.2 Hz/s.

This section demonstrates firstly the decision trees obtained upon the islanding events of CB-1 (see Appendix A.1) open, and fault and CB-1 open in the three types of systems in Table 2.5. Following are the DI and SI of all relay functions, compared to the three types of systems. Moreover, relay performances are investigated in depth under small power mismatch conditions in the substation.

Decision trees

To understand the intelligent relay's performance under small power mismatch, decision trees are obtained in this subsection in three categories: import, export and close-mismatch. The decision trees are shown in Figures 2.8, 2.9 and 2.10. Operating conditions such as import and export in the following figures are referring to the power flowing into and out of the distribution feeder; while close-mismatch stands for the small power mismatch at the utility substation.

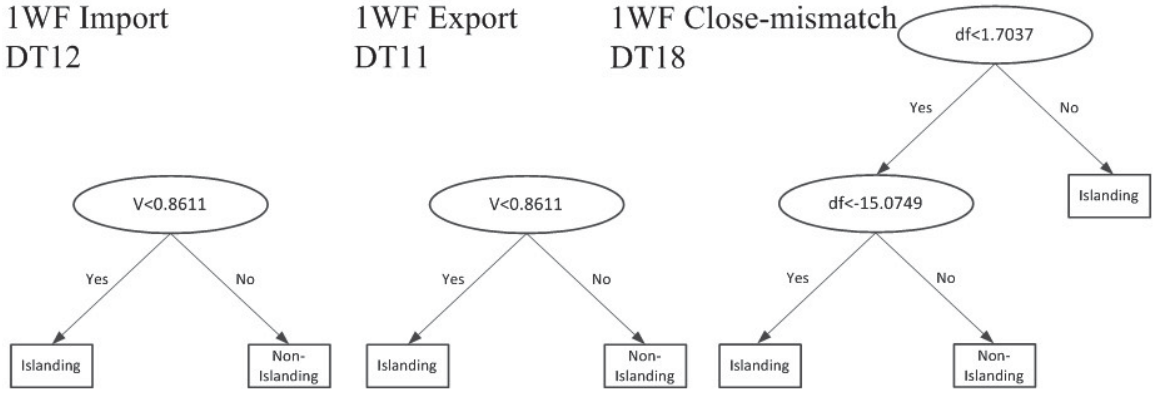

Fig. 2.8 IR logics in the one-WF system under small power mismatch study.

DI and SI under different DER systems

The quantification of DI and SI are shown in Section 2.2. The performance indices of the intelligent relay, frequency relay, voltage relay and ROCOF relay are all listed. Since there are 12 settings for ROCOF relays, only ROCOF with the best indices are shown in the figures. Relay performances are shown in Figure 2.11. It needs to be noted that the DI and SI of location A (DER1) are presented here in the two-WF systems.

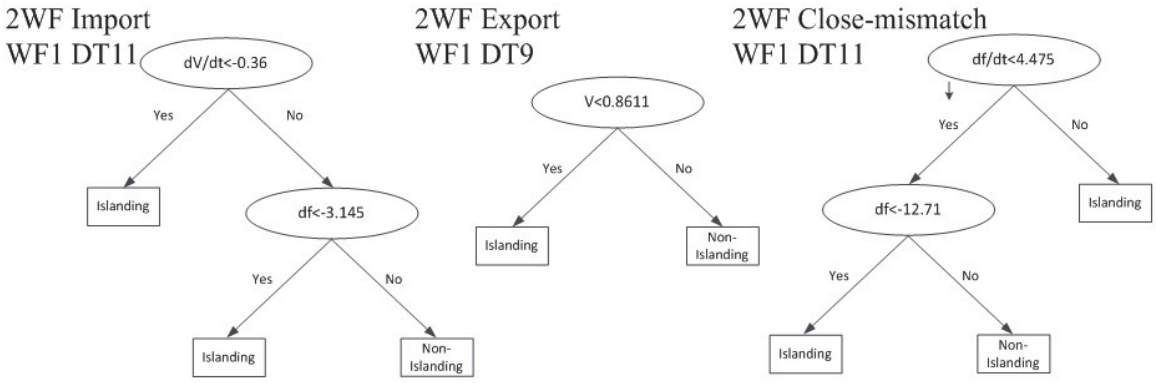

Fig. 2.9 IR logics in the two-WF system under small power mismatch study.

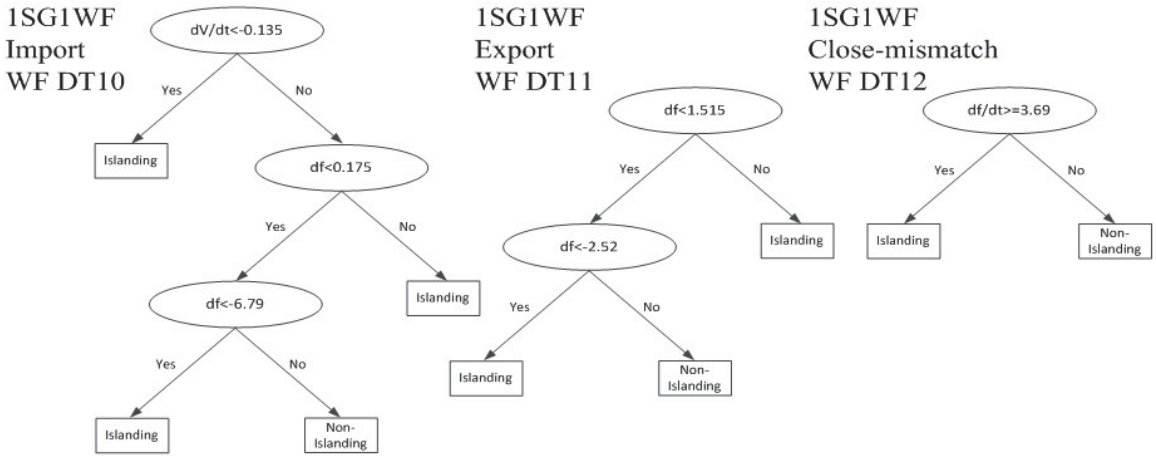

Fig. 2.10 IR logics in the hybrid system under small power mismatch study.

Small power mismatch performance

Due to the frequency-dominated nature of the obtained decision trees, the frequency relay is investigated in particular. In operating conditions of very small power mismatch at the substation, performances of frequency relays and IRs are presented for 1WF and hybrid systems in Table 2.6 and 2.7 respectively. These results are only used to signify the fact that standard relays cannot detect islanding events under small power mismatch. In reality, the power mismatch values are limited by the measurement accuracy under small power mismatch.

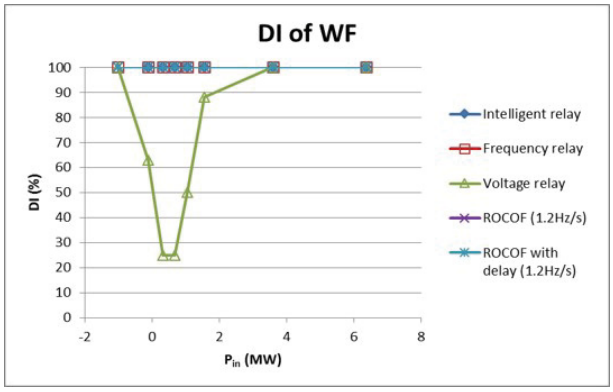

(a) IR dependability index in the one-WF system.

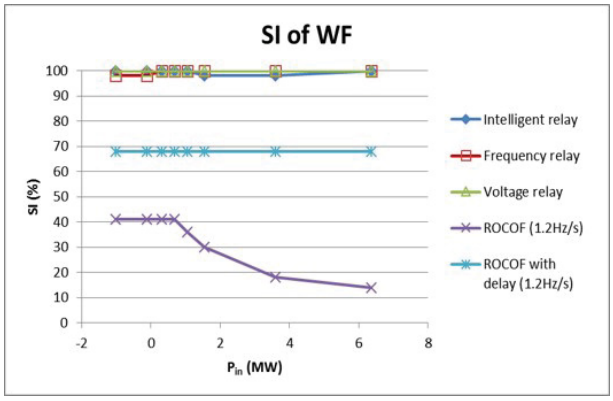

(b) IR security index in the one-WF system.

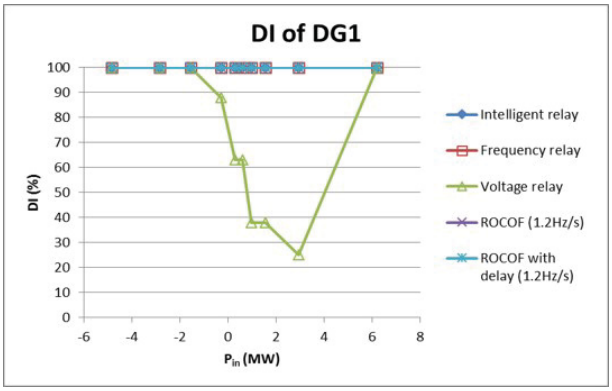

(c) IR dependability index in the two-WF system.

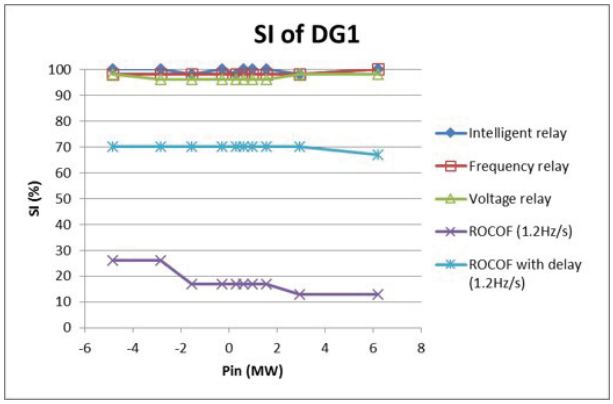

(d) IR security index in the two-WF system.

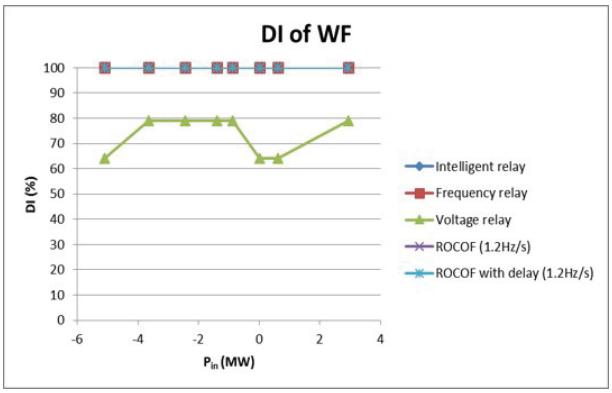

(e) IR dependability index in the hybrid system.

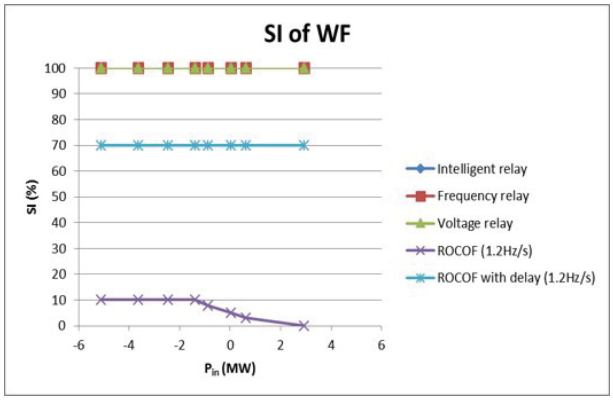

(f) IR security index in the hybrid system.

Fig. 2.11 IR DI and SI under different DER systems.

Table 2.6 Frequency relay performances in 1WF system under small mismatch conditions.

Case	P_{in} (kW)	Q_{in} (kVar)	Freq. Relay (DI%/SI%)	IR (DI%/SI%)	Note
1	-22	-6	99/99	99/100	All cases detected by FR
2	-1	-2.6	88/99	98/99	FR failed at only CB-1 open event
3	-22	-2.6	88/99	99/100	FR failed at only CB-1 open event
4	-1	-6	99/99	99/100	All cases detected by FR

Table 2.7 Frequency relay performances in hybrid system under small mismatch conditions.

Case	P_{in} (kW)	Q_{in} (kVar)	Freq. Relay (DI%/SI%)	IR (DI%/SI%)	Note
1	6	-52	88/99	99/100	FR failed at only CB-1 open event
2	66	-54	99/99	99/99	All cases detected by FR
3	6	-81	99/99	98/100	All cases detected by FR
4	66	-81	63/99	99/100	Inertia increases by 5 times; FR failed in more cases

2.4.3 Discussion

The islanding detection capability of intelligent relays in synchronous DG systems is studied in [110]. This section is corroborating the ability of IR in inverter-based DER systems and hybrid systems. In synchronous DG system, high inertia exists because of the rotating mass of the synchronous generators, while in inverter-based DER systems, although there is a permanent magnet synchronous machine in the wind turbine, inertia response is isolated by the back-to-back converter in some of the wind turbine applications such as type-4 wind turbines. Therefore, frequency deviation becomes obvious in pure inverter-interfaced DER systems. It seems that conventional relays are performing very well in hybrid systems or even pure inverter-based systems, however, in some special and realistic cases, conventional relays may fail to detect islanding events whereas IR has better dependability and security.

The main findings from the previous results comprise the following points:

- Decision trees of IR are mainly frequency-based in pure inverter-based and hybrid systems. From Figures 2.8 to 2.10, among the three systems, the frequency is the

dominant feature for islanding detection. In high power mismatch, export or import, some other features such as V, dV/dt may appear. Yet in close-mismatch cases, frequency deviation is the most effective feature.

- Relay comparisons. As shown in Figure 2.11, IRs are performing the best in both DI and SI. Conventional relays (frequency relays) are also performing well in most of the cases. As an example, 1.2 Hz/s ROCOF with delay is very dependable but not very secure as in the SI figures. Instead, voltage relays are secure but not dependable.
- Small power mismatch performances. As indicated in Table 2.6 and 2.7, when the power mismatch is small enough, as most of the possible conventional IDMs, frequency relay falls in its NDZ. The conventional relays can no longer detect islanding. From Table 2.6 and 2.7, it is clear that frequency relay could not work in some of the feeder operating conditions. In Table 2.6, as the reactive power mismatch decreases, frequency relay fails at islanding event of CB-1 open. In contrast, the performance of frequency relay would not be affected if active power mismatch at the substation decreases to a certain value. This is validated by [117], and quoted as reactive power mismatch dominates the boundaries of over/under frequency relays. Similarly, in hybrid system frequency relay also reaches its NDZ but at a higher reactive power mismatch -54 kVar, instead of -2.6 kVar in one inverter system. Meanwhile, if one increases the inertia of the synchronous generator in the hybrid system and keeps the same power mismatch at the substation, the performance of frequency relay becomes worse because of the high inertia and less obvious frequency deviation. The DI drops to 63% since the inertia in the system increases by five times.
- Frequency relay works well for substation islanding when power mismatch is not very small; whereas intelligent relay can detect both substation islanding and downstream islanding, as long as these operating conditions are trained before getting the optimal DTs.

2.5 Conclusions

Multifunction IR protection scheme can be modelled and tested using comprehensive strategy to get multiple function blocks to integrate islanding and fault detection, fault type recognition and FRT selective blocking functions in the same IR. Results also show that the proposed islanding and fault detection functions can be programmed in existing protective

relays, and the relay responds as expected. HIL real-time simulation results illustrate that both proposed IR and standard protective elements are effective in detecting islanding and fault events in inverter-interfaced distribution systems. However, the proposed IR is able to avoid more nuisance tripping events comparing to standard elements. In addition, the detection times of IR are faster than standard elements by 10.5% and 44.7% in islanding and fault detection.

This chapter discusses as well the performance of IR method in islanding detection of inverter-based DER and hybrid distribution systems. The proposed IR is capable of detecting islanding events in inverter-interfaced systems using frequency and some other features such as rate of change of frequency, each symmetrical component of voltage, phase voltage, rate of change of active power at PCC in its DTs. The performances of other conventional relays, for instance, frequency relays, voltage relays, ROCOF relays are studied and compared with IR. Among them, although performing well in high power mismatches, conventional relays fail in low-power mismatch operating conditions. As the inertia of the system increases, frequency relay is becoming worse in detecting islanding events. In contrast, IR has good performance since it is trained to be intelligent enough to detect these extreme cases. However, the enhanced method needs to be proposed to solve the insensitivity issue of the islanding IRs. In Chapter 3 a novel IR-based islanding detection method which improves the islanding detection under small power mismatch is proposed.

Chapter 3

Islanding Detection Function

3.1 Introduction

This chapter covers the islanding detection function of the proposed IR. A new methodology for reducing the boundary limits of islanding detection schemes using an NDZ-based training/testing strategy to generate DT logics is proposed. In other pattern recognition based islanding protection studies, training effort is equally distributed according to active and reactive power imbalance. Those training strategies are inefficient not only in NDZ reduction but also in utilizing computational resources. In addition, the obtained DT logics is successfully implemented in a real digital relay. The proposed methodology is validated using hardware-in-the-loop (HIL) technique. This chapter is organized as follows: Section 3.2 presents the background of NDZ in islanding detection. Section 3.3 develops the proposed model and the performance indicators required to analyze the decision tree learning algorithm. Then the methodology for reducing the NDZ is elaborated on in Section 3.4. Section 3.5 demonstrates the case study and testing results. The discussions and conclusions are shown in Section 3.6 and Section 3.7.

3.2 The Concept of Non-detection Zones

The NDZ concept is an index to evaluate the performance of islanding protection [117]. This performance index is defined by power imbalance (measured at distribution system point-of-common coupling (PCC)) and plotted in ΔP-ΔQ space as shown in Fig. 3.1. Usually, at the PCC between the local electric power system (Local EPS) and area EPS, power

mismatches both in active and reactive power vary within a certain range, depending on the generation of DERs and the system loading. When power mismatches are large enough prior to grid disconnection, most widely-used standard functions, such as under/over voltage and under/over frequency functions can easily detect such islanding events. However, in scenarios of small power mismatches, voltage and frequency deviations after islanding are not significant enough to be detected by those standard relay functions.

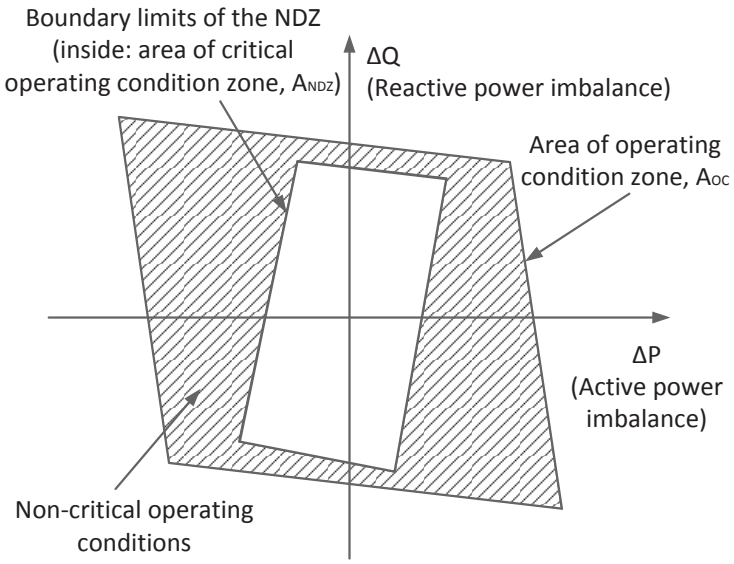

Fig. 3.1 Typical boundary limits of system operating conditions.

In different types of distributed generation, NDZs are of different shapes. In synchronous generator (SG) based systems, the NDZ of the voltage function is influenced by reactive power imbalance (Fig. 3.2(a)), which at the same time defines the top and bottom boundaries, and also by active power imbalance level to a lesser degree [55]. Meanwhile, active power mismatch determines the performance of frequency function, which results in the left and right boundaries.

As for the inverter-based systems, the size of the NDZ, in terms of active power and reactive power mismatch at PCC, depends on the inverter control strategy. For a constant power control strategy, the following relationships define the boundary limits of the NDZ [117]:

$$(\frac{V}{V_{max}})^2 - 1 \leq \frac{\Delta P}{P} \leq (\frac{V}{V_{min}})^2 - 1 \tag{3.1}$$

$$Q_f \cdot (1 - (\frac{f}{f_{min}})^2) \leq \frac{\Delta Q}{P} \leq Q_f \cdot (1 - (\frac{f}{f_{max}})^2) \tag{3.2}$$

where ΔP and ΔQ are the power mismatch before the grid is disconnected. P and Q are the power output of inverter-based DER. V_{max}, V_{min}, f_{max} and f_{min} are the over/under voltage and frequency limits respectively. Q_f is the quality factor of the local load circuit, defined as $Q_f = R\sqrt{C/L}$ in a parallel RLC circuit.

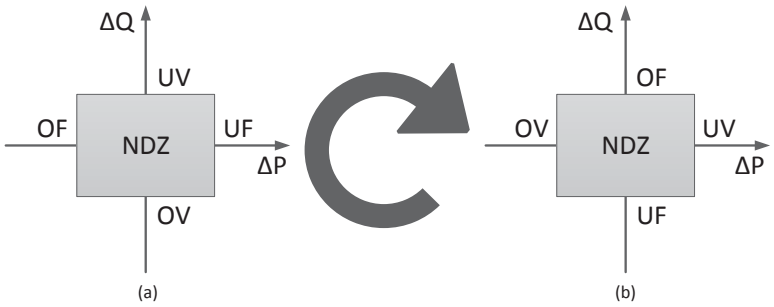

Fig. 3.2 NDZ shapes of Over/Under Frequency and Voltage (OF/UF and OV/UV) functions in (a) synchronous generator and (b) inverter based systems.

3.3 Decision Tree Learning Algorithm

The details of the IR training process can be found in Section 2.2. According to the distribution feeder configuration, typical islanding events are simulated off-line. During these simulation events, the voltage and current measurements at the DG point of common coupling (PCC) are captured and stored for data-mining analysis. Based on the data obtained, additional features that may have clear variation patterns or characteristics during islanding and fault conditions are calculated, such as frequency, rate of change of frequency, active and reactive power, etc. After the data is processed and organized, the data-mining tool Matlab Statistics and Machine Learning Toolbox [118] is utilized to find the determinant features and the detection logics in the form of Decision Trees (DTs). The optimal DT with the highest Dependability Index and Security Index is chosen to be embedded into the IRs. IR performance analysis will be conducted with independent testing events.

The proposed methodology uses the classification and regression tree algorithm to train IRs and obtain IR logics. More than 30 electrical features are tested in the inverter-based,

SG-based and hybrid systems, while in the end, 12 features (see Appendix A.7) are selected using sequential feature selection method. In order to capture the skewed characteristics of NDZ (explained in Section 3.2) under different DER technologies, features x_9 to x_{12} are included. Therefore, there are 12 elements in the vector $\bar{X}$ according to Eq. (2.1). It also means that the nodes in any acquired DTs are limited to the 12 types. It is assumed in this thesis a maximum permissible DER islanding protection tripping time of 734 ms [2]. Thus, for a certain event, either islanding or non-islanding, 44 cycles of the monitored 12 features (which are also the elements in the vector $\bar{X}$) are stored in the matrix T_i^j upon the occurrence of one event. Furthermore, a number of events are simulated and the obtained vector $\bar{X}$ is expanded in such a way. This process is also called training of the DTs. These training events are substantial and determine the capability of the final DTs when differentiating islanding from non-islanding events.

In order to quantify the NDZ performance graphically, the concept of non-detection zone area index R_{NDZ} is introduced in this chapter. It simply calculates the ratio between the area of NDZ and the area of the zone that defines all operating conditions.

$$R_{NDZ} = \frac{A_{NDZ}}{A_{OC}} \times 100\% \tag{3.3}$$

where A_{NDZ} and A_{OC} are defined as the area of NDZ and operating conditions as seen in Fig. 3.1.

3.4 The Proposed Non-detection Zone Reduction Methodology

In this section, the proposed NDZ reduction methodology is presented and explained in detail, namely: Establishing NDZ, Reducing NDZ Band and Generating Intelligent Relay Logics.

3.4.1 Establishing NDZ

The flow chart of the proposed methodology is shown in Fig. 3.3. This is a complete methodology from defining the target DG to generating IR logics, then to the testing and verification of the proposed IR while reducing the NDZ.

As shown in Fig. 3.3, once the target DG is specified, a load change is applied to emulate various load and generation scenarios in a real system. Load change could be realized

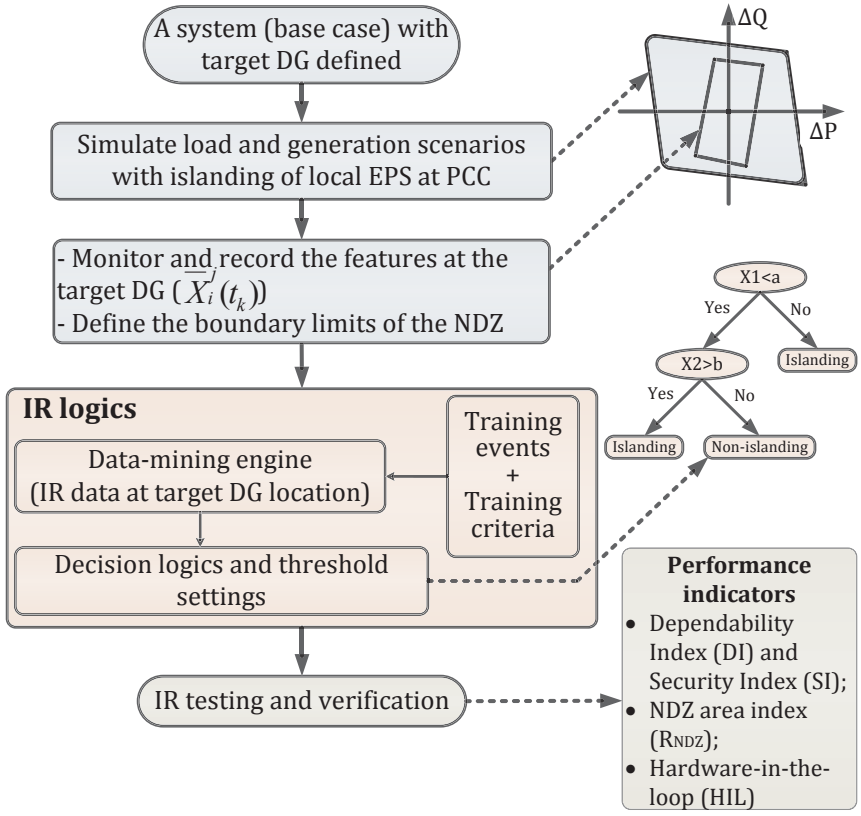

Fig. 3.3 Methodology for creating islanding IR with reduced NDZ.

by a small increment or decrement in active and/or reactive power [119]. Meanwhile, it is needed to emulate islanding events by disconnecting the area electric power system substation at the PCC. This step helps define non-critical operating conditions as shown on the side. Actually, the smaller the change is, the more accurate the NDZ boundaries are, however, the computational cost gets higher. The next step is to monitor and record the islanding features at the target DG. The simulation is then continued until all of the possible operating conditions are covered in the course of defining the NDZ boundaries. After all of the operating conditions are simulated, the islanding detection responses of standard voltage and frequency elements of the relay are defined and plotted for the target DG. Subsequently, the NDZ boundary limits are defined and plotted (refer to the shape in Fig. 3.1). It also defines the critical operating conditions at the target DG location, which can not be detected by a standard relay. The proposed methodology uses this identified NDZ boundary as an initial pattern (boundary limits) for reducing NDZ consequently.

3.4.2 Reducing NDZ Band

Once the NDZ of a standard relay is defined, the goal of creating IR training database is clear: minimizing the NDZ area. Critical operating conditions are delimited already by the NDZ of standard relay functions using the proposed method in the previous steps, while a general range of system operating conditions can be obtained in the ΔP-ΔQ space according to local load variation data and DG generation. Explicitly, the following two types of system operating conditions need to be determined first in the IR training stage, and some training criteria are suggested:

- Critical operating condition corresponding to the small power mismatch within the identified NDZ band. This operating condition is hard to detect due to small deviations in frequency and voltage. IR training should be focused here so that NDZ could be largely reduced.
- Non-critical operating condition including system operating condition outside of the NDZ band but inside the system operating boundaries. This operating condition is easy to be detected due to large deviations in frequency and voltage. IR training points should be covered in all of the four quadrants to guarantee a good overall performance.

Generally, in non-critical area, the further the operating condition is from the origin of ΔP-ΔQ space, the easier it is to be detected. Therefore a detailed knowledge of boundary limits of non-critical operating conditions is not required and the system operating conditions can be acquired from estimation. In other pattern recognition methods [38], [110], the two-dimensional training/testing strategy is not established. Training effort is either distributed according to active power imbalance or equally delivered in the ΔP-ΔQ space with certain ΔP and ΔQ combinations. Those training strategies are inefficient not only in NDZ reduction but also in utilizing computational resources. With the proposed training criteria, IR training set can be selected in an effective and optimal way that reduces the NDZ.

3.4.3 Generating Intelligent Relay Logics

In addition to training criteria, in order to achieve good dependability and security performance, the islanding response data at the target DG location is tested under all types of islanding and non-islanding training events. The purpose here is for the IR to adapt to

more realistic events than only CB opening event seen in the NDZ plot.

Then the captured IR data of target DG location is processed by the data-mining engine. According to the algorithm and implementation principle discussed in Section 3.3, the decision logics and threshold settings are generated and well pruned.

The last step in the flow chart is IR testing and verification. Testing operating conditions are placed in a larger range than in IR training and in more islanding and non-islanding events. The IR performance is evaluated according to the following performance indicator: DI/SI, R_{NDZ} and HIL. DI and SI indicate whether the relay is dependable and capable of avoiding nuisance tripping. The NDZ area index R_{NDZ} illustrates the quantified area of the relay's NDZ. Since the generated relay logics and threshold settings are based on real electrical features, they can be modelled and programmed in a digital relay for real-time HIL testing.

3.5 Case Study

This section is divided into four parts: Benchmark System and Relay Settings, Simulation Events, Off-line Simulation Results and Analysis and Hardware-in-the-loop Validation Results and Analysis.

3.5.1 Benchmark System and Relay Settings

The benchmark system under investigation in this chapter can be found in Appendix A.6. In this chapter, standard islanding protective functions and IRs are implemented at the high voltage side of the DG transformer (see R_1 and R_2 in Fig. A.3). The setting of the standard relay functions is according to [120] and the work in [110], [121]. They are with the same setting as the islanding detection device in Table 2.3. The feasible system operating conditions are defined between 36%-96% of total system loading and the time delay of the IRs is set to be 100 ms.

3.5.2 Simulation Events

The events that are used for IR training and testing are listed in Table 3.1. These events can be classified, according to their nature, into 9 types: normal operating conditions, load shedding, fault and load shedding, load adding, fault-ride-through, topology change,

parallel feeder islanding, circuit breaker open, and fault and circuit breaker open. Some of these events are explained in the following:

Table 3.1 Simulation events in islanding detection.

Event Type	Cases Trained	Cases Tested	Event Description
Normal operating condition	6	3	9 different steady-state operations, within the power range of 30% to 100% of total system loading.
Load shedding	60	30	Load shedding at main and branch buses, include shedding of single and multiple loads.
Fault and load shedding	45	45	Fault and load shedding at main and branch buses, include shedding of single and multiple loads.
Load adding	60	30	Load adding at main and branch buses, include adding of single and multiple loads.
FRT	45	27	Delayed fault events for the future FRT capability of DGs.
Topology change	18	9	Topology A: CB-15 open; Topology B: CB-10, 11 or 12 is open, CB-15 is close.
Parallel feeder islanding	18	9	When the islanding occurs at the shorter parallel feeder, IRs of DG1 and DG2 should detect it is not an islanding event for themselves.
Circuit breaker open	45	27	Circuit breaker open at main and branch buses feeder, some of these events might be an islanding event to one DG and a non-islanding event to the other.
Fault and circuit breaker open	45	27	Fault and circuit breaker open at main and branch buses feeder, same as above.

Fault-ride-through (FRT)

Various delayed faults scenarios are conducted to train the intelligent relay to learn the fault events which it should "ride-through" without tripping DGs. This thesis uses the typical

Canadian FRT curve suggested in [10]. What the IRs are capable of, learning from the FRT training events, is not to violate the FRT requirements of grid codes within a predefined time associated with the FRT curve. In other words, the IRs are trained to recognize any delayed fault and keep their protected DGs connected to the grid in collaboration with the DG FRT controller. Consequently, during the IR training, the events of delayed fault (marked as "-1" since they are non-islanding events) are simulated and corresponding data of the monitored 12 features are stored for further processing. In the trained FRT events, delayed faults at various locations and with different fault types (three-phase, single-line-to-ground, double-line and double-line-to-ground) are incorporated into the FRT capability.

The integration of advanced inverter function – FRT/LVRT capability with the proposed methodology can be achieved through predefined setting logics that provide responses corresponding to particular sets of parameters, which has potential to restore a temporary ride-through condition and to remove the need for disconnections during under/over voltage and/or frequency conditions. The proposed IR is applicable in and compatible with the context of grid code requirements [120], [122] on advanced inverter functions such as Low-Voltage or Low-Frequency Ride-Through (LVRT/LFRT). Since the inverter control of the inverter-based DER is designed to respect a certain Voltage/Frequency Ride-Through curve according to local grid code requirements, the key to islanding detection relay is not to override such scenarios by false tripping of DGs. This can be easily realized through IR tripping logics with inverter LVRT/LFRT controller's supervision.

Topological change and parallel feeder islanding

The proposed NDZ reduction methodology is able to detect scenarios such as topological change and parallel feeder islanding. In the loop-type distribution grid of Fig. A.3, high service reliability is guaranteed by connecting CB-15 when there is an upstream permanent fault resulting to an islanding at the short feeder. During the transition from Topology A to B (see Table 3.1), the IRs should view this as a non-islanding event. On the other hand, islanding events that occur at a parallel feeder are not islanding events of the other feeder. The parallel feeder islanding events are simulated at the shorter feeder, therefore the IRs at R_1 and at R_2 should differentiate those non-islanding events from real islanding events that occur at the same feeder as the IRs.

3.5.3 Off-line Simulation Results and Analysis

Using the benchmark system of Fig. A.3, 360 power mismatch conditions are simulated to describe overall system operating conditions. For the IR training database of the benchmark system, 11 system operating conditions are chosen according to Section 3.4. Each operating condition is consistently trained in 342 cases and tested in a disjoint set of 207 cases according to Table 3.1.

The obtained DT at the PCC of SG is shown in Fig. 3.4, where frequency deviation is the dominant feature. The root threshold on frequency deviation is much stricter than that of a standard frequency relay. Thus, the three-layer DT makes an accurate islanding detection model. However, for the WF, DT is more complicated because of its inverter-based characteristics and further location in the feeder (location B of Fig. A.3). Its DT logic is shown in Fig. 3.5. The effectiveness of the IRs is tested in a larger range than the feasible system operating conditions—from 30% to 100% of total system loading.

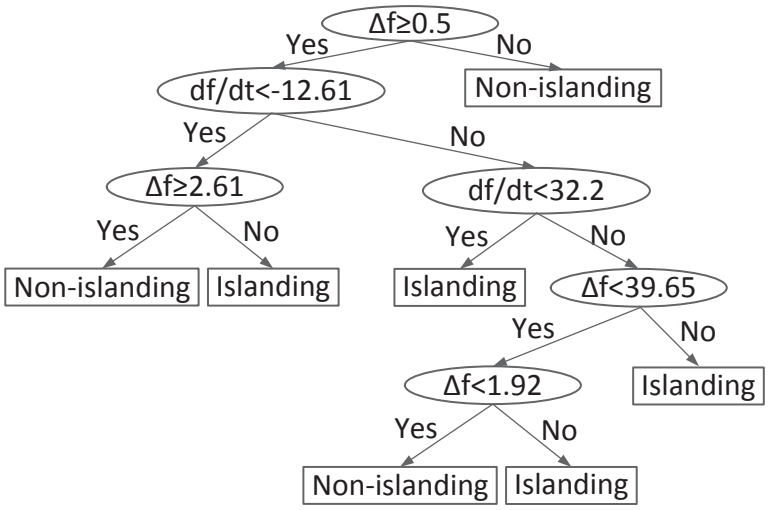

Fig. 3.4 Decision logics of IR at the PCC of SG with WF in power control mode.

At the target DG locations, shown as A and B in Fig. A.3, comparisons are made between standard islanding relay functions and the IRs. In Fig. 3.6, the NDZs of standard relay functions are delimited with the WF having constant power control. Boundaries corresponding to OF/UF and OV/UV functions are marked as well. In this thesis, under-voltage function is not violated in the system under study.

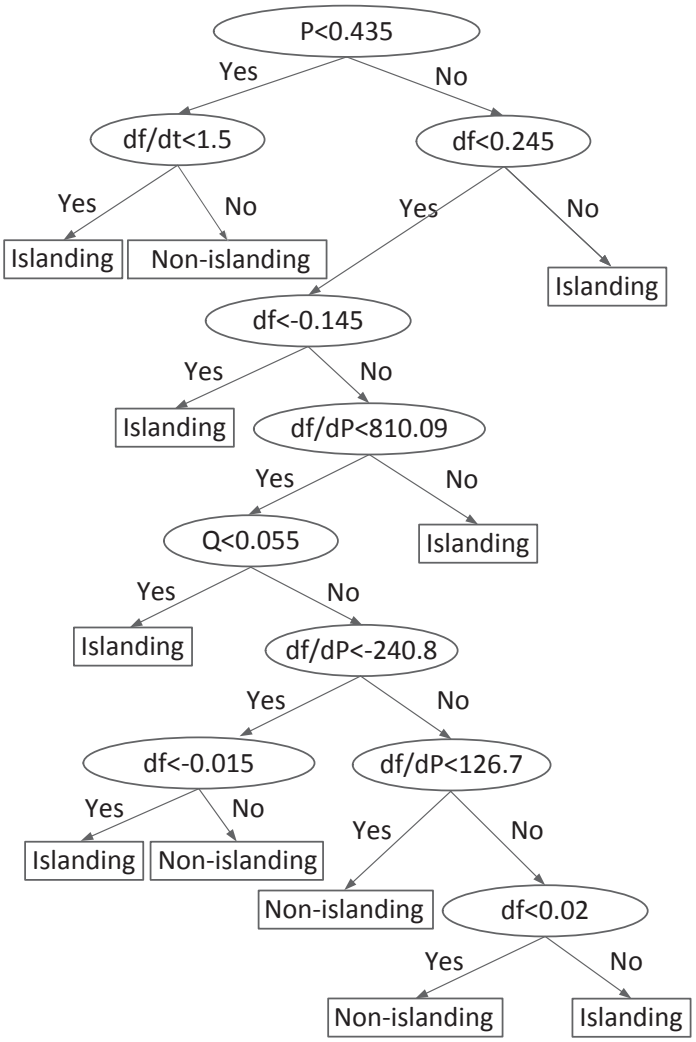

Fig. 3.5 Decision logics of IR at the PCC of WF with WF in power control mode.

Different voltage control strategies of the WF have been considered as shown in Fig. 3.7. It exhibits a wider power mismatch area under the same load variation level. It means that, upon the inception of islanding, WF with constant power control has stricter power generation and consequently less NDZ area compared to WF with voltage control that tries to maintain the collapsed voltage by increasing reactive power resulting in less reactive power mismatch. P/f (active power and frequency) control of DER is not considered in this thesis because the frequency is assumed to be maintained by the main grid in this study.

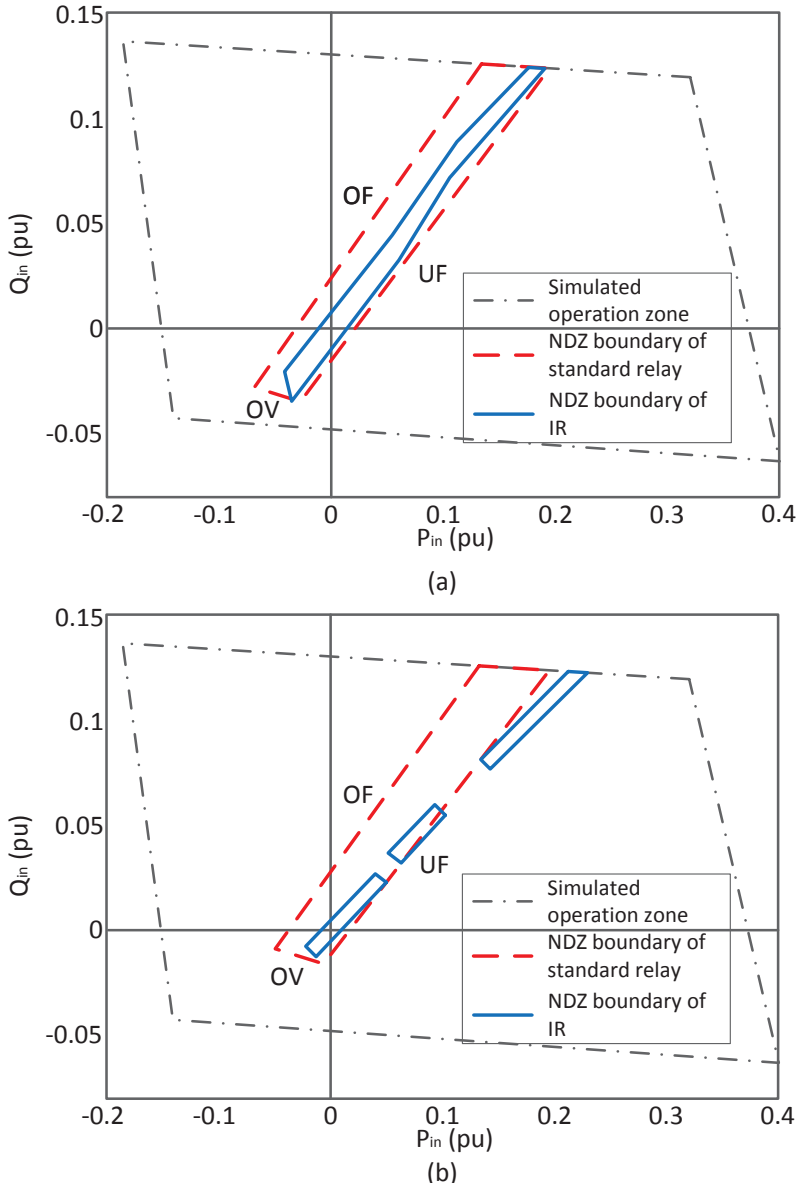

Fig. 3.6 NDZ of the standard relay and IR functions at (a) the PCC of SG in power control mode and (b) the PCC of WF in power control mode.

3.5.4 Hardware-in-the-loop Validation Results and Analysis

The proposed methodology is validated in a real-time simulator by connecting a real digital relay in the loop. Chapter 5 provides more details of the setup. According to the available digital relay's word bits, IR logic in Fig. 3.4 is programmed in the digital relay logic. The

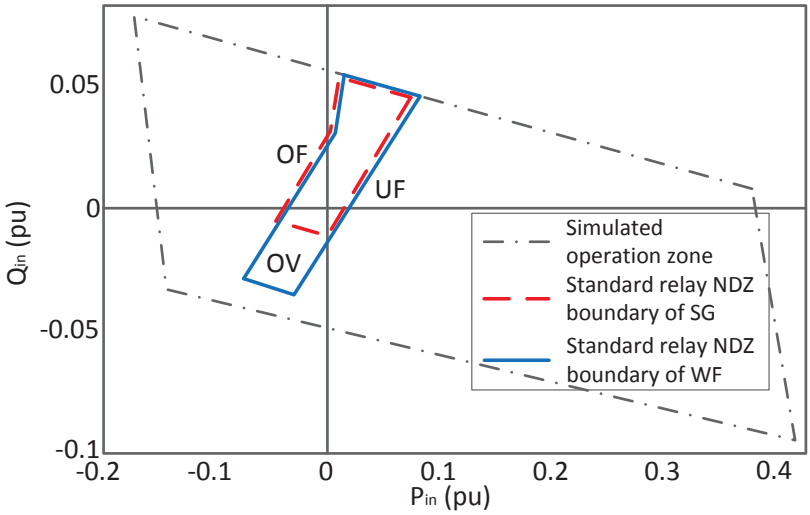

Fig. 3.7 NDZ of the standard relay at the PCC of SG and WF with WF in voltage control mode.

HIL simulation results of reduced NDZ in the case study are demonstrated in Fig. 3.8.

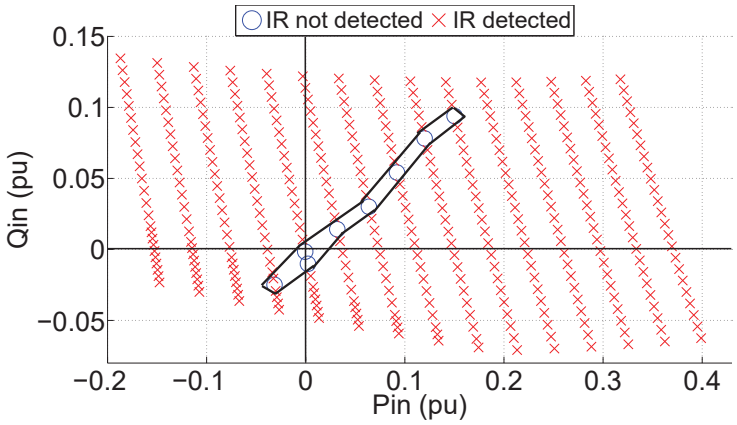

Fig. 3.8 HIL experimental NDZ of digital relay programmed with IR logics of Fig. 3.4 at the PCC of SG with WF in power control mode.

The proposed IR logics are tested and compared with standard relay functions. Table 3.2 shows the R_{NDZ} values of standard relay functions and the proposed IRs at different target DG locations according to Fig. 3.6. This table indicates that the NDZ areas of the proposed IR decreased more than a half of those of standard relay functions for SG and WF. When tested in HIL, the IR result is even better, only 2.78% of the entire area is not detected. Note that N/A here results from the fact that some of the elements in Fig. 3.5

are not supported by the employed commercial relay.

Table 3.2 Relay performance comparison of different relays (SG: Synchronous Generator, WF: Wind Farm, DI: Dependability Index, SI: Security Index).

Performance indicator	Standard relay functions	The proposed IR	The proposed IR tested in HIL
R_{NDZ_SG} [%]	9.11 (Fig. 3.6a)	4.19 (Fig. 3.6a)	2.78 (Fig. 3.8)
R_{NDZ_WF} [%]	8.14 (Fig. 3.6b)	2.00 (Fig. 3.6b)	N/A
DI_{SG} [%]	98.1	99.8	98.5
SI_{SG} [%]	95.0	99.7	96.6
DI_{WF} [%]	97.8	99.5	N/A
SI_{WF} [%]	80.0	99.9	N/A

The dependability and security performance results of the standard relay functions, the proposed IR and the IR in HIL are also provided in Table 3.2. It is seen that the proposed IR is exhibiting a higher DI/SI than standard relay functions. IRs at the WF PCC show a similar performance as ones at the SG PCC. From the perspective of standard relay functions, they are less dependable than the proposed IRs, while the SIs of the standard relay functions represent an undesirable nuisance tripping behavior at both locations.

The HIL validation of the proposed methodology exhibits practical applicability. The advanced industrial technology of numerical relay algorithms has realized the implementation of custom protection functions using relay logic programming. Therefore, intelligent decision tree logics obtained can be programmed into a standard industrial numerical relay as shown in this subsection, which also reduces hardware requirements. Future development of signal processing algorithm will allow the implementation of even more complicated logics than the one in Fig. 3.5.

3.5.5 Under-trained DT Logic

If the IR is not trained appropriately according to the proposed methodology, the resultant NDZ would have a significant area (its R_{NDZ} might be even larger than the one of

standard relay functions) outside of the NDZ boundary of the standard relay. Under this circumstance, the active and reactive power mismatch would be so large that the associated voltage and frequency deviations upon islanding violate the IEEE 1547 Standard [14]. The DT, in this case, is called under-trained DT logic.

With the same system setting as the one in Fig. 3.6 but different DT training strategy, an example of the under-trained DT logic can be found in Fig. 3.9. The DT behind this figure lacks training in the fourth quadrant of the ΔP-ΔQ space, The outcome is the undetected triangle-like area in that quadrant. A corrective measure to solve this problem is to add an extra training condition located in the middle of this triangle-like area in the fourth quadrant. As long as the training strategy follows the proposed method in Section 3.4.2, a newly trained DT logic with negligible NDZ can be generated while satisfying the IEEE standard, as shown in Fig. 3.6a.

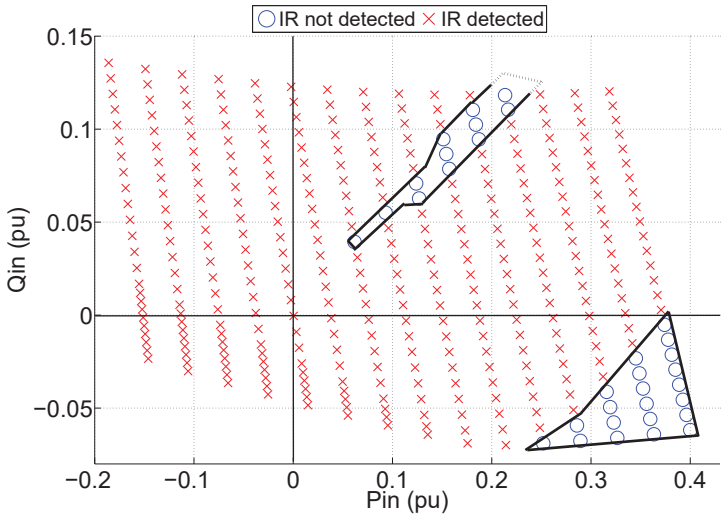

Fig. 3.9 An example of the under-trained DT.

3.6 Discussions

3.6.1 Comparison with Other Methods

This subsection compares the proposed method with other intelligence based methods. The results can be seen from Table 3.3.

Table 3.3 Comparison with other methods.

Method	Measure-ment	Feature	DI, SI	Events & DG types	Hardware Realization
In [38]	V, I	8 (wavelet coefficients, wavelet energy)	$> 95\%$, $> 96\%$	6, conventional DER, inverter-based DER	Difficult, need to design a microcontroller
In [123]	V	3 (wavelet coefficient, wavelet energy)	N/A, accuracy $> 98\%$	7, conventional DER	N/A
In [110]	V, I	11 (basic physical quantity)	$> 98\%$, $> 48\%$	5, conventional DER	N/A
In the proposed methodology	V, I	12 (basic physical quantity)	$> 99\%$, $> 99\%$	9, conventional DER, inverter-based DER	Easy, can be integrated into digital relays

The comparison is made among four DT based methods. All four methods measure voltage and current except for the one in [38] measuring only voltage. The work in [38] and [123] utilizes discrete wavelet transform (DWT) to obtain islanding detection features and DT to classify different events. Same mother wavelet (DB4) is selected in the two DWT-based papers, but [38] uses 4 levels of voltage and current wavelet decomposition coefficients (8 features) and [123] uses 3 levels of voltage wavelet decomposition coefficients (3 features). While the work in [110] and the proposed methodology in this chapter take advantage of only discrete Fourier transform (DFT) and DT. Fewer features are used in [123] due to the fact that inverter-based DER is not under investigation. The inertia-less characteristic of inverter-based DER increases the difficulty of islanding detection and therefore requires more features for detection. Besides DG types, the event type under study also alters the detection difficulty level. All of the four methods have the following two types of islanding

events: circuit breaker opening and circuit breaker opening after a fault. For non-islanding events, there are 4 types of them in [38], 5 types in [123] and 3 types in [110]. While in this thesis, extra events such as FRT, topological changes and parallel feeder islanding are taken into account. The proposed method in [110] was tested using these non-islanding events, showing a low SI value. Moreover, the work in both [38] and this chapter is validated in a laboratory environment. However, the proposed methodology in this chapter is promising due to the following reasons: 1) it requires low computational burden and its calculation is more reliable comparing to the DWT-based method; 2) the IR can be easily programmed into digital/numerical relays and does not require any micro-controller design and 3) the proposed islanding detection methodology has a reduced NDZ comparing to other decision tree based methods.

3.6.2 DER Technologies and Controls

The proposed methodology can be utilized for both SG-based and inverter-interfaced DERs. As illustrated in Fig. 3.6, both SG and WF have similar shapes located in the ΔP-ΔQ space. Which DER technology results in the NDZ shape is not necessary information for the proposed IR training technique. The technique focuses on the delimited NDZ shapes obtained from the NDZ establishing procedures in Section 3.4.1, followed by the NDZ reducing criteria. Once the IR gets trained/tested appropriately, a negligible NDZ can be achieved. The results can be seen in the IRs' NDZ boundaries of Fig. 3.6(a) and (b). Their non-detection zone area indices are both below 4.2%, as indicated in Table 3.2.

Similarly, this NDZ reduction methodology is feasible for DERs with various control strategies. Section 5.4 demonstrates the NDZs of WF with power control mode in Fig. 3.6 (b) and with voltage control mode in Fig. 3.7. After both NDZs are delimited, critical and non-critical operating conditions can be identified. IR training strategies can be subsequently designed, without the need to know the specific DER control modes.

3.7 Conclusions

This chapter proposed a complete procedure for constructing intelligent islanding relays while reducing non-detection zones. It firstly proposed a methodology to establish and reduce NDZ in islanding schemes. IR decision logics and threshold settings can be obtained

through this methodology to achieve a superior relay performance. In addition, the proposed NDZ reduction method is applicable to both DER technologies and different DER control strategies due to its pattern recognition nature. Besides the reduced NDZ performance, the proposed IR is capable of detecting a myriad of islanding and non-islanding events using decision tree learning method.

The generated IR logics are proved to be effective in reducing the NDZ boundary limits at target DG locations as shown in Fig. 3.6 - 3.7 and Table 3.2. The concept of non-detection zone area index is introduced as well to quantify the NDZ performance. This methodology reduces more than 54% of NDZ area comparing to standard relay functions, without jeopardizing dependability and security performance. It is also concluded that the IR using proposed methodology has a much smaller NDZ and higher dependability and security index (as indicated in Table 3.2) in the overall performance. Extensive field tests and fault recorder data would be considered and applied in the future work to compare the simulations with real-world conditions, and to see the efficacy of the proposed pattern recognition methodology under field data. Furthermore, this thesis managed to implement intelligence in a standard numerical relay with decision tree logics. The proposed pattern recognition methodology is also realized and validated in the laboratory HIL environment.

Chapter 4

High Impedance Fault Detection Function

4.1 Introduction

This chapter extends the functionality of the multifunction intelligent relay by incorporating a HIF detection approach. It has been decades for researchers and engineers to seek a solution to high impedance fault (HIF) detection. HIF is associated with the downed or undowned conductor. The downed conductor is the one that falls on the poorly conductive surface, while undowned conductor involves contacts with the tree limb, sand, asphalt, grass, soil, concrete and so on. HIF produces little or no fault current. Typical fault currents range from 10 to 50 amps, with an erratic waveform [64]. Hence, it is hard to detect HIF since its current is usually too low to reach overcurrent relay's pickups. Besides, with the irregular, non-linear and asymmetric attributes, HIF detection becomes more difficult and challenging.

HIF normally exists in distribution power systems with voltages ranging from 4 kV to 34.5 kV. Upon the occurrence of HIF, its immediate vicinity is imposed with potential danger, which is hazardous to public safety. Therefore effective HIF detection is required to detect all of the HIFs while avoiding false tripping to maintain the continuity of power supply. In addition, HIFs cannot always be recorded in the fault report to relay engineers and the reported cases are therefore less than what line crews observe from the field. It was revealed in [64] in one case study that conventional protection cleared only 17.5% of

staged HIFs.

A high-impedance fault looks very similar to a small, noisy, poorly behaved single-phase load [89]. Meanwhile, some normal system events such as capacitor switching or motor starting are possible to mislead the detection of HIFs. It is therefore very difficult to find unique characteristics to discriminate HIFs from non-HIFs. Different system loading conditions, amount of local generations, weather conditions such as humidity and temperature, type of materials in contact with the conductor are all variables that can have a subtle affect on HIFs behaviours. Machine learning method is working well to detect what it has been trained to detect, but the inexhaustible uncertainty and stochasticity of HIFs require an online learning or adaptive HIF detector to achieve satisfactory performance.

4.2 HIF modeling

There are mainly three ways of modeling HIF. The first one is called transient analysis of control systems (TACS) controlled switch, which was proposed in [124]. This model emulates arc conduction, re-ignition and extinction. The advantage of this model is the adjustable phase difference between the applied voltage and fault current. Some modifications of the TACS controlled switch are shown in [125], [78].

The second way of modeling HIF is the employment of two anti-parallel dc-sources connected via two diodes, plus two variable resistors. The primitive model came from a fixed resistance at the point of fault [126]. The nonlinear impedances was then included to add the non-linearity of fault current [73]. Later on, the model is extended with two anti-parallel DC-sources connected via two diodes [127], which modelled the asymmetric nature, as well as the intermediate arc extinction around current zero. The above model was then modified by adding one [93] or two [95], [96], [128] variable resistances in series with the DC sources. This kind of model is able to model the effective impedance and thus the randomness of the resulting fault current.

The third way originates from the Kizilcay model [129] which utilizes a dynamic arc model derived from the viewpoint of control theory based on the energy balance in the arc column [130]. A branch with an arcing fault can be modeled as an arc in series with a constant resistance R_0, where $R_{arc}(t)$ is the time varying arc resistance. Let $g_{arc}(t) = 1/R_{arc}(t)$ be the arc conductance, which is also time-varying. Thus,

$$v_f(t) = i_f(t) \cdot R_0 + \frac{i_f(t)}{g_{arc}(t)} \tag{4.1}$$

The arc model that connects $g_{arc}(t)$ and the current of the arc branch $i_f(t)$ is as follows:

$$\frac{dg_{arc}(t)}{dt} = \frac{1}{\tau}\left(\frac{|i_f(t)|}{u_0 + r_0|i_f(t)|} - g_{arc}(t)\right) \tag{4.2}$$

where u_0 is the characteristic arc voltage, r_0 is the characteristic arc resistance, and τ is the arc time constant.

This chapter employs the second way of modeling HIF since it fully captures the random, irregular and unsymmetrical characteristics of HIFs. Fig. 4.1 shows the HIF model used in this chapter. This model connects one phase of the power line to the ground. Two variable resistors are both changing randomly and model the dynamic arcing resistance. Two sets of diodes and DC sources are connected in an anti-parallel configuration. The two DC sources are randomly varying as well, which model the asymmetric nature of HIF. The positive half cycle of HIF current is achieved when $V_{ph} > V_p$, while negative half cycle when $V_{ph} < V_n$. When $V_n < V_{ph} < V_p$, the current equals to zero, which represents the period of arc extinction. In order to generate a fault current between 10 and 100 A in the 25 kV benchmark system (discussed in Section 4.3.3), the model settings are provided in Table 4.1. The obtained HIF current waveforms and V-I characteristics are presented in Fig. 4.2 and 4.3. Testing results of this HIF model reveal a good modeling performance and are validated in the simulation and field test results of [83], [131] and [132].

Table 4.1 HIF model settings.

Component	Value range	Values change every
V_p	$5 \sim 6$ kV	0.1 ms
V_n	$7 \sim 8$ kV	0.1 ms
R_p	$200 \sim 1500$ Ω	0.1 ms
R_n	$200 \sim 1500$ Ω	0.1 ms

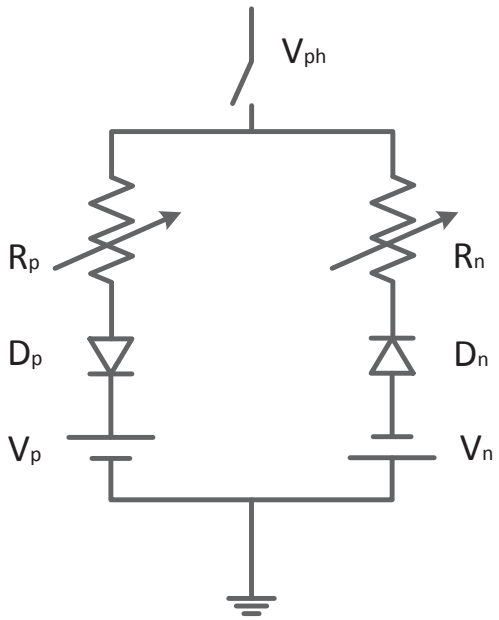

Fig. 4.1 HIF two anti-parallel dc-source model.

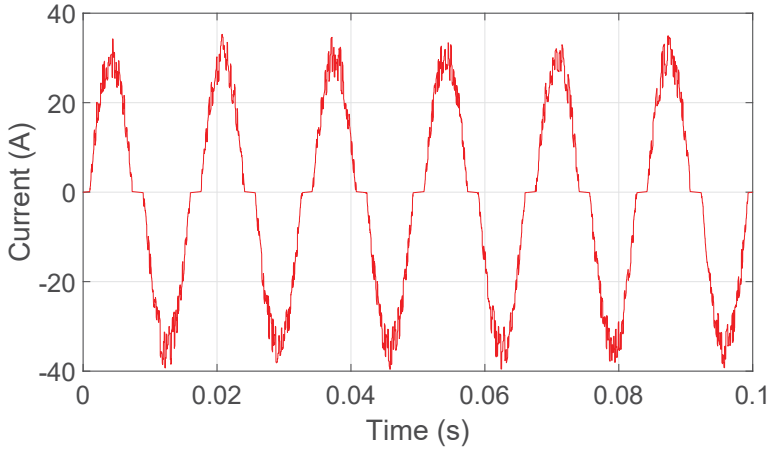

Fig. 4.2 HIF current waveform.

4.3 Feature Selection

Feature selection significantly affects the performance of pattern recognition based methods. This chapter has studied 246 candidate electrical features by measuring the current and voltage at the point of common coupling (PCC). These features include discrete Fourier

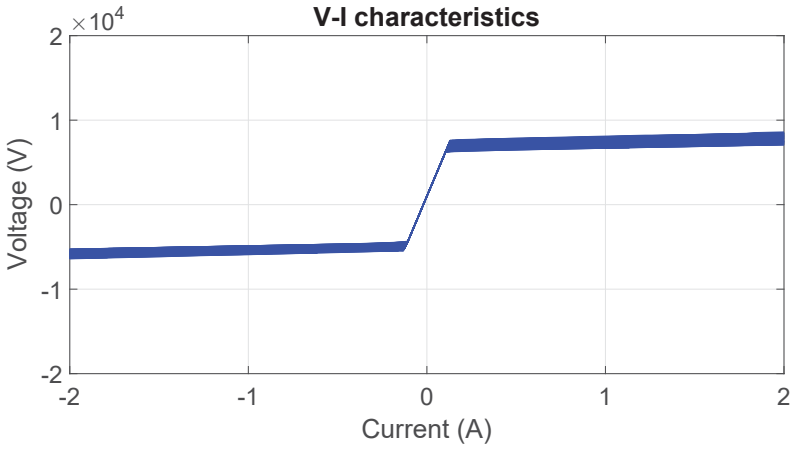

Fig. 4.3 HIF V-I characteristics.

transform and Kalman filter estimated features. In addition to all conventional features in protection, some artificial electrical features such as the rate of change of frequency over active power, the rate of change of power factor, the angle difference between voltage harmonics, and so on are also included. Prior to the proposed HIF detection features, the benchmark system and event under study are presented.

4.3.1 Variable-importance in Feature Evaluation

Decision tree based algorithm in machine learning can provide protection engineers with optimal relay logics and settings in distribution network protection [133]. However, it is a significant challenge to find out the key features to HIF given the fact of its randomness and irregularity. In another word, an effective and unbiased feature evaluator is required to calculate the merit of each tested feature before the classification between HIF event and non-HIF event. The proposed method takes advantages of the information gain and minimum description length (MDL)-based discretization algorithm to select important features during HIF. The MDL score is called variable of importance in this chapter. A detailed mathematical formulation of the MDL-based algorithm is presented in Appendix A.8.

4.3.2 Pool of Candidate Features

In this study, 246 features are investigated as candidate features. These features are extracted through two techniques: discrete Fourier transform (DFT) and Kalman filter (KF).

Both techniques appear simple and reliable to engineers. Many applications utilizing these techniques can be found in engineering field [134], [135].

The candidate feature pool contains conventional features and invented features as shown in Table 4.2. In DFT-based features, conventional features include frequency (df), rate of change of frequency (df/dt), active power (P), rate of change of active power (dP/dt), power factor (pf), rate of change of power factor (dpf/dt), reactive power (Q), rate of change of reactive power (dQ/dt), power angle (ϕ), rate of change of power angle ($d\phi/dt$), harmonic magnitude of voltage from the first order to the sixth ($H_{V1} \sim H_{V6}$), harmonic magnitude of current from the first order to the sixth ($H_{I1} \sim H_{I6}$), three-phase voltage (V_{abc}), sequence component of voltage (V_{012}), three-phase current (I_{abc}), sequence component of current (I_{012}), rate of change of three-phase current (dI/dt), rate of change of three-phase voltage (dV/dt), line voltage (V_{ll}), angle of sequence component of voltage ($\theta_{V_{012}}$), angle of sequence component of current ($\theta_{I_{012}}$), angle of sequence component of voltage at its first order harmonic ($\theta_{H_{V1\_012}}$), angle of sequence component of current at its first order harmonic ($\theta_{H_{I1\_012}}$), angle of sequence component of voltage at its third order harmonic ($\theta_{H_{V3\_012}}$), angle of sequence component of current at its third order harmonic ($\theta_{H_{I3\_012}}$). While the invented features in DFT-based technique consist of: rate of change of frequency over active power (df/dP), rate of change of frequency over reactive power (df/dQ), rate of change of voltage over active power (dV/dP), rate of change of voltage over reactive power (dV/dQ), rate of change of harmonic magnitude of voltage from the first order to the sixth ($dH_{V1}/dt \sim dH_{V6}/dt$), angle difference between negative and zero sequence voltage ($\theta_{V_2} - \theta_{V_0}$), angle difference between negative and zero sequence current ($\theta_{I_2} - \theta_{I_0}$). The invented features are designed according to literature and a great number of experimental simulations.

In KF-based features, conventional features include the in-phase component of current from the first to the sixth order ($KF\_I\_cos\_H1 \sim H6$), the in-quadrature components of current from the first to the sixth order ($KF\_I\_sin\_H1 \sim H6$), the in-phase component of voltage from the first to the sixth order ($KF\_V\_cos\_H1 \sim H6$) and the in-quadrature components of voltage from the first to the sixth order ($KF\_V\_sin\_H1 \sim H6$) estimated from KF. While the invented features in KF-based technique consist of: DC component of voltage (KF_V_DC), 10 Hz inter-harmonic element of voltage ($KF\_V\_10Hz\_inter - harmonic$) estimated from KF. The implementation details of KF-based features can be found in [136].

Table 4.2 Candidate Feature Pool.

Feature Type	Conventional Feature	Invented Feature
DFT-based	$df, df/dt, P, dP/dt, pf,$ $dpf/dt, Q, dQ/dt, \phi, d\phi/dt,$ $H_{V1} \sim H_{V6}, H_{I1} \sim H_{I6},$ $V_{abc}, V_{012}, I_{abc}, I_{012}, dI/dt,$ $dV/dt, V_{ll}, \theta_{V_{012}}, \theta_{I_{012}},$ $\theta_{H_{V1\_012}}, \theta_{H_{I1\_012}}$ $\theta_{H_{V3\_012}}, \theta_{H_{I3\_012}}$	$df/dP, df/dQ,$ $dV/dP, dV/dQ,$ $dH_{V1}/dt \sim dH_{V6}/dt,$ $\theta_{V_2} - \theta_{V_0}, \theta_{I_2} - \theta_{I_0}$
KF-based	$KF\_I\_cos\_H1 \sim H6,$ $KF\_I\_sin\_H1 \sim H6,$ $KF\_V\_cos\_H1 \sim H6,$ $KF\_V\_sin\_H1 \sim H6$	$KF\_V\_DC,$ $KF\_V\_10Hz\_inter\_$ $harmonic$

To be noted that harmonic phase angles are in harmonic degrees and are the phase difference between the zero crossing of the fundamental frequency reference and the next zero crossing in the same direction of the harmonic.

4.3.3 System and Event Under Study

Benchmark System

The benchmark system utilized can be found form Appendix A.1. The system configuration under different DER Technologies is presented in Table 4.3.

Table 4.3 System Configuration under Different DER Technologies.

System Type	Location A	Location B
Synchronous machine based system	SG	N/A
Inverter-based system	WF	N/A
Hybrid system	SG	WF

Events Under Study

Comprehensive scenarios are considered in the event category (refer to Table 4.4). A loading condition ranging from 30% to 100%, in a step of 10%, is simulated. Furthermore, eight loading conditions and three DG technologies are examined respectively on top of the base case scenario. Therefore, the number of fault and non-fault events are calculated as follows:

1. Fault event: since two types of fault, summing up to 13 cases, are included, the number of fault events with one fault impedance, one fault location and one fault impedance is $(10 + 3) \times 8 \times 3 = 312$. Given 6 simulated fault impedances, 4 fault inception angles and 3 fault locations, the total number of fault events add up to $312 \times 6 \times 4 \times 3 = 22464$.
2. Non-fault event: it comprises normal state, load switching (adding and shedding) and capacitor switching events. Therefore the total number of non-fault events equals to $(1 + 6 + 2) \times 8 \times 3 = 216$.

The simulated events result in an imbalanced dataset, as calculated above. With imbalanced datasets, an algorithm could get insufficient information about the minority class to make an accurate prediction. Therefore, the synthetic minority over-sampling technique (SMOTE) is employed to generate synthetic samples and shift the classifier learning bias towards minority class [137].

Table 4.4 Event Category of System Under Study.

Event Category	Event Type	Number of Events
System Operating Condition	Loading Condition (30%-100%)	8
	DER Tech. (SG, inverter, hybrid)	3
Fault Event	Type 1: SLG, LLG, LL, LLLG	10
	Type 2: Downed conductor	3
	Fault impedance	6
	Inception Angle (0°, 30°, 60°, 90°)	4
	Fault location	3
Non-fault Event	Normal State	1
	Load Switching	6
	Capacitor Switching	2

4.3.4 Effective Feature Set

In the end, after mining the collected data, applying the feature ranking algorithm and selecting the effective feature set (EFS) by considering the comprehensive performance in different distribution systems, an EFS is proposed in Table 4.5.

Table 4.5 Effective Feature Set of HIF Detection in Three Types of Distribution Systems.

Fault Type	Feature
SLG, LL, LLG	$V_2, I_2, (\theta_{V_2} - \theta_{V_0}), (\theta_{I_2} - \theta_{I_0})$ $KF\_V\_cos\_H3, KF\_V\_sin\_H3$
LLLG	$V_{ll}, V_{ph}, H_{V1}, \theta_{H_{V1\_1}}$ $KF\_I\_cos\_H1, KF\_I\_sin\_H1$

4.4 Typical Waveforms

Typical waveforms of the proposed EFS upon HIF are shown in this subsection. A single-line-to-ground HIF is applied in a hybrid distributed generation system (refer to Section 2.4.2 Table 2.5) when $t = 0.3$ second. The exemplary waveforms of all effective features are illustrated in Fig. 4.4.

4.5 Fault Scenario Analysis

In this section, the EFS is evaluated in terms of different fault impedances, fault inception angles and fault locations. The quantifier used in the evaluation is the variable of importance explained in Section 4.3.1.

4.5.1 Fault Impedance Variations

The variable-of-importance values are plotted under different fault impedances. Fig. 4.5 depicts the variable-importance performances of each feature in EFS upon single-line-to-ground (SLG) fault, line-to-line (LL) fault, line-to-line-to-ground (LLG) fault and three-line (LLLG) fault. It is concluded from this figure that:

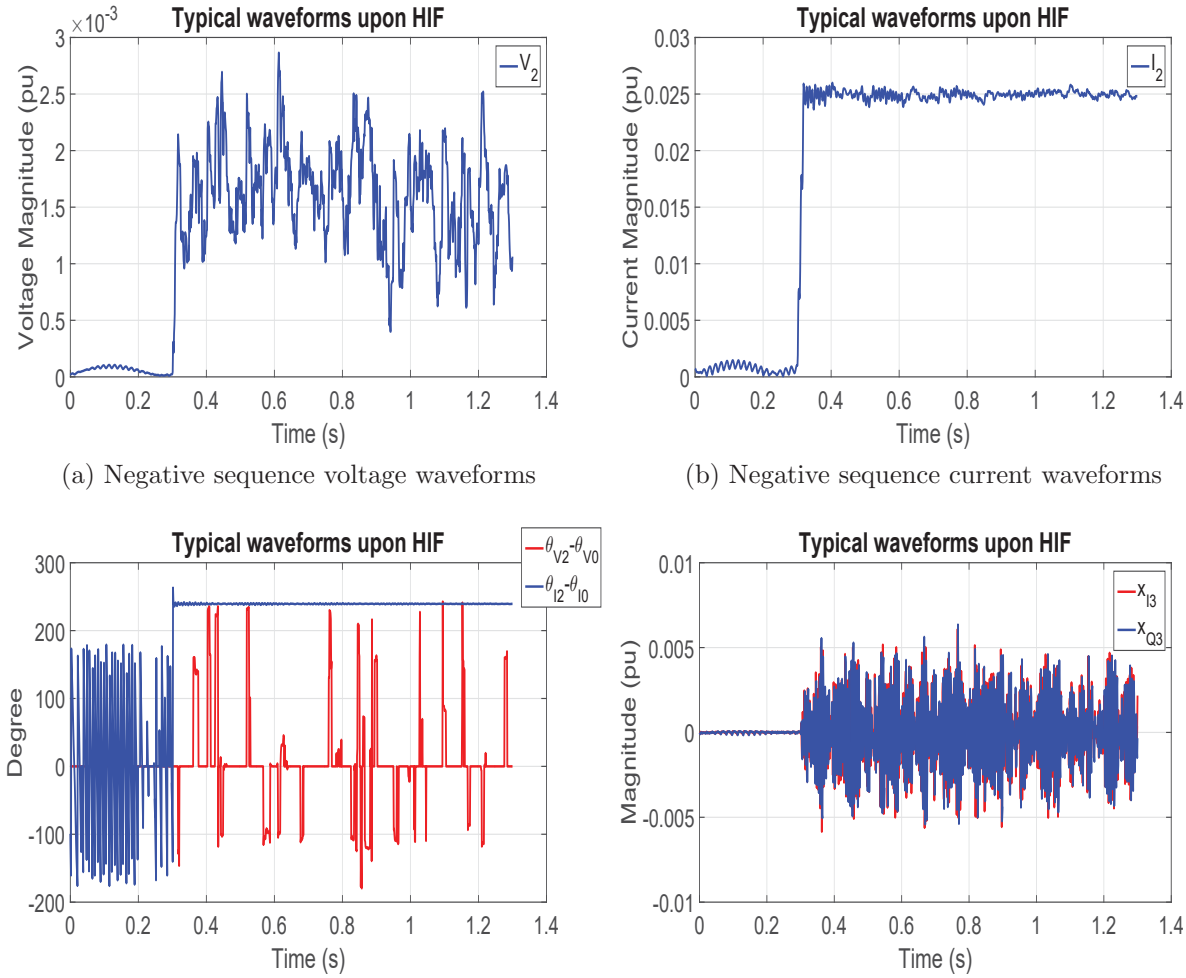

(a) Negative sequence voltage waveforms

(b) Negative sequence current waveforms

(c) Angle difference waveforms between zero and negative sequence voltage and current

(d) 3rd order in-phase and in-quadrature components

Fig. 4.4 Typical waveforms under HIF.

1. The negative sequence of voltage and current are most reliable features that can keep unaffected during any unbalanced fault upon a varying fault impedance.
2. The feature of the angle difference between negative sequence voltage and zero sequence voltage is reliable under LL and LLLG fault but vulnerable to high fault impedance.
3. The third harmonic components estimated from KF gets deteriorated when the fault impedance increases.
4. The proposed three-phase HIF detection features are all performing very well except

for the fundamental in-quadrature component of current estimated from KF.

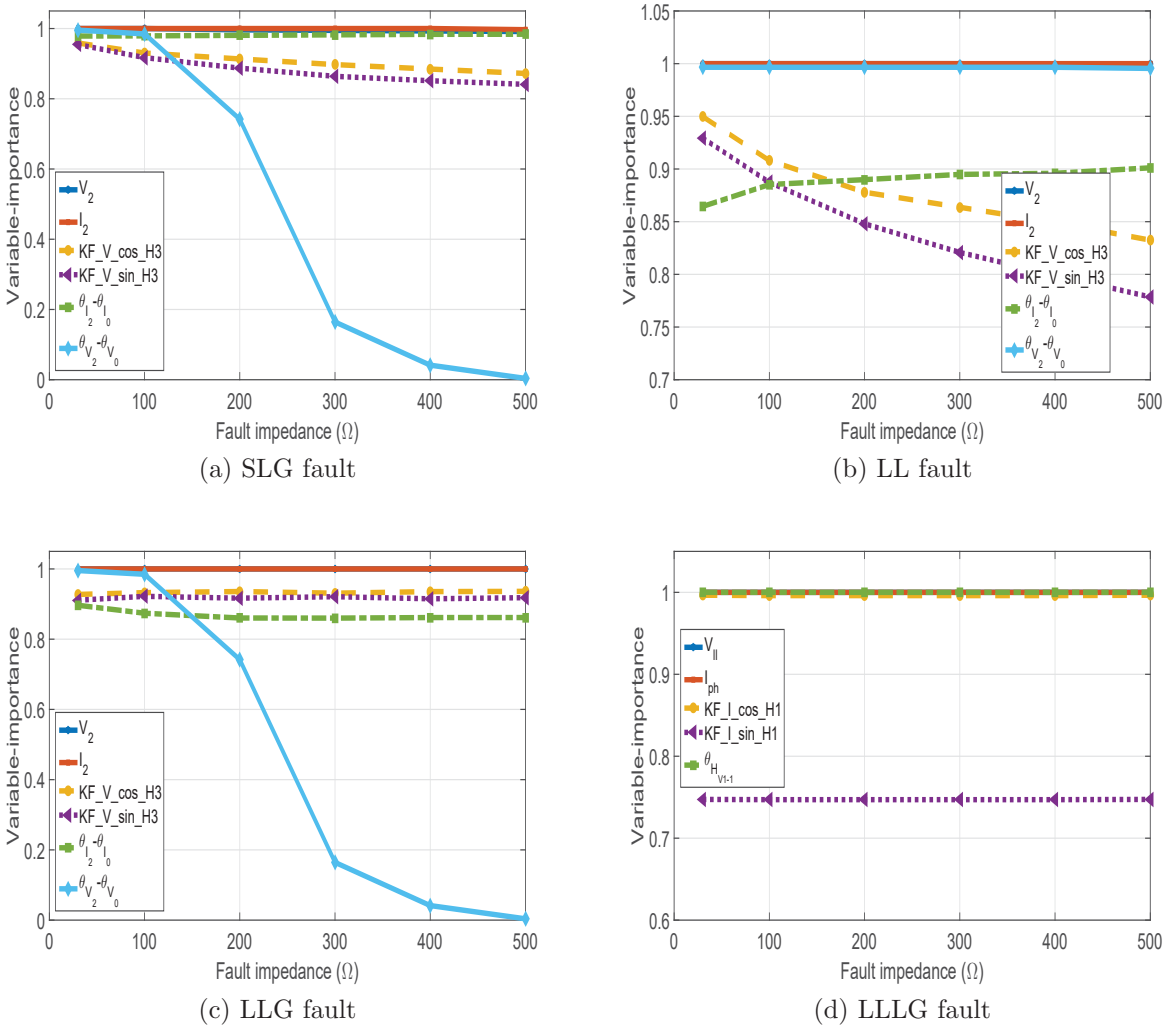

(a) SLG fault (b) LL fault

(c) LLG fault (d) LLLG fault

Fig. 4.5 Variable-importance of all features under each type of fault in a grounded system.

4.5.2 Fault Inception Angle Variations

The affect of fault inception angle is examined as well in this study. The results in unbalanced fault and three phase faults are shown in Fig. 4.6 and Fig. 4.7 respectively. The results in both figures include a varying impedance from 30 Ω to 500 Ω.

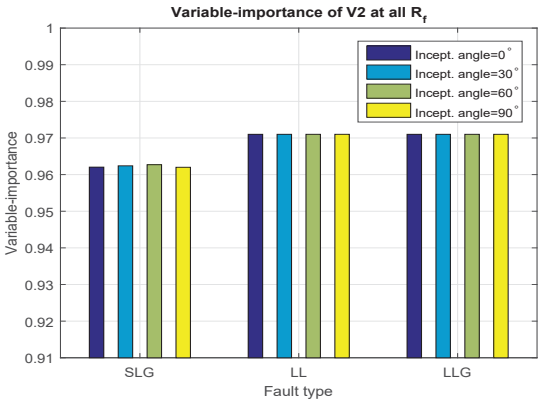

(a) Feature of V_2

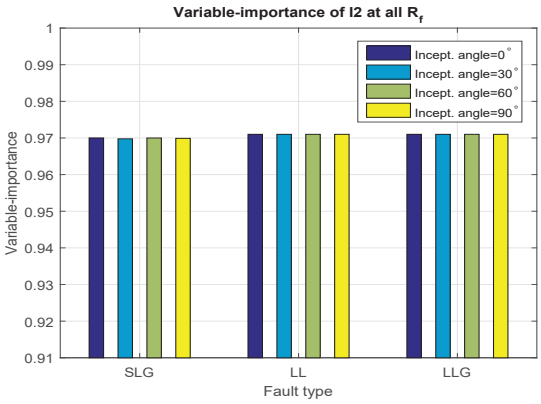

(b) Feature of I_2

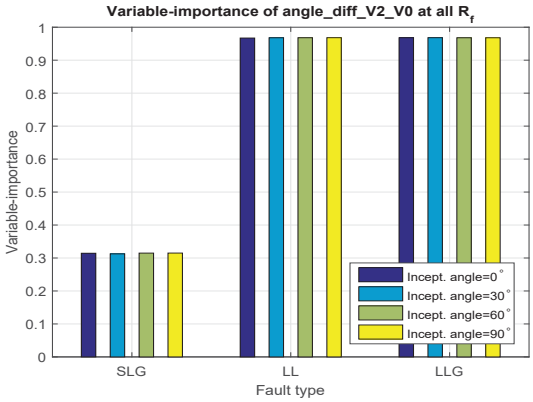

(c) Feature of $\theta_{V_2} - \theta_{V_0}$

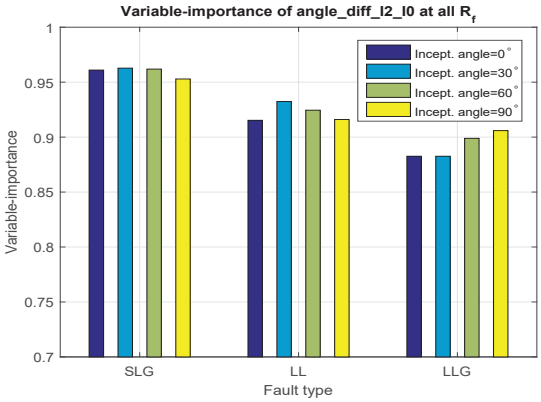

(d) Feature of $\theta_{I_2} - \theta_{I_0}$

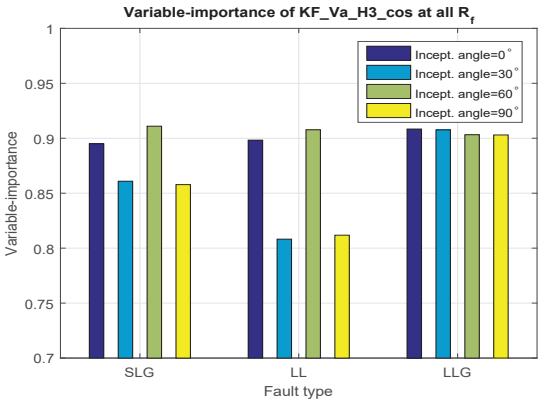

(e) Feature of $KF\_V\_cos\_H3$

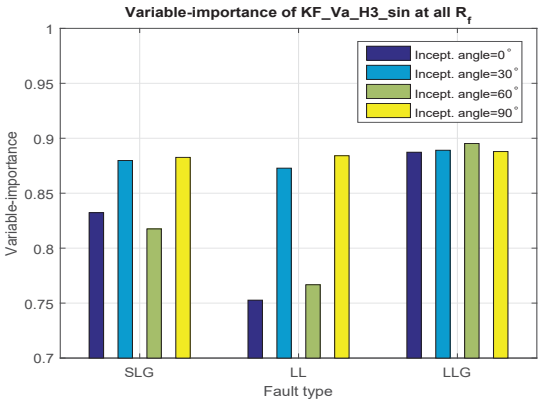

(f) Feature of $KF\_V\_sin\_H3$

Fig. 4.6 Variable-importance of all features at different fault inception angles.

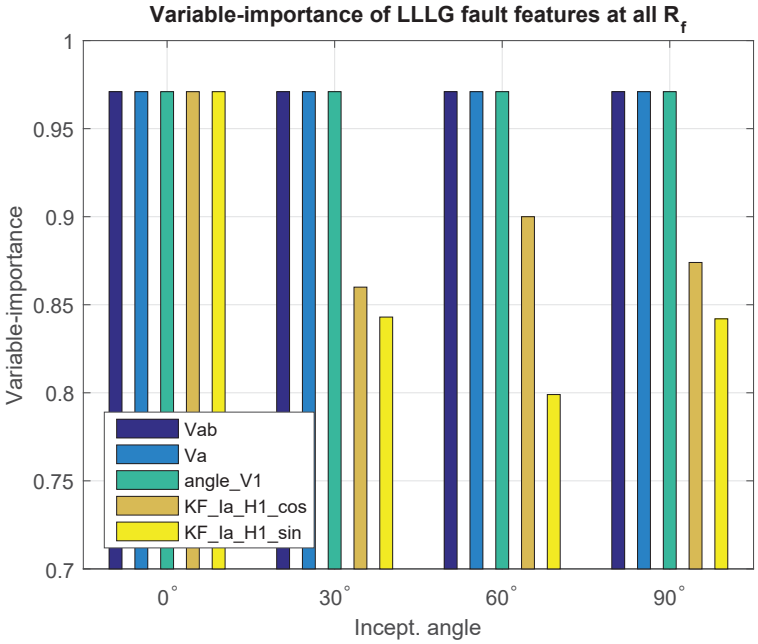

Fig. 4.7 Variable-importance of LLLG fault features at different fault inception angles.

It is seen that in general, the fault inception angle is not a significant factor that can perturb variable importance. The angles of 30°and 60°may result in a subtle decrease in the variable of importance of the KF estimated third harmonic, but the change is limited. For a three-phase fault, the first order harmonic components of current estimated by KF have a performance drop in non-zero angles.

4.5.3 Fault Location Variations

The variable-importance of the features in EFS is presented at three fault locations (refer to Appendix A.1):

- Location 1: Fault near Bus B-3;
- Location 2: Fault near Bus B-11;
- Location 3: Fault near Bus B-19;

The result is demonstrated in Fig. 4.8, including all fault impedance in Section 4.5.1 and all fault inception angles in Section 4.5.2. As indicated from this figure, the feature of negative sequence current keeps being unaffected at each location, however, the negative sequence of voltage is so low at location 1 and 2 that the variable of importance becomes

very low. The reason for that is the strong voltage source from the substation is ideally balanced; therefore the negative sequence voltage deviation contributed from the HIF is weak. At location 3, since it is far from the substation, the negative sequence voltage becomes a good HIF indicator again. To a negligible extent, it is similar for the variable of importance performance of other features that the further the fault location is, the less compromised the features are.

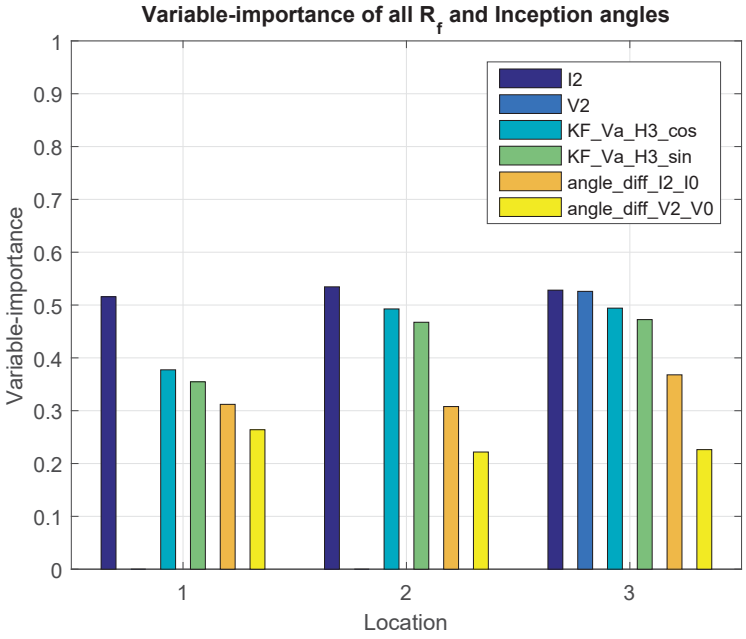

Fig. 4.8 Variable-importance at different fault locations.

4.6 Pattern Recognition Based HIF Detection Method

The proposed HIF detection method follows the flow chart in Fig. 4.9. It comprises three parts: data collection, feature selection and determination of classifiers. Data collection is also viewed as training as in other pattern recognition based methods. In this chapter, HIFs are applied to the types of single-line-to-ground fault, line-to-line fault, line-to-line-to-ground fault and three-phase fault at different locations and/or with different fault impedances along the benchmark distribution feeder. Non-HIF events contain normal operating conditions, capacitor switching and loading switching. Moreover, this chapter

investigates the HIF pattern in three types of distribution systems (explained in Section 2.4.2) before coming up with the EFS.

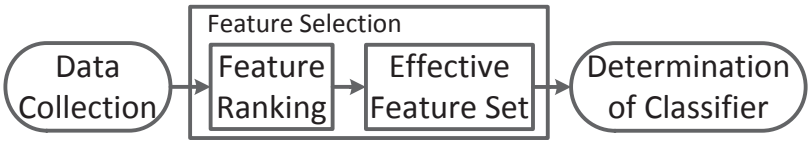

Fig. 4.9 The proposed pattern recognition flow chart of HIF detection.

The details of feature processing will be mentioned in the next subsection. The third part in Fig. 4.9 is about the selection of classifiers that can achieve the best performance in accuracy, dependability and security. Besides pre-programming the selected classifier model into the HIF detector after learning the entire dataset at once (this is called batch learning), one could as well design the HIF detector that is capable of online machine learning. It means that the HIF detector receives the current and voltage signals in a sequential order and updates its prediction model (classifier) at each step. Thus, the proposed method explores classifiers of batch learning and online learning.

4.6.1 Testing Results

The benchmark system is shown in Appendix A.1. Two distributed generators (DGs) can be connected at location A and B respectively. Three types of distribution systems can be therefore modelled: (1) The synchronous generator (SG) based system is developed by connecting an SG to location A and no DG at location B; (2) The inverter-interfaced system is with only type-4 wind turbines at location A and no DG at location B; and (3) The hybrid DG system has a SG connected at location A and wind turbine generators at location B. The proposed method is tested in grounded SG-based systems, inverter-interfaced systems, and hybrid systems, with the 246 features (discussed in Section 4.3) implemented. 1944 HIF events and another 1944 non-HIF events (they may not be necessary with the same number) are simulated for the training and feature processing. The types of testing events are similar to those of training events, but the events are different (either at different locations or with different parameter values). There are totally 972 HIF and 972 non-HIF events in the testing in the aforementioned three types of distribution systems. The detection performances are tested firstly with the full feature set and then with EFS. In addition, five classical classifiers (Naive Bayes, Support Vector Machine, k-nearest neighbour, J48

and random forest) from Weka [138] are compared in order to find the best classifier. The performance results with full features available are shown in Table 4.6, while the results with proposed EFS are shown in Table 4.7, where the accuracy is defined as the ratio of the number of correctly classified events to the total number of events, dependability index (DI) is the ratio of the of detected HIF events to the total number of HIF events and security index (SI) is the ratio of the of detected non-HIF events to the total number of non-HIF events. To limit problems such as over-fitting and inaccuracy in prediction, each classifier model in Table 4.6 is acquired through 10-folder cross-validation.

Table 4.6 Batch learning performance of HIF detection with the full feature set.

Classifier	Accuracy (%)	DI (%)	SI (%)
NaiveBayes	86.7	86.1	87.4
LibSVM (Gaussian kernel)	76.3	69.1	80.8
k-nearest neighbour	97.6	97.6	97.6
J48	99.0	99.0	99.0
RandomForest	99.1	99.0	99.1

Table 4.7 Batch learning performance of HIF detection with the effective feature set.

Classifier	Accuracy (%)	DI (%)	SI (%)
NaiveBayes	80.3	76.8	82.9
LibSVM (Gaussian kernel)	93.7	93.6	93.9
k-nearest neighbour	98.6	98.6	98.6
J48	99.1	99.1	99.1
RandomForest	99.1	99.1	99.1

The proposed EFS and HIF detection method are tested in four online machine learning classifiers as well. Table 4.8 and 4.9 demonstrate the online machine learning performance of the proposed HIF detection method with full and effective feature sets, respectively. The mean DI and SI are calculated and listed in the two tables.

Table 4.8 Online learning performance of HIF detection with the full feature set.

Classifier	Mean DI & SI (%)
Naive Bayes	89.9 & 97.9
Online Accuracy Updated Ensemble	98.6 & 89.9
Hoeffding Adaptive Tree	97.9 & 98.6
k-nearest neighbour	83.8 & 97.9

Table 4.9 Online learning performance of HIF detection with the effective feature set.

Classifier	Mean DI & SI (%)
Naive Bayes	80.4 & 95.7
Online Accuracy Updated Ensemble	97.0 & 80.4
Hoeffding Adaptive Tree	95.7 & 80.4
k-nearest neighbour	96.9 & 97.0

4.6.2 Discussions

According to the batch learning testing results, the proposed method with the EFS has similar performance as the one with the full feature set. Therefore it comes to the conclusion that the EFS requires a very small number of signal channels without compromising the overall detection performance. At the same time, tree-structured classifiers such as J48 and random forest present much better performance over other classifiers in batch learning. The online learning result tables reveal the fact that the number of detection features does affect the performance of the classifiers. However, the classifier of k-nearest neighbour shows a satisfactory performance with the EFS, which is almost as good as the best performing classifier Hoeffding adaptive tree when detecting with full feature set.

4.7 HIF Detection Logic

Inspired by the tree structure of the machine learning classifier model, the author further explores the decision tree structures. A HIF detection logic, based on the previously identified EFS, is proposed. Statistically, since three-phase faults take up only 2%-3% of the

fault occurrences [139], a HIF detection logic is designed in this regard for unbalanced HIF only. As for LLLG type HIFs, a simple and feasible logic pattern is difficult to generalize after observing and analyzing the obtained decision tree structures. Therefore a decision tree based classifier model is recommended for the detection of three-phase balanced HIF – although relatively rare.

The proposed HIF detection logic is targeted to be implemented in a microprocessor based digital relay. Similar to conventional digital relays, the proposed relay technique takes the voltage and current signals as its input. In addition, DFT and KF are required for corresponding feature extraction. Before the explanation of the proposed HIF detection logic, the logic circuit is presented first in Fig. 4.10.

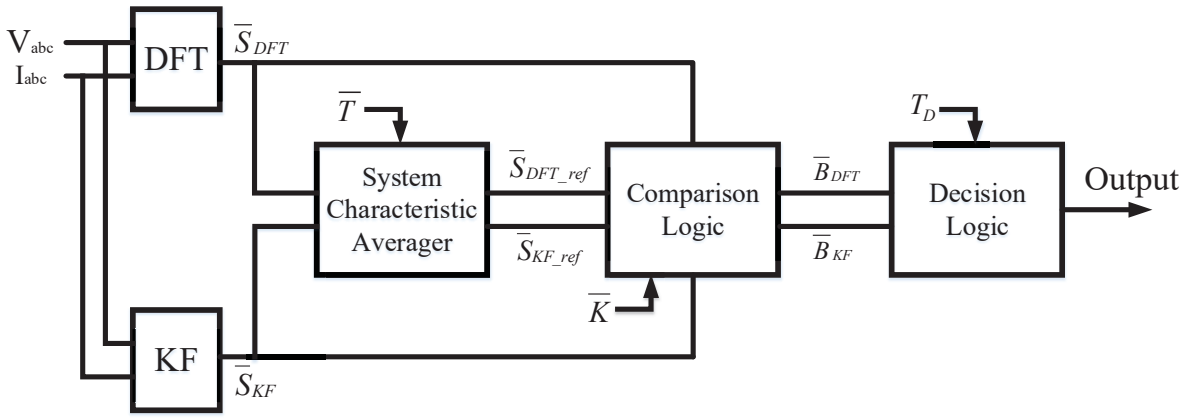

Fig. 4.10 The proposed HIF detection logic.

As indicated in the detection logic, three-phase voltage and current signals are sent to DFT and KF for feature extraction. The utilized features are based on the EFS explained in Table 4.5 in Section 4.3.4. Therefore, the extracted instantaneous signals after the DFT and KF blocks are:

$$\bar{S}_{DFT} = \{s_1, s_2\, s_3, s_4\} = \{V_2, I_2, \theta_{V_2} - \theta_{V_0}, \theta_{I_2} - \theta_{I_0}\} \tag{4.3}$$

$$\begin{aligned} \bar{S}_{KF} &= \{s_5, s_6, s_7, s_8, s_9, s_{10}\} \\ &= \{KF\_V_a\_cos\_H3, KF\_V_b\_cos\_H3, KF\_V_c\_cos\_H3, KF\_V_a\_sin\_H3, \\ &\quad KF\_V_b\_sin\_H3, KF\_V_c\_sin\_H3\} \end{aligned} \tag{4.4}$$

4.7.1 System Characteristic Averager

The System Characteristic Averager has a memory that stores the signals for a predefined duration of $\bar{T} = \{t_1, t_2, t_3, t_4, t_5, t_6, t_7, t_8, t_9, t_{10}\}$. In other words, $\bar{T}$ is the time constant that is a vector of ten elements associated with $\bar{S}_{DFT}$ and $\bar{S}_{KF}$. To avoid signal spikes, a limiter is implemented for each signal channel. Meanwhile, the time constant $\bar{T}$ is set according to the system characteristics of each individual signal. A small t_i $(i = 1, 2, ...10)$ can avoid severe step change of signal but a large t_i costs more data storage and computational efforts. The output of the System Characteristic Averager block provides the reference value s_{i_ref} $(i = 1, 2, ...10)$ for the Comparison Logic. A reliable average value is a prerequisite to successful detection.

4.7.2 Comparison Logic

The block of Comparison Logic is depicted in Fig. 4.11. Based on the feature extraction technique discussed in Section 4.3, the extracted instantaneous signal s_i can be understood as the system background signal superimposed by the extra signal contributed from the HIF behaviour. The comparison is therefore made between the extracted instantaneous signal s_i and its reference value s_{i_ref}.

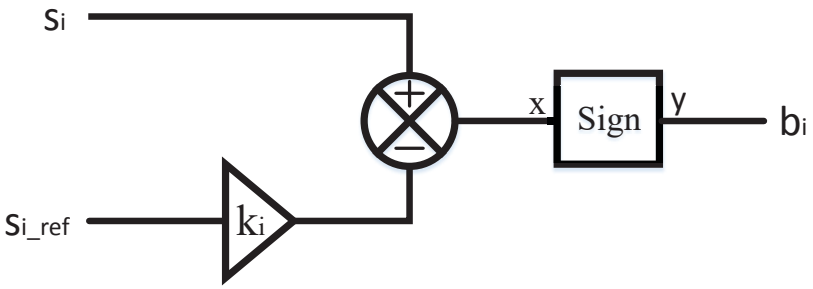

Fig. 4.11 Comparison Logic in the proposed HIF detection logic.

The sensitivity gain of k_i is incorporated in order to 1) set the margin of detection and 2) add a handle to the detection sensitivity. Where the undefined parameter of $\bar{K}$ stands for:

$$\bar{K} = \{k_1, k_2, k_3, k_4, k_5, k_6, k_7, k_8, k_9, k_{10}\} \tag{4.5}$$

After the summation block in Fig. 4.11, a Sign function is employed to provide the following decision making:

- When $x > 0$, $y = 1$;
- When $x \leqslant 0$, $y = 0$.

The output of the comparison logic is the comparison assertion bit of b_i $(i = 1, 2, ...10)$, the $\bar{B}$, which is the input to the decision logic.

4.7.3 Decision Logic

The decision logic, as shown in Fig. 4.12, is the execution part of the HIF detection logic.

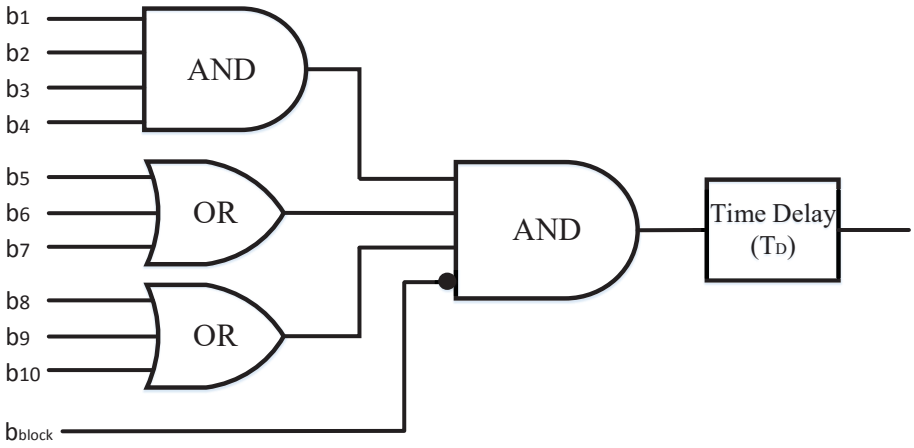

Fig. 4.12 Decision Logic in the proposed HIF detection logic.

The AND gate before the time delay has four inputs:

1. The ANDed signal of all four DFT-based assertion bits. If any of the four signals are not asserted, the decision logic will not trip.
2. KF-estimated in-phase components of third harmonic voltage. If none of the three-phase in-phase components of third harmonic estimated from the KF gets asserted, the decision logic will not trip.
3. KF-estimated in-quadrature components of third harmonic voltage. If none of the three-phase in-quadrature components of third harmonic estimated from the KF gets asserted, the decision logic will not trip.
4. The blocking bit b_{block}. If this bit is 1, the detection logic is blocked and none of HIF events can be detected; if this bit is 0, HIF detection is enabled.

A time delay of T_D is implemented. The appropriate selection of T_D can effectively avoid the false tripping resulting from normal switching, which might contribute to third harmonics.

4.8 Conclusions

The pattern recognition based method is conducted for each and every system separately with different training and testing sets, similar to other pattern recognition methods in Section 1.1.3 . Conventional relays are widely used for their universality; however, they have their own limitations on detecting HIFs (dependability and security performance issues). On the other hand, the proposed pattern recognition method demonstrates an excellent HIF protection performance for a specific system based on Table 4.7 and 4.9 , given the fact that machine learning and big data processing capability will no longer be a problem in the future.

The EFS has included critical features that are capable of differentiating HIF and non-HIF events in distribution systems with different groundings and DER technologies. The features in the EFS originate from engineering estimation method of Kalman filter and signal processing technique of discrete Fourier transform, therefore it is simple and reliable in power system protection. The results show as well the possibility of an online learning HIF detector. The embedded classifier model could learn incrementally at each step to detect any HIF that it has learned in the past.

Chapter 5

Real-time Hardware-in-the-loop Validation

5.1 Introduction

The development of real-time digital simulators has made HIL testing accessible. An HIL simulation is often used to minimize the risk of investment through the use of a prototype once the underlying theory is established through a real-time simulator [140]. This cost-effective technique brings protection engineers and researchers the following benefits [141]: 1) rapid simulation speed for large grid network studies; 2) automated repetitive testing in a variety of normal and disturbance conditions and 3) protection algorithm development and evaluation.

This chapter demonstrates the real-time HIL setup of the proposed multifunction IR in Chapter 2 and the NDZ reduction methodology in Chapter 3. Since the results of the former method are already shown in Section 2.4, the rest of this chapter focuses on the method of generating HIL-based islanding intelligent relay (IIR) logics – a real-time HIL method derived from Chapter 3, concentrating on the hardware-based NDZ reduction.

5.2 Real-time HIL Simulation Setup

With a real relay connected in the simulation loop, the proposed intelligent islanding relay (IIR) can be implemented and validated through hardware experiment. On the other hand, the advantages of the real relay can be fully explored. The generated IIR logic can be

programmed into any existing proprietary numerical relay. In addition, GOOSE function inside such a relay is utilized for IED (Intelligent Electronic Device) communication, which makes the integration of the proposed method with electric substation automation systems easy.

This section describes the laboratory hardware and software setup of the proposed method. The present section includes three parts: the HIL setup, the relay logic implementation and the detection performance acquisition using IEC 61850 Communication Protocol.

5.2.1 HIL Setup

The proposed method is implemented on a real-time platform. A real-time digital simulator and a digital relay are required. The electric network is emulated on the real-time simulator. The simulator employed in this study is equipped with a Xilinx ML605 board for analog signal outputs. The analog signals of three-phase currents and voltages at the target DG location of the distribution feeder are sampled and sent through a band cable from the simulator's analog I/O card. The other end of the band cable is connected to the calibrated input interface of the main board of the digital relay. This interface is called low-level test interface, which bypasses the relay's internal transformer and is accessible by removing the relay front panel [142]. The real-time simulator's analog output has a voltage range of $\pm$16V. For each phase at a particular DG connection bus, there are two channels, one for voltage and the other for current. Therefore at one DG location, six wires are required to transmit the signals. Those wires should be connected to the relay by respecting the low-level test interface connector configuration. Besides, before setting the CT and PT ratios of the relay, the scale factors for input module need to be calculated properly according to input channels, input channel nominal rating, input values and corresponding output values. This information can be found in the manual of the relay. In order to acquire a reliable and accurate detection time, both the real-time simulator and the commercial relay are connected to one local area network (LAN) through a network switch using Ethernet cables. The above setup contains the electrical layer of the HIL simulation in a laboratory environment. Its functional diagram is illustrated in Fig. 5.1 (a).

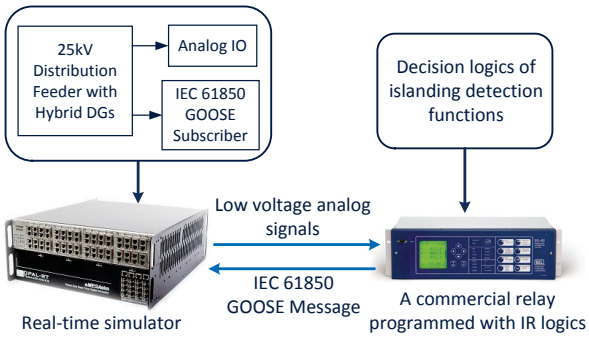

(a) Hardware-In-the-Loop functional diagram

Protective Relay	Setting	Time Delay
Over Frequency	60.5 Hz	100 ms
Under Frequency	59.7 Hz	100 ms
Over Voltage-I	>1.2 pu	100 ms
Over Voltage-II	1.1 pu-1.2 pu	500 ms
Under Voltage	<0.8 pu	100 ms

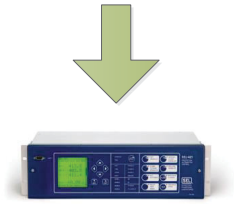

(b) Standard relay logic setting

Fig. 5.1 HIL functional diagram and standard relay logic settings

5.2.2 Relay Logic Implementation

Relay logic functions are programmed into the relay using available word bits, timers and basic logic functions. The relay logic functions contain two parts: standard islanding protective relay functions and IIR function. The standard relay functions are enabled and set according to Fig. 5.1 (b) using the built-in elements of over/under frequency and voltage. The protective logics are programmed in the Protection Free-Form Logic Settings in AcSELerator QuickSet [143]. As shown in Fig. 5.1 (b), the relay's measured system frequency and voltage values are stored in two variables. Along with the other predetermined threshold values, these two variables are stored in the Protection Math Variable (PMV). These PMVs are then built through logic operators to represent each standard element. Time delays in the relay logic setting of Fig. 5.1 (b) are realized by the timer function and the timer provides an output of the established relay elements.

On the other hand, IIR function originates from the decision tree (DT) logics by applying the proposed method (described in Section 5.3). The obtained DT logics are programmed into the digital relay using the available elements and logic operators. The output of standard relay functions and IIR is assigned to particular variables of the relay for displaying and tripping output. For example, relay logic variable PSV01 (Table 5.1) represents the first Protection SELogic Variable (PSV). It is used to monitor time keeping status of

assigned function – intelligent relay corresponding to PSV01.

5.2.3 Performance Acquisition Using IEC 61850 Communication Protocol

IEC 61850 communication protocol is utilized in this HIL application for transmitting the trip signal. GOOSE is one of the IEC 61850 protocols that define the communication rules among IEDs in electric substation automation. Utilizing of GOOSE adds a practical dimension of IIR implementation in modern distribution systems. Benefits of using GOOSE are listed as follows: 1) Provide standard storing/transferring/exchanging data packages from the proposed relay for event recording and future analysis, 2) Potential of relay-relay or relay-substation communication and coordination and 3) High interoperability of devices from different vendors.

Data acquisition of the proposed method is realized through appropriate setting of hardware devices and various GOOSE message blocks. An Ethernet switch is employed to connect the host computer, the relay and the real-time simulator for information exchange using GOOSE message in this application. Once an islanding event occurs and the relay detects it, a tripping signal associated with the programmed relay function output gets asserted. As shown in the first column of Table 5.1, certain PSV (as programmed in Fig. 5.1 (b)) becomes asserted if its logic equation is satisfied. Meanwhile, a GOOSE message with the updated status becomes available in the LAN. This GOOSE message is from a GOOSE publisher and contains information such as element status and tripping time. The output of GOOSE subscriber will follow the relay logic output PSV if the GOOSE subscriber gets correctly configured through an IED Capability Description (ICD) file. The ICD file not only defines the complete capability of an IED (here it is the protective relay) but also assists on establishing control signal tailored for GOOSE message communication by utilizing the specified multi-cast address and identifier of the IED. Meanwhile, the subscriber in the simulation model of the simulator interprets the GOOSE messages according to the ICD file obtained from the IED.

Fig. 5.2 shows the relay real-time simulation performance recorder. It comprises of an IEC61850 GOOSE Subscriber and Publisher as well as other logic controllers. The output of the subscriber (shown in the second column of Table 5.1) is associated with the assigned PSVs. Followed by a flip-flop after each subscriber port, the output of the performance recorder, in other words, the status of monitored functions, is stored in a separate file for

Table 5.1 An example: relay variables of relay function output

Relay Logic Variable	GOOSE Subscriber Output Port	Function
PSV01	Ind01	Intelligent Relay
PSV14	Ind14	OUF
PSV15	Ind15	OUV
PSV16	Ind16	Standard elements (PSV14 OR PSV15)

further result processing, for instance, plotting NDZs and other associated performance indicators. The triggering control of file writing block helps saving data storage space.

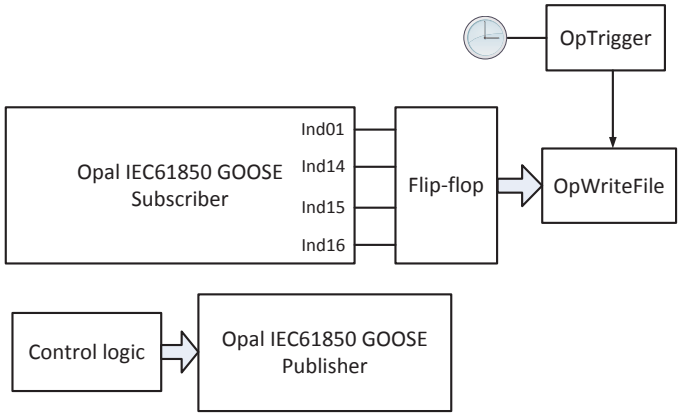

Fig. 5.2 Relay real-time simulation performance recorder.

5.3 Method for Generating HIL-based IIR Logics

The proposed method starts by identifying the targeted DG location, and is followed by three core stages (indicated in Fig. 5.3), namely: A) Defining the boundary limits of the NDZ, B) Creating IIR training database and C) Training and testing of IIR. The output of stages A and B is the IIR training database. Lastly, in stage C, the generated IIR detection logics are tested and verified using a real digital relay for further analysis and performance comparison with standard relay functions. The three stages are explained in details as follows.

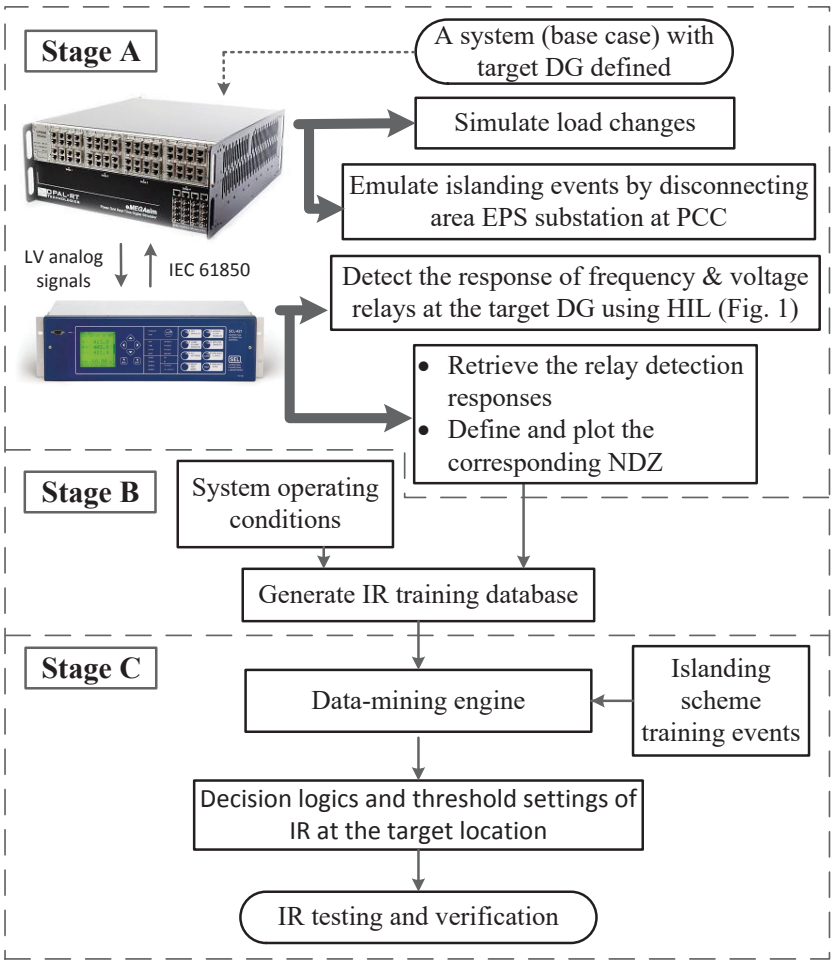

Fig. 5.3 Method for creating HIL-based IIR with reduced NDZ

5.3.1 Defining the Boundary Limits of the NDZ (Stage A)

The boundary limits of NDZ are determined by frequency and voltage functions under prescribed detection time and type of DER technologies. Therefore, a systematic method is required to define the NDZ boundaries taking into account various possible operating conditions and system configurations. The entire process is run in HIL environment so as to get an accurate NDZ area. A script of Python Application Programming Interface (API) that controls the simulations in the real-time simulator is created to automate all of the events.

As shown in Fig. 5.3 Stage A, once the target DG is specified, a load change is applied

to emulate the actual load change at the normal operating condition in a real system. Load change could be realized by a small increment or decrement in active and/or reactive power [119]. The smaller the change is, the more accurate the NDZ boundaries are, however, the computational cost gets higher. The next step is to emulate islanding events by disconnecting the area electric power system substation at PCC using a real-time simulator. Meanwhile, the frequency and voltage functions are monitored and recorded at the target DG location with a real commercial relay connected in the loop. The simulations are then continued until all of the possible operating conditions are covered in the course of defining the NDZ boundaries. After all of the operating conditions are simulated, the islanding detection responses of standard voltage and frequency elements of the relay are defined and plotted for the target DG. Subsequently, the NDZ boundary limits are defined and plotted, which is the output of Stage A. It also defines the critical operating conditions at the target DG location.

5.3.2 Creating IIR Training Database (Stage B)

The proposed approach for creating HIL-based IIR training database in order to minimize the produced NDZ is given in Fig. 5.3 Stage B. There are two factors that affect the power mismatch levels in an island: one is the daily variation of the feeder load and the other is the location of islanding formation. Feasible system operating conditions can be obtained from the daily load variation data. Whereas critical operating conditions are delimited by the NDZ of standard relay functions using the proposed method in the previous subsection. The two types of system operating conditions are defined in Section 3.4.2.

It should be noted that critical operating conditions are within the NDZ boundaries of standard relay functions (refer to Fig. 5.1 (b) for relay function settings). However, for non-critical operating conditions, their frequency and voltage deviations are large enough to be detected by standard relay functions. Once the above two types of conditions are identified, one can choose a good number of points within the system operating condition boundaries as the training sets.

5.3.3 Training and Testing of IIR (Stage C)

The third stage of the proposed method is the training and testing of HIL-based IIR. The islanding response data at the target DG location is captured accordingly under all types of

islanding and non-islanding training events, such as CB opening, faults with CB tripping, load adding, load shedding, fault with load shedding, capacitor switching, etc. [144], to adapt for more realistic events than only CB open event seen in the NDZ plot. The following islanding events are included: 1) all possible tripping of circuit breakers that are liable to assume the conditions of islanding formation; 2) islanding formed in the area EPS transmission system; 3) events that could trip all breakers and reclosers that could island the DG under study; 4) faults on the PCC bus with instantaneous and delayed fault clearing times.

12 IIR features (see Appendix Section A.7 for details) are proposed in this IDM. The feature of the rate of change of frequency over reactive power is included as well according to [145]. The resulting database is then processed by a data-mining engine [118], which generates an optimized DT. A DT is a hierarchical model for supervised learning where the local region is identified in a sequence of recursive splits in a smaller number of steps [112]. This section employs classification trees, where Gini index [113] is used as the impurity measure to quantify a good split in the DT based classification technique.

In IIR testing, operating conditions are tested in a larger range than in IIR training and in more islanding and non-islanding events. The generated DT is the islanding detection logics and threshold settings which can be implemented in a real-time environment and programmed into a real digital relay. Thus, performance verification of HIL-based IIR is made possible in the HIL environment. Relay performances in terms of islanding detection time, dependability and security index (DI/SI), as defined in [110], can be obtained. In addition, performance comparison with real standard relay functions can be therefore conducted.

5.4 Case Study and Result Analysis

The benchmark system can be found in Appendix A.1. In this section, standard islanding protective functions and IIRs are implemented at the high voltage side of the DG transformer (see R_1 and R_2 in Fig. A.1), according to standing standards, operating practices and protection coordination requirements [120], [146]. The feasible system operating conditions are defined between 36%-96% of total system loading. Using the benchmark system stated in the previous section, 360 power mismatch conditions are simulated to describe overall system operating conditions. For the IIR training database of the benchmark sys-

tem, 11 system operating conditions are chosen according to Section 5.3.2. Each operating condition are consistently trained under 34 events (8 islanding events and 26 non-islanding events). Therefore it sums up to 88 islanding and 286 non-islanding events in total. The training events are located at CB-1, 3, 6 and 8 as shown in Fig. A.1). For each CB location, there are CB opening as well as Fault with CB tripping events, therefore there are 8 islanding events associated with each operating condition. The obtained HIL-based DTs at two target DG locations are shown in Fig. 5.4.

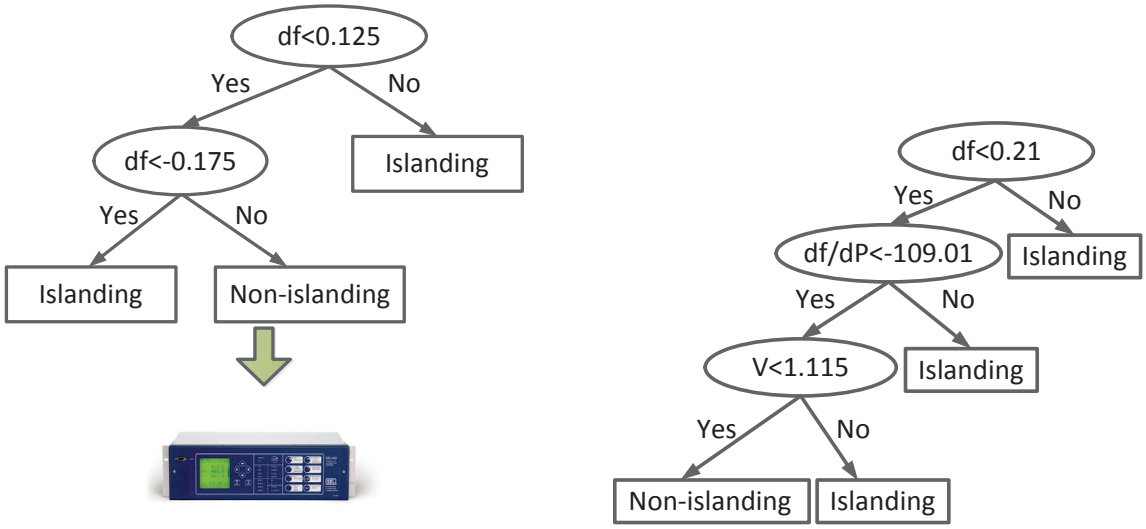

(a) At location R_1 (PCC of SG) (b) At location R_2 (PCC of WF)

Fig. 5.4 Decision logics of IIR

The HIL experimental NDZs of standard relay functions (real relay) are shown in Fig. 5.5 (a) for location R_1 and Fig. 5.5 (b) for location R_2. The NDZs of Simulink modeled IIR are shown in Fig. 5.5 (c) for location R_1 and Fig. 5.5 (d) for location R_2. The HIL experimental NDZs of standard relay functions are delimited by the over/under frequency relay (O/UF) and over/under voltage relay(O/UV), which are marked near their associated boundaries respectively in Fig. 5.5 (a) and (b). In addition, the cases that are detected by frequency relay (FR) and voltage relay (VR) are marked differently as shown in the figure. It can be seen that the HIL experimental NDZ of standard relay functions at R_1 is larger than the one at R_2. The voltage response tends to deviate more at the PCC of WF than SG. The NDZs of Simulink modeled IIR at R_1 and R_2 represent a significant change in NDZ areas — IIR trips in a larger area in the ΔP-ΔQ space than standard relay functions

which can be seen in Fig. 5.5 (c) and (d).

According to the available digital relay word bits of the digital relay, IIR logic in Fig. 5.4 (a) is implemented in the digital relay logic. The HIL experimental NDZ results of IIR are shown in Fig. 5.6. This result also indicates a similar performance as in Fig. 5.5 (c). The resulting NDZ area is negligible. Meanwhile, the irregular NDZ shape reveals the non-ideal simulation environment due to the connection of a real digital relay in the closed loop. Results of islanding relay detection time are extracted from GOOSE messages. Table 5.2 reveals that by taking the average time of all detected cases (more in the proposed IIR than in standard relay function, out of 70 testing islanding cases), the detection time of standard relay functions and proposed IIR are 0.588 second and 0.425 second respectively.

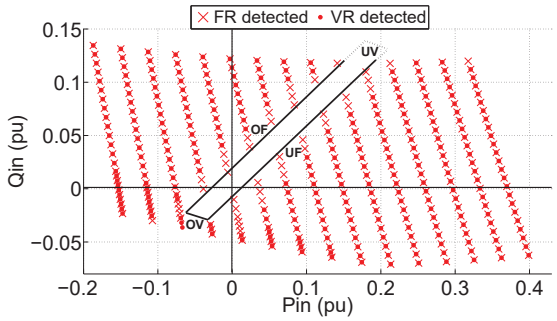

(a) HIL experimental NDZ of standard relay functions at R_1 (PCC of SG)

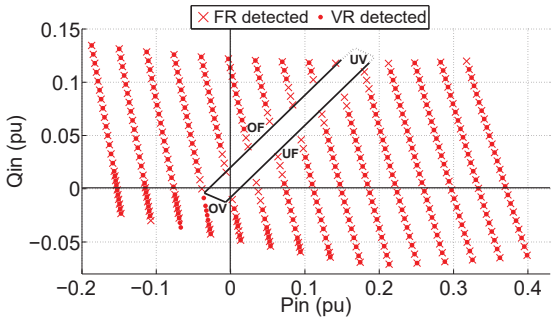

(b) HIL experimental NDZ of standard relay functions at R_2 (PCC of WF)

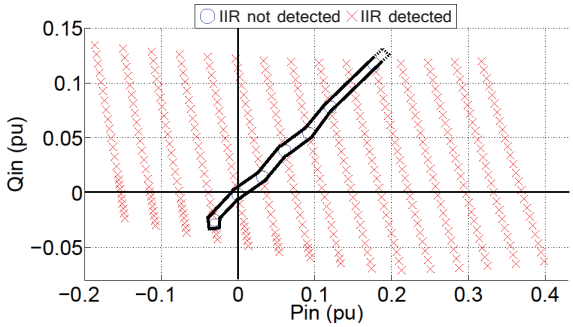

(c) NDZ of Simulink modeled IIR at R_1 (PCC of SG)

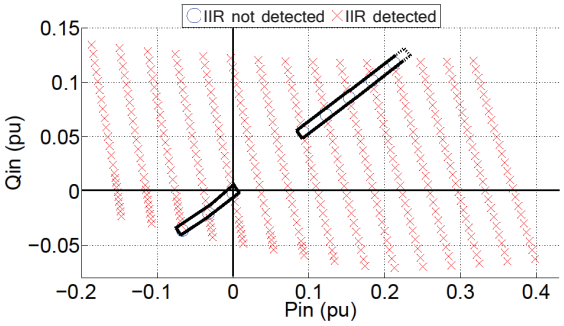

(d) NDZ of Simulink modeled IIR at R_2 (PCC of WF)

Fig. 5.5 HIL experimental NDZ results of IIR

In order to quantify the NDZ performance graphically, the concept of NDZ area ratio R_{NDZ} is utilized again as explained in Section 3.3. It simply calculates the ratio between the area of NDZ and the area of all operating conditions.

Table 5.2 Performance comparison of the proposed approach

Relay function	Percent of detected cases	Detection time
Standard relay functions	77.1%	0.588
The proposed IIR programmed in SEL relay with HIL	97.1%	0.425

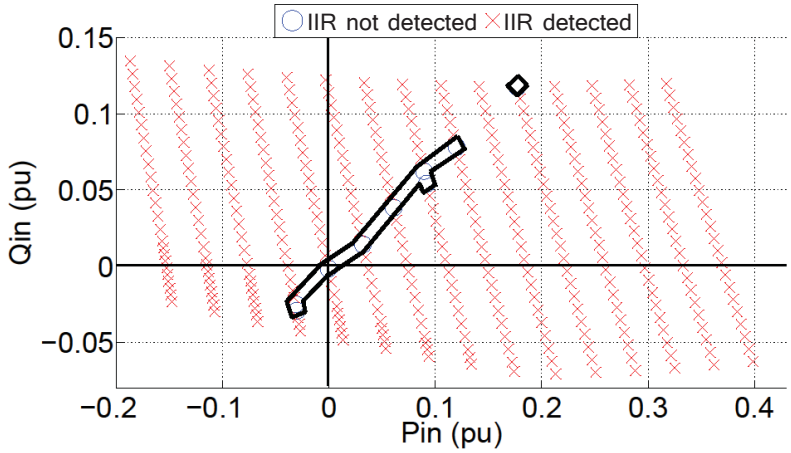

Fig. 5.6 HIL experimental NDZ of IIR at R_1 (PCC of SG)

The proposed IIR logics are tested and compared with standard relay functions. Fig. 5.7 shows the R_{NDZ} values of standard relay functions and the proposed IIRs at different target DG locations according to Figures 5.5. This table indicates that the NDZ areas of the proposed IIR decreased from 6.24% to 2.9% for SG and from 5.46% to 2.55% for WF, comparing to standard relay functions. When tested in HIL, the IIR result is even better, only 1.91% of the entire area is not covered. Note that N/A here results from the fact that some of the features in Fig. 5.4 (b) are not supported by this digital relay.

In the case study of this chapter, 5 operating conditions within the critical area of NDZ obtained from standard relay functions are randomly selected, and 10 operating conditions are randomly chosen within the non-critical area of NDZ. For each operating conditions, 54 events, which include 8 new islanding events and 46 new non-islanding events, are tested. In sum, there are 120 islanding events and 690 non-islanding events tested under different levels of system operating conditions and scenarios.

The benefits of using HIL setup compared to the Simulink one are 1) higher simulation

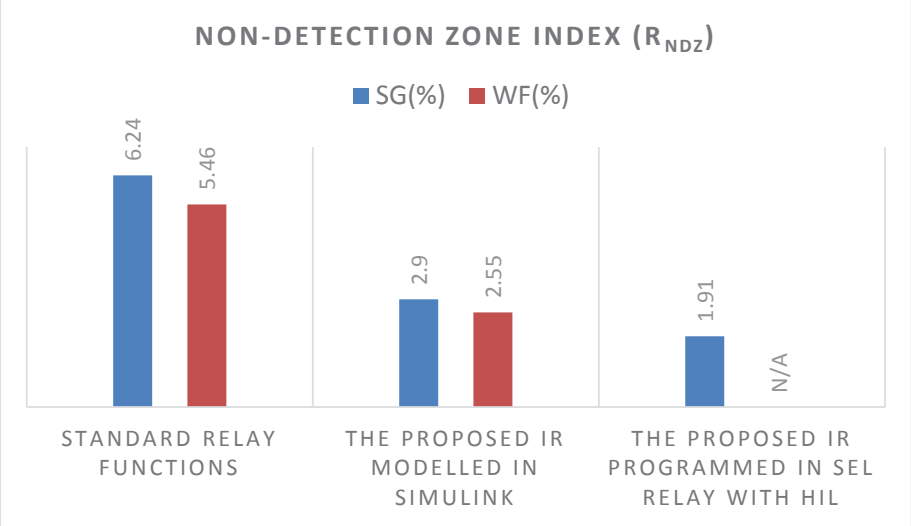

Fig. 5.7 Non detection zone area comparison

speed and therefore better fitting into machine learning method, 2) added value of real relay connection, implementation and validation.

The dependability and security test results of the standard relay functions, the proposed IIR and the HIL-based IIR are provided in Table 5.3. It is seen that the proposed IIR is exhibiting a higher DI/SI than standard relay functions, whose results are obtained from HIL experiments. IIRs at the WF PCC show a similar performance as ones at SG. From the perspective of standard relay functions, they are less dependable than the proposed IIRs, while their SI represents an undesirable nuisance tripping behaviour at both locations.

Table 5.3 Relay performance comparison at two DG locations

Device		@R_1 (%)	@R_2 (%)
Standard relay functions	DI	96.7	95.8
	SI	88.7	88.3
The proposed IIR modelled	DI	98.3	98.3
in Simulink	SI	94.2	94.8
The proposed IIR programmed	DI	99.2	N/A
in SEL relay with HIL	SI	95.5	N/A

5.5 Conclusions

This chapter proposed a real-time HIL based IDM to minimize the NDZ by adding a realistic dimension. This method employs decision-tree-learning algorithm to detect and differentiate islanding and non-islanding events, meanwhile, with the help of real-time simulator, defining the NDZ boundary, generating IIR logics, training and testing the IIRs can all become efficient. Consequently, the proposed method gets well fitted into the context of pattern recognition based method, making it more realistic and applicable in massive and complex training/testing scenarios. The generated HIL-based IIR logics are validated to be effective in reducing NDZ areas. Numerically, the NDZ area ratios drop by more than 53% in both DG locations. Moreover, a hidden advantage of the proposed NDZ reduction method is its universality to both DG technologies due to the pattern recognition nature. Besides, testing results show that the proposed method has also achieved a superior dependability and security performance as evidenced in Table 5.3. The combination of real-time HIL simulation and advanced pattern recognition algorithm have been proved to be a prosperous technique that takes full advantage of the real-time simulator's computational capability on a large amount of simulations and the HIL technique.

The proposed IIR shows promising dependability and security besides a reduced NDZ, however, the proposed method is limited by the network modeling and real-time simulation techniques. On the other hand, extensive field tests and fault recorder data would be considered and applied in the future work to compare the simulations with real-world conditions, and to see the efficacy of the proposed pattern recognition methodology under field data.

Chapter 6

Summary and Conclusions

6.1 Thesis Summary

The goal of this thesis is to address DER interconnection protection problems with the integrated renewable energies. As observed from practical applications, conventional relays have difficulties in detecting islanding and high impedance fault events in some circumstances. Particularly, with a deep penetration level of DERs, new distribution network behaviours, different from the ones in conventional networks, arise, such as: limited fault current contribution, bidirectional power flow, intermittent availability of renewable energy, low system inertia and the advanced DER function modes and grid code requirements. Consequently, a series of pattern recognition based intelligent protective schemes is proposed to address the DER interconnection issues in this background. The thesis defines the problems and scope in DER interconnection protection. The scope of this work is defined in two categories: islanding detection and protection of faulty distribution feeders.

Multifunction relay is not a new term for protection engineers, however, this thesis proposes a data-mining based intelligent protection method in modern distribution networks. The method includes problem identification, data preparation, data-mining detail and performance analysis. Importantly, the architecture of the proposed multifunction IR scheme is presented. The classification algorithm that utilizes Gini index to build the DTs is implemented in the proposed scheme. With Gini splitting criterion, DT firstly grows in its entirety, then trimmed in a bottom-up fashion to avoid over-fitting and pruned using cross-validation. The idea of big data is introduced to the intelligent relay's training and testing stages. To improve data utilization, the non-tripping events, differentiated

from islanding and fault events, are defined as non-tripping events and obtained at one attempt. Training and testing strategy is refined and combined for a better inter-function coordination possibility. The proposed multifunction IR scheme is simple and versatile. By extracting all necessary signals from a common bus, each function has its own detection logic. It can detect not only islanding but also identify different fault types. Furthermore, the fault IR logic is supervised by the FRT selective blocking logic which effectively avoids false-tripping and coordinating with inverters' FRT function.

To improve the utilization, assimilation and recognition of simulation data and elevate the islanding detection performance in the most challenging scenarios — small active and reactive imbalance at the point of disconnection, an NDZ reduction methodology is proposed. Through the study of NDZ behaviour in the synchronous generator and inverter-interfaced distribution systems, the limitation of conventional standard relays is characterized. This limitation is quantified and plotted as the preparation of the proposed methodology. Traditional data-mining based methods do not address the islanding problem utilizing the NDZ plane or just equally distribute the data training selection, however, this methodology defines critical operating condition and non-critical operating condition, then allocate training effort accordingly. During IR training, different DER technologies, advanced inverter functions and topological changes of distribution networks are integrated. The concept of non-detection zone area index is introduced here to quantify and evaluate the performance of IRs and standard relays. Moreover, in the discussion section, the proposed methodology is horizontally compared with three other intelligence based methods from literature. Comparison is performed in terms of signal measurement, number of features, DI and SI, simulation event and DER type and hardware realization.

HIF has been a challenging task to detect in distribution networks. To capture the randomness and irregularity of this certain type of fault, a two anti-parallel dc-source model is implemented with proper HIF model settings. The fault waveform and V-I characteristics are validated by other work. A large candidate feature pool is created. The proposed feature selection method utilizes information gain and minimum description length to evaluate the variable-importance of each feature. The acquired top features are named as EFS in this thesis. Through fault scenarios analysis, the EFS presents a satisfied performance under different fault impedance, fault inception angle and fault locations. The variable-importance scores of some features might drop during some scenarios: for instances, the angle difference between negative sequence and zero sequence voltage decreases when fault

impedance gets larger, or the negative sequence voltage that is affected by the substation voltage. However, the variable-importance of other features is very stable and reliable in the same scenario. The general performance is not compromised. A pattern recognition based HIF detection method is then proposed. The batch learning method is firstly validated to be an effective tool using the proposed EFS. Batch learning classifiers such as J48 and random forest achieve a larger than 99% performance in terms of accuracy, DI and SI. The dimension of online learning applicability of the proposed EFS is demonstrated as well. Using the k-nearest neighbour online classifier, the mean DI and SI reach 96.9% and 97.0% respectively. Besides, a simple and practical HIF detection logic is proposed according to the EFS. This detection logic utilizes DFT and KF for reliable feature extraction. Through the system characteristic averager, a reference feature value is obtained and then sent to comparison logic. Through the sensitivity gain $\bar{K}$, the summation block and the sign function, the assertion bit of a particular feature is set high or low. The EFS features are then ANDed with a delay to make the tripping decision.

One of the advantages of employing decision tree based pattern recognition method is its applicability through HIL. The hardware connection is realized through a real-time simulator that models the 25 kV distribution feeder with hybrid DGs, and a commercial relay that is programmed with IR logics. Meanwhile, since standard relay elements are available in the commercial relay, results comparison can be accomplished within the same run of simulation. Relay logic, either from the standard elements or from the IIRs, are programmed using the commercial relay's setting software. Simultaneously, the embedded GOOSE message function of the relay is sent from the message publisher to the subscriber. An HIL-based IIR with reduced NDZ is proposed. This method validates the proposed simulation-based NDZ reduction method from the hardware perspective. The corresponding NDZ, NDZ area index and detection time are therefore the results of real-world measurement. Practicality and applicability of the proposed islanding detection method are therefore validated.

6.2 Conclusions

Solutions to DER interconnection protection are proposed in this thesis using pattern recognition based intelligent relay schemes. It is concluded that:

- A pattern recognition based multifunction intelligent relay scheme is designed and

realized. This scheme successfully combines the training of islanding and fault events, reducing the training data set. The proposed multifunction IR scheme outperforms standard islanding and fault detection relays as indicated in the dependability and security indices. Meanwhile, the average detection time of the proposed detection scheme is much smaller than that of the standard relays. Cases that the DGs should "ride-through" are blocked during FRT tests. Fault types are well differentiated during fault type tests. HIL simulation validates the fault and islanding detection functions and shows the dimension of applicability.

- The proposed non-detection zone reduction methodology introduces the critical operating condition and non-critical operating conditions in the ΔP-ΔQ space. The IR training strategy is designed according to the non-detection zone results, independent from DER control and interconnection technologies. Therefore the decision making efficiency is improved, so are the utilization, assimilation and recognition of the simulation data. Indicated by the testing results, the NDZ area ratio is greatly reduced while the DI and SI are increased. Through the comparison with other methods, the proposed methodology demonstrates its feasibility in various event and DG types. The hardware realization is proved to be superior to other methods.
- The proposed high impedance fault detection features are selected through advanced attribute selection technique from a large feature pool. The combination of features under balanced and unbalanced faults are original features to HIF detection. Utilizing these simple and practical features, the proposed HIF detection logic is effective in detection HIF events and capable of avoiding malfunctioning. Furthermore, the proposed logic can detect HIF occurring at any location and with a wide range of fault impedance in various type of distribution networks.

6.3 Recommendations for Future Work

Based on the established methods, contributions and conclusions, the following areas of interest are recommended in the future work:

1. Big-data based deep learning for distribution network protection with a large amount of DER integration. The major issues of distribution networks with deep DER penetration, including advanced inverter functions, complex topological change and the plug-and-play of DGs, are expected to be resolved by this advanced algorithm.

Big data obtained from IEDs is facing challenges including storage, analysis, search, sharing, transfer, visualization, querying, updating and information privacy. The big data analysis can shed new light on fault detection and network behaviour prediction.

2. The inclusion of other functions to the multifunction IR scheme. Since the future distribution networks are evolving to become more intelligent, islanding and fault detection are getting more challenging and complicated. The rapidly developed pattern recognition technique might be a solution to DER interconnection protection in the future. The multifunction IR scheme can be incorporated with other advanced inverter technologies such as advanced inverter control techniques, volt-var management, dynamic reactive current support, voltage-watt management. The non-detection zones and dynamic responses are influenced by this inverter techniques.
3. Adaptive intelligent relays for DER interconnection protection in grid-connected and microgrid mode. The microgrid operation of distribution feeders is out of the scope of this thesis. However, it will be interesting to include the mode transition and microgrid mode of distribution network where DER interconnection protection is still favourable and necessary. Meanwhile, the coordination of the protective schemes should be maintained in each mode.
4. The proposed online HIF detection method can be extended to the development of an online intelligent relay. This relay performs online learning algorithm which is incrementally learning as required and updating its detection criteria as it is learning. The learning process can be based on both field events and data sent from a real-time simulator that models the network and fault cases. By the time artificial intelligence application gets reliable in a real-time system, a novel machine-learning-based relay will be commercialized. This kind of relay does not have straightforward protective logics. The decision making is achieved through its sophisticated internal classification rules. Hundreds of thousands of contingency scenarios, uncertainty from the renewable energies and advanced inverter functions can all be managed to provide the best protection decisions at its current state.

Appendix A

Benchmark Systems

A.1 Benchmark System 1

The benchmark system (Fig. A.1 [147]) is a 60 Hz distribution feeder energizing a nominal load of 11 MW at a nominal three-phase trunk line-to-line voltage of 25 kV. It contains SG rated at 4.17 kV, 9 MVA and WF rated at 575 V, 6.6 MVA. A shunt capacitor bank (1.2 MVAR) is located on the main distribution line as means for voltage regulation. The substation, WF and SG are connected to the 25 kV network through their own dedicated transformers. The substation transformer is delta-connected at the 120 kV utility. The line parameters and load profile can be found in [147].

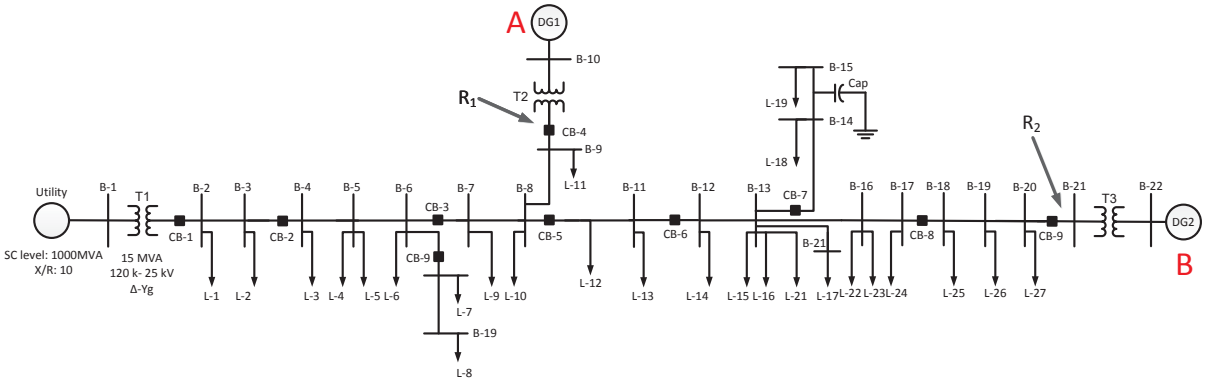

Fig. A.1 Single line diagram of distribution feeder under study.

A.2 Synchronous Generator Modeling

The SG employed in the thesis is represented by a full 6^{th} order SG model. The excitation system of the SG is configured to operate in power factor control mode. In addition, the mechanical power input of SG is assumed to be constant. These assumptions meet the standard of IEEE 1547 [1] and represent SG in compliance with standard transient stability analysis practice. The parameters of SG can be found in Table A.1.

Table A.1 Synchronous generator parameters

Parameter	Value
Capacity (MVA)	9
Voltage (kV)	2.4
H (s)	1.07
Tdo' (s)	3.7
Tdo'' (s)	0.05
Tq''	0.05
Xd (pu)	1.56
Xd' (pu)	0.296
Xd'' (pu)	0.177
Xq (pu)	1.06
Xq'' (pu)	0.177
Xl (pu)	0.052
Rs (pu)	0.0036

A.3 Wind Turbine Modeling

The wind turbine model employed in the thesis utilizes type 4 full-converter wind turbines, which contain permanent magnet SG and a back-to-back converter. The current controlled voltage source inverter (Figure A.2) employs constant power control and uses Phase-Locked-Loop (PLL) as synchronization measure. The active power control is realized through DC link control loop to maintain a constant DC link voltage. The parameters of the wind turbine can be found in Table A.2.

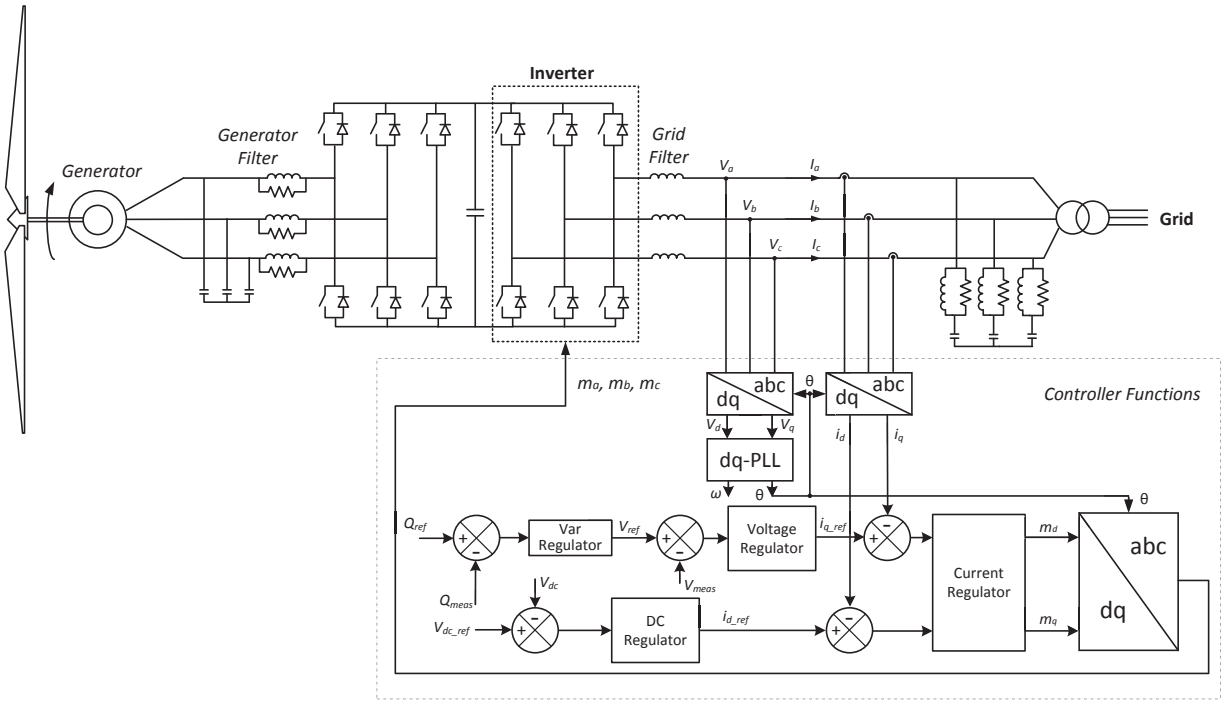

Fig. A.2 Wind turbine control scheme.

A.4 Training and Testing Events for Islanding Detection Function of the Multifunction IR

Table A.3 shows the training and testing events associated with islanding detection in Chapter 2. The training set and testing set are two supplementary subsets from this table without overlapping. Be noticed here that for a certain event, it might be a different event type for each DG, such as the event 4 in this table.

Table A.3: Training and Testing Events for Islanding Detection Function of the Multifunction IR

#	Event	Event Type at Location A	Event Type at Location B
1	CB-1 open	islanding	islanding
2	CB-2 open	islanding	islanding
3	CB-3 open	islanding	islanding
4	CB-4 open	islanding	non-islanding

5	Fault at B-2, CB-1 open	islanding	islanding
6	Fault at B-4, CB-2 open	islanding	islanding
7	Fault at B-7, CB-3 open	islanding	islanding
8	Fault at B-9, CB-4 open	islanding	non-islanding
9	CB-5 open	non-islanding	islanding
10	CB-6 open	non-islanding	islanding
11	CB-7 open	non-islanding	non-islanding
12	CB-8 open	non-islanding	islanding
13	CB-9 open	non-islanding	islanding
14	Fault at B-8, CB-5 open	non-islanding	islanding
15	Fault at B-12, CB-6 open	non-islanding	islanding
16	Fault at B-13, CB-7 open	non-islanding	non-islanding
17	Fault at B-18, CB-8 open	non-islanding	islanding
18	Fault at B-21, CB-9 open	non-islanding	islanding
19	Shed L-1	non-islanding	non-islanding
20	Shed L-14	non-islanding	non-islanding
21	Shed L-15	non-islanding	non-islanding
22	Shed L-18	non-islanding	non-islanding
23	Shed L-19	non-islanding	non-islanding
24	Shed L-20	non-islanding	non-islanding
25	Shed L-23	non-islanding	non-islanding
26	Shed L-24	non-islanding	non-islanding
27	Shed L-25	non-islanding	non-islanding
28	Shed L-26	non-islanding	non-islanding
29	Shed L-2, L-4 and L-5	non-islanding	non-islanding
30	Shed L-7 and L-8	non-islanding	non-islanding
31	Shed L-9 and L-10	non-islanding	non-islanding
32	Fault at L-1, CB-1 open	islanding	islanding
33	Fault at L-14, CB-6 open	non-islanding	islanding
34	Fault at L-15, CB-6 open	non-islanding	islanding
35	Fault at L-18, CB-6 open	non-islanding	islanding

36	Fault at L-19, CB-6 open	non-islanding	islanding
37	Fault at L-20, CB-6 open	non-islanding	islanding
38	Fault at L-23, CB-6 open	non-islanding	islanding
39	Fault at L-24, CB-6 open	non-islanding	islanding
40	Fault at L-25, CB-8 open	non-islanding	islanding
41	Fault at L-26, CB-8 open	non-islanding	islanding
42	Add L-14	non-islanding	non-islanding
43	Add L-15	non-islanding	non-islanding
44	Add L-18	non-islanding	non-islanding
45	Add L-19	non-islanding	non-islanding
46	Add L-20	non-islanding	non-islanding
47	Add L-23	non-islanding	non-islanding
48	Add L-24	non-islanding	non-islanding
49	Add L-25	non-islanding	non-islanding
50	Add L-26	non-islanding	non-islanding
51	Add L-1	non-islanding	non-islanding
52	Add L-2, L-4 and L-5	non-islanding	non-islanding
53	Add L-7 and L-8	non-islanding	non-islanding
54	Add L-9 and L-10	non-islanding	non-islanding

A.5 Training and Testing Events for Fault Detection Function of the Multifunction IR

Table A.4 shows the training and testing events associated with fault detection in Chapter 2. The training set and testing set are two supplementary subsets from this table without overlapping.

Table A.2 Wind turbine parameters

Parameter	Value
Number of wind turbines	3
Capacity (MVA)	2.2
Voltage (kV)	0.575
H (s)	0.62
Tdo' (s)	4.49
Tdo'' (s)	0.0681
Tq''	0.0513
Xd (pu)	1.305
Xd' (pu)	0.296
Xd'' (pu)	0.252
Xq (pu)	0.474
Xq'' (pu)	0.243
Xl (pu)	0.18
Rs (pu)	0.006
Grid-side converter maximum AC current (pu)	1.1

Table A.4 Training and Testing Events for Fault Detection Function of the Multifunction IR

#	Event	Event Type
1	Normal loading	no-fault
2	all CB open events	no-fault
3	Shed different load(s)	no-fault
4	Add different load(s)	no-fault
5	Fault (LL,LLG,SLG,LLL) at different bus(es)	fault
6	Fault (LL,LLG,SLG,LLL) at different bus(es) with ground impedance of 0,5,10,15,20 for ground fault	fault

A.6 Benchmark system 2

Originating from Fig. A.1, the benchmark system 2 (Fig. A.3) comprises two parallel distribution feeders. The first feeder energizes a nominal load of 11 MW at a nominal three-phase trunk line-to-line voltage of 25 kV, 60 Hz. It contains an SG rated at 4.17 kV, 9 MVA and a type 4 inverter-based wind farm (WF) rated at 575 V, 6.6 MVA. A shunt capacitor bank (1.2 MVAR) is located on the main distribution line as means for voltage regulation. The second feeder is shorter and one SG with the same rating as the one in the first feeder is connected at the end. The substation, WF and SG are connected to the 25 kV network through their own dedicated transformers. The substation transformer is delta-connected at the 120 kV utility.

A.7 Selected intelligent relay features

The selected intelligent relay features are shown in Table A.5.

Table A.5 Intelligent relay features

Feature	Definition
$x_1 = \Delta f$	Frequency deviation, Hz
$x_2 = \Delta V$	Voltage deviation, pu
$x_3 = df/dt$	Rate of change of frequency, Hz/s
$x_4 = dV/dt$	Rate of change of voltage, pu/s
$x_5 = dP/dt$	Rate of change of active power, pu/s
$x_6 = pf$	Power factor
$x_7 = dpf/dt$	Rate of change of power factor, pu/s
$x_8 = dQ/dt$	Rate of change of reactive power, pu/s
$x_9 = df/dP$	Frequency vs active power change, Hz/pu
$x_{10} = dV/dQ$	Voltage vs reactive power change
$x_{11} = df/dQ$	Frequency vs reactive power change, Hz/pu
$x_{12} = dV/dP$	Voltage vs active power change

A.8 Minimum description length based algorithm

The MDL-based method relies on the information gain (also known as entropy). Once the information gain of each feature is calculated for the classification variable, those features that contribute more information will have a higher information gain value over others, whereas those that do not add much information will have a lower score and can be removed. The entropy and information gain are defined as follows [148]:

$$\text{Entropy}(S) = -\sum_{i} f_i \log_2 f_i \tag{A.1}$$

where f_i is the frequency of the value i appearing in the dataset. If considering the entropy when subset T has been partitioned in accordance with n outcomes of one feature test X, then

$$\text{Entropy}_x(T) = -\sum_{i=1} \frac{T_i}{T} \text{Entropy}(T_i) \tag{A.2}$$

$$\text{InfoGain(X)} = \text{Entropy}(S) - \text{Entropy}(T) \tag{A.3}$$

Therefore, the information gain of the test feature X when partitioning subset T, can be computed.

The score of variable-importance [149] is a type of selection measures in machine learning. The problem of selecting the best attribute can be stated as the problem of selecting the most compressive attribute [150]. Assuming that all features are discrete, the objective is to find the best features that maximize the selection measure. Let C, A and V denote the number of classes, the number of features and the number of values of the given feature. Then the entropy of the classes (H_C), the values of the given feature (H_A), the joint events class-feature value (H_{CA}) and the classes given the value of the attribute ($H_{C|A}$) can be expressed as follows respectively:

$$H_C = -\sum_{i} p_{i.} \log p_{i.} \tag{A.4}$$

$$H_A = -\sum_{j} p_{.j} \log p_{.j} \tag{A.5}$$

$$H_{CA} = -\sum_i \sum_j p_{ij} \log p_{ij} \tag{A.6}$$

$$H_{C|A} = H_{CA} - H_A \tag{A.7}$$

where $p_{ij} = n_{ij}/n_{..}$, $p_{i.} = n_{i.}/n_{..}$, $p_{.j} = n_{.j}/n_{..}$ and $p_{i|j} = n_{ij}/n_{.j}$. Specifically, $n..$ denotes the number of training instances, $n_{i.}$ the number of training instances from class C_i, $n_{.j}$ the number of instances with the j-th value of the given attribute, and n_{ij} the number of instances from class C_i and with the j-th value of the given attribute.

The information gain is defined as the transmitted information by a given attribute about the object's class:

$$\text{Gain} = H_C + H_A - H_{CA} = H_C - H_{C|A} \tag{A.8}$$

The approximation of the total number of bits that are needed to encode the classes of $n_{..}$ is:

$$\text{Prior MDL}' = n..H_C + \log\binom{n.. + C - 1}{C - 1} \tag{A.9}$$

and the approximation of the number of bits to encode the classes of examples in all subsets corresponding to all values of the selected attribute is:

$$\text{Post MDL}' = \sum_j n_{.j} H_{C|j} + \sum_j \log\binom{n_{.j} + C - 1}{C - 1} + \log A \tag{A.10}$$

The last term ($\log A$) is needed to encode the selection of an attribute among A attributes. However, this term is constant for a given selection problem and can be ignored. The first term is equal to $n_{..}H_{C|A}$. Therefore, the MDL' measure that evaluates the average compression (per instance) of the message by an attribute is defined with the following difference Prior MDL' - Post MDL' normalized with $n_{..}$:

$$\begin{aligned} \text{MDL}' = \text{Gain} + \frac{1}{n..}(&\log\binom{n.. + C - 1}{C - 1} \\ &- \sum_j \log\binom{n_{.j} + C - 1}{C - 1}) \end{aligned} \tag{A.11}$$

However, entropy H_C can be used to derive MDL' if the messages are of arbitrary length. If the length of the message is known, the more optimal coding uses the logarithm of all possible combinations of class labels for given probability distribution:

$$\text{Prior MDL} = \binom{n..}{n_{1.}, ..., n_{C.}} + \log\binom{n.. + C - 1}{C - 1} \tag{A.12}$$

This gives a better definition of MDL:

$$\begin{aligned}\text{MDL} = \frac{1}{n..}(&\binom{n..}{n_{1.}, ..., n_{C.}} - \sum_j \log\binom{n_{.j}}{n_{1j}, ..., n_{Cj}} \\ &+\log\binom{n.. + C - 1}{C - 1} - \sum_j \log\binom{n_{.j} + C - 1}{C - 1})\end{aligned} \tag{A.13}$$

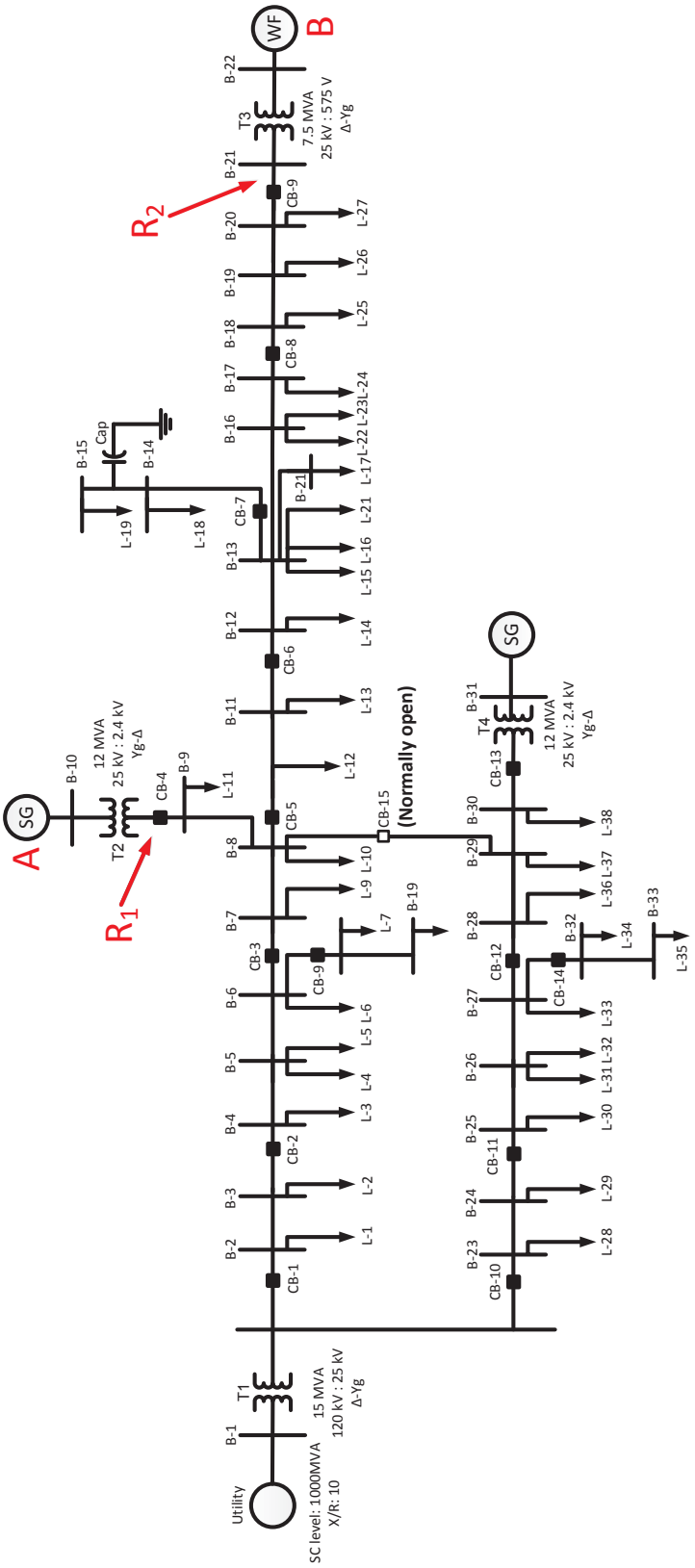

Fig. A.3 Single line diagram of the two parallel distribution feeders under study.

References

[1] "IEEE application guide for IEEE std 1547, IEEE standard for interconnecting distributed resources with electric power systems," *IEEE Std 1547.2–2008*, pp. 1–207, 2009.

[2] Hydro One, "Distributed generation technical interconnection requirementsinterconnection at voltages 50 kv and below," *Toronto, ON, Canada, Rep. no. DT-10-015 REV. 3*, March 2013.

[3] H. One, "Distributed generation technical interconnection requirementsinterconnection at voltages 50 kv and below," *Toronto, ON, Canada, Rep. no. DT-10-015*, vol. 2, p. 161, 2009.

[4] W. Freitas and W. Xu, "False operation of vector surge relays," *Power Delivery, IEEE Transactions on*, vol. 19, no. 1, pp. 436–438, 2004.

[5] F. Coffele, C. Booth, and A. Dyśko, "An adaptive overcurrent protection scheme for distribution networks," *IEEE Transactions on Power Delivery*, vol. 30, no. 2, pp. 561–568, 2015.

[6] Renewable Energy Policy Network for the 21st Century. (2014) The first decades: 2004-2014, 10 years of renewable energy progress. [Online]. Available: http://www.ren21.net/Portals/0/documents/activities/Topical\%20Reports/R\\EN21_10yr.pdf

[7] H. L. Willis, *Distributed power generation: planning and evaluation*. CRC Press, 2000.

[8] B. A. Welchko, T. M. Jahns, W. L. Soong, and J. M. Nagashima, "IPM synchronous machine drive response to symmetrical and asymmetrical short circuit faults," *IEEE Transactions on Energy Conversion*, vol. 18, no. 2, pp. 291–298, June 2003.

[9] R. Tonkoski, L. A. Lopes, and T. H. El-Fouly, "Coordinated active power curtailment of grid connected pv inverters for overvoltage prevention," *IEEE Transactions on Sustainable Energy*, vol. 2, no. 2, pp. 139–147, 2011.

[10] G. Joos, "Wind turbine generator low voltage ride through requirements and solutions," in *Power and Energy Society General Meeting-Conversion and Delivery of Electrical Energy in the 21st Century.* IEEE, 2008, pp. 1–7.

[11] A. Hooshyar and R. Iravani, "Microgrid protection," *Proceedings of the IEEE*, vol. 105, no. 7, pp. 1332–1353, July 2017.

[12] "IEEE standard for interconnecting distributed resources with electric power systems - amendment 1," *IEEE Std 1547a-2014 (Amendment to IEEE Std 1547-2003)*, pp. 1–16, May 2014.

[13] P. Naisani, D. Tholomier, T. Yip, and G. Lloyd, "Protection of distributed generation (DG) interconnection," in *Protective Relay Engineers, 2010 63rd Annual Conference for.* IEEE, 2010, pp. 1–17.

[14] "IEEE standard for interconnecting distributed resources with electric power systems," *IEEE Std 1547-2003*, pp. 1–28, July 2003.

[15] P. Mahat, Z. Chen, and B. Bak-Jensen, "Review on islanding operation of distribution system with distributed generation," in *Power and Energy Society General Meeting, 2011 IEEE*, July 2011, pp. 1–8.

[16] R. Walling, "Application of direct transfer trip for prevention of dg islanding," in *2011 IEEE Power and Energy Society General Meeting*, 2011.

[17] M. Ropp, P. Banschbach, C. Mouw, C. Mettler, and B. Enayati, "Application of pulse based power line carrier permissive (plcp) in distribution system islanding detection," in *2014 IEEE PES T&D Conference and Exposition.* IEEE, 2014, pp. 1–6.

[18] G. N. Ericsson, "Cyber security and power system communication - essential parts of a smart grid infrastructure," *IEEE Transactions on Power Delivery*, vol. 25, no. 3, pp. 1501–1507, July 2010.

[19] D. Reigosa, F. Briz, C. Charro, P. Garcia, and J. Guerrero, "Active islanding detection using high-frequency signal injection," *Industry Applications, IEEE Transactions on*, vol. 48, no. 5, pp. 1588–1597, Sept 2012.

[20] A. Yafaoui, B. Wu, and S. Kouro, "Improved active frequency drift anti-islanding detection method for grid connected photovoltaic systems," *Power Electronics, IEEE Transactions on*, vol. 27, no. 5, pp. 2367–2375, May 2012.

[21] H. Zeineldin and S. Conti, "Sandia frequency shift parameter selection for multi-inverter systems to eliminate non-detection zone," *Renewable Power Generation, IET*, vol. 5, no. 2, pp. 175–183, March 2011.

[22] F. Liu, Y. Kang, Y. Zhang, S. Duan, and X. Lin, "Improved sms islanding detection method for grid-connected converters," *Renewable Power Generation, IET*, vol. 4, no. 1, pp. 36–42, January 2010.

[23] D. Reigosa, F. Briz, C. Blanco, P. Garcia, and J. Manuel Guerrero, "Active islanding detection for multiple parallel-connected inverter-based distributed generators using high-frequency signal injection," *Power Electronics, IEEE Transactions on*, vol. 29, no. 3, pp. 1192–1199, March 2014.

[24] L. A. Lopes and H. Sun, "Performance assessment of active frequency drifting islanding detection methods," *IEEE Transactions on Energy Conversion*, vol. 21, no. 1, pp. 171–180, 2006.

[25] B. Bahrani, H. Karimi, and R. Iravani, "Nondetection zone assessment of an active islanding detection method and its experimental evaluation," *Power Delivery, IEEE Transactions on*, vol. 26, no. 2, pp. 517–525, April 2011.

[26] M. Ciobotaru, V. Agelidis, R. Teodorescu, and F. Blaabjerg, "Accurate and less-disturbing active antiislanding method based on pll for grid-connected converters," *Power Electronics, IEEE Transactions on*, vol. 25, no. 6, pp. 1576–1584, June 2010.

[27] E. Kamyab and J. Sadeh, "Islanding detection method for photovoltaic distributed generation based on voltage drifting," *Generation, Transmission Distribution, IET*, vol. 7, no. 6, pp. 584–592, June 2013.

[28] X. Chen and Y. Li, "An islanding detection algorithm for inverter-based distributed generation based on reactive power control," *Power Electronics, IEEE Transactions on*, vol. 29, no. 9, pp. 4672–4683, Sept 2014.

[29] H. Vahedi, R. Noroozian, A. Jalilvand, and G. Gharehpetian, "A new method for islanding detection of inverter-based distributed generation using dc-link voltage control," *Power Delivery, IEEE Transactions on*, vol. 26, no. 2, pp. 1176–1186, April 2011.

[30] X. Wang, W. Freitas, V. Dinavahi, and W. Xu, "Investigation of positive feedback anti-islanding control for multiple inverter-based distributed generators," *IEEE Transactions on Power Systems*, vol. 24, no. 2, pp. 785–795, May 2009.

[31] P. Du, Z. Ye, E. Aponte, J. Nelson, and L. Fan, "Positive-feedback-based active anti-islanding schemes for inverter-based distributed generators: Basic principle, design guideline and performance analysis," *Power Electronics, IEEE Transactions on*, vol. 25, no. 12, pp. 2941–2948, Dec 2010.

[32] L. A. Lopes and Y. Zhang, "Islanding detection assessment of multi-inverter systems with active frequency drifting methods," *IEEE Transactions on power Delivery*, vol. 23, no. 1, pp. 480–486, 2008.

[33] H. Vahedi and M. Karrari, "Adaptive fuzzy sandia frequency-shift method for islanding protection of inverter-based distributed generation," *Power Delivery, IEEE Transactions on*, vol. 28, no. 1, pp. 84–92, Jan 2013.

[34] I. PVPS, "Evaluation of islanding detection methods for photovoltaic utilityinteractive power systems," *Report IEA PVPS T5-09*, 2002.

[35] W. Freitas, W. Xu, C. M. Affonso, and Z. Huang, "Comparative analysis between rocof and vector surge relays for distributed generation applications," *IEEE Transactions on Power Delivery*, vol. 20, no. 2, pp. 1315–1324, 2005.

[36] P. Mahat, Z. Chen, B. Bak-Jensen, and C. L. Bak, "A simple adaptive overcurrent protection of distribution systems with distributed generation," *IEEE Transactions on Smart Grid*, vol. 2, no. 3, pp. 428–437, 2011.

[37] H. Samet, F. Hashemi, and T. Ghanbari, "Islanding detection method for inverter-based distributed generation with negligible non-detection zone using energy of rate of change of voltage phase angle," *Generation, Transmission Distribution, IET*, vol. 9, no. 15, pp. 2337–2350, 2015.

[38] N. Lidula and A. Rajapakse, "A pattern recognition approach for detecting power islands using transient signals–Part I: Design and implementation," *IEEE Transactions on Power Delivery*, vol. 25, no. 4, pp. 3070–3077, 2010.

[39] H. Laaksonen, "Advanced islanding detection functionality for future electricity distribution networks," *Power Delivery, IEEE Transactions on*, vol. 28, no. 4, pp. 2056–2064, Oct 2013.

[40] M. A. Farhan and K. S. Swarup, "Mathematical morphology-based islanding detection for distributed generation," *IET Generation, Transmission & Distribution*, vol. 10, no. 2, pp. 518–525, 2016.

[41] H. Vahedi, G. Gharehpetian, and M. Karrari, "Application of duffing oscillators for passive islanding detection of inverter-based distributed generation units," *Power Delivery, IEEE Transactions on*, vol. 27, no. 4, pp. 1973–1983, 2012.

[42] J. Vieira, W. Freitas, W. Xu, and A. Morelato, "Performance of frequency relays for distributed generation protection," *Power Delivery, IEEE Transactions on*, vol. 21, no. 3, pp. 1120–1127, July 2006.

[43] K. El-Arroudi, G. Joós, I. Kamwa, and D. T. McGillis, "Intelligent-based approach to islanding detection in distributed generation," *Power Delivery, IEEE Transactions on*, vol. 22, no. 2, pp. 828–835, 2007.

[44] O. Faqhruldin, E. El-Saadany, and H. Zeineldin, "A universal islanding detection technique for distributed generation using pattern recognition," *Smart Grid, IEEE Transactions on*, vol. 5, no. 4, pp. 1985–1992, July 2014.

[45] B. Matic-Cuka and M. Kezunovic, "Islanding detection for inverter-based distributed generation using support vector machine method," *IEEE Transactions on Smart Grid*, vol. 5, no. 6, pp. 2676–2686, Nov 2014.

[46] S. D. Kermany, M. Joorabian, S. Deilami, and M. A. Masoum, "Hybrid islanding detection in microgrid with multiple connection points to smart grids using fuzzy-neural network," *IEEE Transactions on Power Systems*, 2016.

[47] M. O. Faruque and V. Dinavahi, "Hardware-in-the-loop simulation of power electronic systems using adaptive discretization," *IEEE transactions on industrial electronics*, vol. 57, no. 4, pp. 1146–1158, 2010.

[48] V. Jalili-Marandi, L.-F. Pak, and V. Dinavahi, "Real-time simulation of grid-connected wind farms using physical aggregation," *IEEE Transactions on industrial electronics*, vol. 57, no. 9, pp. 3010–3021, 2010.

[49] A. Myaing and V. Dinavahi, "Fpga-based real-time emulation of power electronic systems with detailed representation of device characteristics," *IEEE Transactions on Industrial Electronics*, vol. 58, no. 1, pp. 358–368, Jan 2011.

[50] W. Zhu, S. Pekarek, J. Jatskevich, O. Wasynczuk, and D. Delisle, "A model-in-the-loop interface to emulate source dynamics in a zonal dc distribution system," *IEEE Transactions on Power Electronics*, vol. 20, no. 2, pp. 438–445, March 2005.

[51] D. Motter, J. C. Vieira, and D. V. Coury, "Development of frequency-based anti-islanding protection models for synchronous distributed generators suitable for real-time simulations," *IET Generation, Transmission & Distribution*, vol. 9, no. 8, pp. 708–718, 2015.

[52] B. Lundstrom, B. Mather, M. Shirazi, and M. Coddington, "Implementation and validation of advanced unintentional islanding testing using power hardware-in-the-loop (phil) simulation," in *Photovoltaic Specialists Conference (PVSC), 2013 IEEE 39th.* IEEE, 2013, pp. 3141–3146.

[53] P. Crolla, A. Roscoe, A. Dyśko, and G. Burt, "Methodology for testing loss of mains detection algorithms for microgrids and distributed generation using real-time power

hardware-in-the-loop based technique," in *Power Electronics and ECCE Asia (ICPE & ECCE), 2011 IEEE 8th International Conference on*. IEEE, 2011, pp. 833–838.

[54] M. Almas and L. Vanfretti, "RT-HIL implementation of hybrid synchrophasor and goose-based passive islanding schemes," *IEEE Transactions on Power Delivery*, vol. PP, no. 99, pp. 1–1, 2015.

[55] J. Vieira, W. Freitas, W. Xu, and A. Morelato, "An investigation on the nondetection zones of synchronous distributed generation anti-islanding protection," *Power Delivery, IEEE Transactions on*, vol. 23, no. 2, pp. 593–600, 2008.

[56] X. Li, A. Dysko, I. Abdulhadi, and R. King, "Hardware prototype and real-time validation of the satellite communication based loss-of-mains protection," in *Developments in Power System Protection (DPSP 2014), 12th IET International Conference on*. IET, 2014, pp. 1–6.

[57] Y. Zhou, H. Li, and L. Liu, "Integrated autonomous voltage regulation and islanding detection for high penetration pv applications," *Power Electronics, IEEE Transactions on*, vol. 28, no. 6, pp. 2826–2841, 2013.

[58] D. Bejmert and T. Sidhu, "Investigation into islanding detection with capacitor insertion-based method," *IEEE Transactions on Power Delivery*, vol. 29, no. 6, pp. 2485–2492, 2014.

[59] R. Teodorescu, M. Liserre, and P. Rodriguez, *Grid converters for photovoltaic and wind power systems*. John Wiley & Sons, 2011, vol. 29.

[60] E. Muljadi, N. Samaan, V. Gevorgian, J. Li, and S. Pasupulati, "Short circuit current contribution for different wind turbine generator types," in *Power and Energy Society General Meeting, 2010 IEEE*. IEEE, 2010, pp. 1–8.

[61] J. Keller and B. D. Kroposki, *Understanding fault characteristics of inverter-based distributed energy resources*. National Renewable Energy Laboratory, 2010.

[62] M. Adamiak, C. Wester, M. Thakur, and C. Jensen, "High impedance fault detection on distribution feeders," *GE Industrial solutions*, 2006.

[63] M. Sedighizadeh, A. Rezazadeh, and N. I. Elkalashy, "Approaches in high impedance fault detection-a chronological review," *Advances in Electrical and Computer Engineering*, vol. 10, no. 3, pp. 114–128, 2010.

[64] J. Tengdin and R. Westfall, "High impedance fault detection technology report of psrc working group d15," 1996.

[65] J. Carr, "Detection of high impedance faults on multi-grounded primary distribution systems," *IEEE Transactions on Power Apparatus and Systems*, vol. 4, no. PAS-100, pp. 2008–2016, 1981.

[66] R. E. Lee and M. Bishop, "Performance testing of the ratio ground relay on a four-wire distribution feeder," *IEEE transactions on power apparatus and systems*, no. 9, pp. 2943–2949, 1983.

[67] A. V. Mamishev, B. D. Russell, and C. L. Benner, "Analysis of high impedance faults using fractal techniques," *IEEE Transactions on Power Systems*, vol. 11, no. 1, pp. 435–440, Feb 1996.

[68] I. Zamora, A. Mazon, K. Sagastabeitia, and J. Zamora, "New method for detecting low current faults in electrical distribution systems," *IEEE Transactions on Power Delivery*, vol. 22, no. 4, pp. 2072–2079, 2007.

[69] K. Sagastabeitia, I. Zamora, A. Mazón, Z. Aginako, and G. Buigues, "Low-current fault detection in high impedance grounded distribution networks, using residual variations of asymmetries," *IET Generation, Transmission & Distribution*, vol. 6, no. 12, pp. 1252–1261, 2012.

[70] M.-S. Choi, S.-J. Lee, D.-S. Lee, and B.-G. Jin, "A new fault location algorithm using direct circuit analysis for distribution systems," *Power Delivery, IEEE Transactions on*, vol. 19, no. 1, pp. 35–41, 2004.

[71] J. Zhu, D. L. Lubkeman, and A. A. Girgis, "Automated fault location and diagnosis on electric power distribution feeders," *Power Delivery, IEEE Transactions on*, vol. 12, no. 2, pp. 801–809, 1997.

[72] D. Jeerings and J. Linders, "A practical protective relay for down-conductor faults," *IEEE Transactions on Power Delivery*, vol. 6, no. 2, pp. 565–574, 1991.

[73] D. Yu and S. H. Khan, "An adaptive high and low impedance fault detection method," *IEEE transactions on power delivery*, vol. 9, no. 4, pp. 1812–1821, 1994.

[74] M. Aucoin and B. D. Russell, "Detection of distribution high impedance faults using burst noise signals near 60 Hz," *IEEE transactions on power delivery*, vol. 2, no. 2, pp. 342–348, 1987.

[75] J. R. Macedo, J. W. Resende, C. A. Bissochi, D. Carvalho, and F. C. Castro, "Proposition of an interharmonic-based methodology for high-impedance fault detection in distribution systems," *IET Generation, Transmission & Distribution*, vol. 9, no. 16, pp. 2593–2601, 2015.

[76] C.-H. Kim, H. Kim, Y.-H. Ko, S.-H. Byun, R. K. Aggarwal, and A. T. Johns, "A novel fault-detection technique of high-impedance arcing faults in transmission lines using the wavelet transform," *IEEE Transactions on Power Delivery*, vol. 17, no. 4, pp. 921–929, 2002.

[77] M. Michalik, W. Rebizant, M. Lukowicz, S.-J. Lee, and S.-H. Kang, "High-impedance fault detection in distribution networks with use of wavelet-based algorithm," *IEEE Transactions on Power Delivery*, vol. 21, no. 4, pp. 1793–1802, 2006.

[78] W. C. Santos, F. V. Lopes, N. S. D. Brito, and B. de Souza, "High impedance fault identification on distribution networks," *IEEE Transactions on Power Delivery*, vol. PP, no. 99, pp. 1–1, 2016.

[79] F. B. Costa, B. Souza, N. Brito, J. Silva, and W. Santos, "Real-time detection of transients induced by high-impedance faults based on the boundary wavelet transform," *IEEE Transactions on Industry Applications*, vol. 51, no. 6, pp. 5312–5323, 2015.

[80] W. H. Kwon, G. W. Lee, Y. M. Park, M. C. Yoon, and M. H. Yoo, "High impedance fault detection utilizing incremental variance of normalized even order harmonic power," *Power Delivery, IEEE Transactions on*, vol. 6, no. 2, pp. 557–564, 1991.

[81] A. A. Girgis, W. Chang, and E. B. Makram, "Analysis of high-impedance fault generated signals using a kalman filtering approach," *Power Delivery, IEEE Transactions on*, vol. 5, no. 4, pp. 1714–1724, 1990.

[82] M. Sarlak and S. Shahrtash, "High impedance fault detection using combination of multi-layer perceptron neural networks based on multi-resolution morphological gradient features of current waveform," *IET generation, transmission & distribution*, vol. 5, no. 5, pp. 588–595, 2011.

[83] S. Gautam and S. M. Brahma, "Detection of high impedance fault in power distribution systems using mathematical morphology," *IEEE Transactions on Power Systems*, vol. 28, no. 2, pp. 1226–1234, 2013.

[84] A. Ghaderi, H. A. Mohammadpour, H. L. Ginn, and Y.-J. Shin, "High-impedance fault detection in the distribution network using the time-frequency-based algorithm," *IEEE Transactions on Power Delivery*, vol. 30, no. 3, pp. 1260–1268, 2015.

[85] N. I. Elkalashy, M. Lehtonen, H. A. Darwish, A.-M. I. Taalab, and M. A. Izzularab, "Dwt-based detection and transient power direction-based location of high-impedance faults due to leaning trees in unearthed mv networks," *Power Delivery, IEEE Transactions on*, vol. 23, no. 1, pp. 94–101, 2008.

[86] F. Jota and P. Jota, "High-impedance fault identification using a fuzzy reasoning system," in *Generation, Transmission and Distribution, IEE Proceedings-*, vol. 145, no. 6. IET, 1998, pp. 656–661.

[87] M. Haghifam, A. Sedighi, and O. Malik, "Development of a fuzzy inference system based on genetic algorithm for high-impedance fault detection," *IEE PROCEEDINGS GENERATION TRANSMISSION AND DISTRIBUTION*, vol. 153, no. 3, p. 359, 2006.

[88] A. N. Milioudis, G. T. Andreou, and D. P. Labridis, "Detection and location of high impedance faults in multiconductor overhead distribution lines using power line communication devices," *Smart Grid, IEEE Transactions on*, vol. 6, no. 2, pp. 894–902, 2015.

[89] C. L. Benner and B. D. Russell, "Practical high-impedance fault detection on distribution feeders," *Industry Applications, IEEE Transactions on*, vol. 33, no. 3, pp. 635–640, 1997.

[90] C. Kim, B. D. Russell, and K. Watson, "A parameter-based process for selecting high impedance fault detection techniques using decision making under incomplete knowledge," *Power Delivery, IEEE Transactions on*, vol. 5, no. 3, pp. 1314–1320, 1990.

[91] A. F. Sultan, G. W. Swift, and D. J. Fedirchuk, "Detection of high impedance arcing faults using a multi-layer perceptron," *Power Delivery, IEEE Transactions on*, vol. 7, no. 4, pp. 1871–1877, 1992.

[92] C. Kim and B. D. Russell, "A learning method for use in intelligent computer relays for high impedance faults," *Power Delivery, IEEE Transactions on*, vol. 6, no. 1, pp. 109–115, 1991.

[93] Y. Sheng and S. M. Rovnyak, "Decision tree-based methodology for high impedance fault detection," *IEEE Transactions on Power Delivery*, vol. 19, no. 2, pp. 533–536, 2004.

[94] A.-R. Sedighi, M.-R. Haghifam, O. Malik, and M.-H. Ghassemian, "High impedance fault detection based on wavelet transform and statistical pattern recognition," *IEEE Transactions on Power Delivery*, vol. 20, no. 4, pp. 2414–2421, 2005.

[95] T. Lai, L. Snider, E. Lo, and D. Sutanto, "High-impedance fault detection using discrete wavelet transform and frequency range and rms conversion," *Power Delivery, IEEE Transactions on*, vol. 20, no. 1, pp. 397–407, 2005.

[96] A. Etemadi and M. Sanaye-Pasand, "High-impedance fault detection using multi-resolution signal decomposition and adaptive neural fuzzy inference system," *IET generation, transmission & distribution*, vol. 2, no. 1, pp. 110–118, 2008.

[97] M. Sarlak and S. M. Shahrtash, "High-impedance faulted branch identification using magnetic-field signature analysis," *IEEE Transactions on Power Delivery*, vol. 28, no. 1, pp. 67–74, 2013.

[98] Y. Wang and V. Dinavahi, "Low-latency distance protective relay on fpga," *IEEE Transactions on Smart Grid*, vol. 5, no. 2, pp. 896–905, 2014.

[99] Y. Wang and V. Dinavahi, "Real-time digital multi-function protection system on reconfigurable hardware," *IET Generation, Transmission & Distribution*, vol. 10, no. 10, pp. 2295–2305, 2016.

[100] H. Muda and P. Jena, "Sequence currents based adaptive protection approach for dns with distributed energy resources," *IET Generation, Transmission & Distribution*, vol. 11, no. 1, pp. 154–165, 2017.

[101] F. Coffele, C. Booth, A. Dyśko, and G. Burt, "Quantitative analysis of network protection blinding for systems incorporating distributed generation," *IET Generation, Transmission & Distribution*, vol. 6, no. 12, pp. 1218–1224, 2012.

[102] V. A. Papaspiliotopoulos, G. N. Korres, V. A. Kleftakis, and N. D. Hatziargyriou, "Hardware-in-the-loop design and optimal setting of adaptive protection schemes for distribution systems with distributed generation," *IEEE Transactions on Power Delivery*, vol. 32, no. 1, pp. 393–400, 2017.

[103] MATLAB Statistics and Machine Learning Toolbox Release 2013a. Natick, Massachusetts: The MathWorks Inc., 2013.

[104] Q. Cui, S. Li, K. El-Arroudi, and G. Joos, "Multifunction intelligent relay for inverter-based distributed generation," in *13th International Conference on Development in Power System Protection 2016 (DPSP)*, March 2016, pp. 1–6, **Best Paper Award**.

[105] Q. Cui, K. El-Arroudi, and G. Joos, "Islanding detection of hybrid distributed generation under reduced non-detection zone," *IEEE Transactions on Smart Grid*, vol. PP, no. 99, pp. 1–1, 2017.

[106] Q. Cui, K. El-Arroudi, and G. Joos, "Real-time hardware-in-the-loop simulation for islanding detection schemes in hybrid distributed generation systems," *IET Generation, Transmission & Distribution*, vol. PP, no. 99, pp. 1–8, 2017.

[107] Q. Cui, K. El-Arroudi, and G. Joos, "An effective feature extraction method in pattern recognition based high impedance fault detection," in *2018 IEEE Power Energy Society Innovative Smart Grid Technologies Conference (ISGT)*, Feb. 2018, pp. 1–5, accepted, to appear.

[108] Z. Ye, R. Walling, L. Garces, R. Zhou, L. Li, and T. Wang, *Study and development of anti-islanding control for grid-connected inverters*. National Renewable Energy Laboratory, 2004.

[109] S. L. R. P. D. Mascarella, K. El-Arroudi and G. Joós, "Real-time testing of relay-fuse coordination implemented with iec 61850 goose messaging using industrial relays," in *2015 CIGRÉ Canada Conference*, August 2015.

[110] H. G. Far, A. J. Rodolakis, and G. Joos, "Synchronous distributed generation islanding protection using intelligent relays," *Smart Grid, IEEE Transactions on*, vol. 3, no. 4, pp. 1695–1703, 2012.

[111] A. R. H. Ayres and G. Joós, "Distributed generation fault interconnection protection using intelligent relays," in *2012 CIGRÉ Canada Conference*, September 2012.

[112] E. Alpaydin, *Introduction to machine learning*. MIT press, 2014.

[113] L. Breiman, J. Friedman, C. J. Stone, and R. A. Olshen, *Classification and regression trees*. CRC press, 1984.

[114] M. Leblanc, L. Evans, P. Gardner, N. Scott, and S. Whittaker, "Canadian grid code for wind development-review and recommendations," *Garrad Hassan and CANWEA, Ottawa, Tech. Rep*, vol. 11163, pp. 2006–075, 2005.

[115] M. Altin, Ö. Göksu, R. Teodorescu, P. Rodriguez, B.-B. Jensen, and L. Helle, "Overview of recent grid codes for wind power integration," in *Optimization of Electrical and Electronic Equipment (OPTIM), 2010 12th International Conference on*. IEEE, 2010, pp. 1152–1160.

[116] K. A. Saleh, E. Moursi, M. Shawky, and H. H. Zeineldin, "A new protection scheme considering fault ride through requirements for transmission level interconnected wind parks," *Industrial Informatics, IEEE Transactions on*, vol. 11, no. 6, pp. 1324–1333, 2015.

[117] Z. Ye, A. Kolwalkar, Y. Zhang, P. Du, and R. Walling, "Evaluation of anti-islanding schemes based on nondetection zone concept," *Power Electronics, IEEE Transactions on*, vol. 19, no. 5, pp. 1171–1176, 2004.

[118] *MATLAB Statistics and Machine Learning Toolbox (R2013a)*. Natick, Massachusetts: The MathWorks Inc., 2013.

[119] "IEEE standard conformance test procedures for equipment interconnecting distributed resources with electric power systems," *IEEE Std 1547.1–2005*, pp. 1–54, July 2005.

[120] Canadian Standards Association, "Interconnection of distributed resources and electricity supply systems," *CAN/CSA-C22.3 NO. 9-08 (R2015)*, pp. 1–58, 2015.

[121] A. Foss and K. Leppik, "Design and implementation of an anti-islanding protection strategy for distributed generation involving multiple passive protections," in *Electrical Power & Energy Conference (EPEC)*. IEEE, 2009, pp. 1–4.

[122] B. Seal, F. Cleveland, and A. Hefner, "Distributed energy management (der): Advanced power system management functions and information exchanges for inverter-based der devices, modelled in iec 61850–90-7," *IEC TC57 WG17, Tech. Rep*, 2012.

[123] M. Heidari, G. Seifossadat, and M. Razaz, "Application of decision tree and discrete wavelet transform for an optimized intelligent-based islanding detection method in distributed systems with distributed generations," *Renewable and Sustainable Energy Reviews*, vol. 27, pp. 525–532, 2013.

[124] D. C. T. Wai and X. Yibin, "A novel technique for high impedance fault identification," *IEEE Transactions on Power Delivery*, vol. 13, no. 3, pp. 738–744, 1998.

[125] S. Nam, J. Park, Y. Kang, and T. Kim, "A modeling method of a high impedance fault in a distribution system using two series time-varying resistances in emtp," in *Power Engineering Society Summer Meeting, 2001*, vol. 2. IEEE, 2001, pp. 1175–1180.

[126] R. Lee and M. Bishop, "A comparison of measured high impedance fault data to digital computer modeling results," *IEEE Transactions on Power Apparatus and systems*, no. 10, pp. 2754–2758, 1985.

[127] A. Emanuel, D. Cyganski, J. Orr, S. Shiller, and E. Gulachenski, "High impedance fault arcing on sandy soil in 15 kv distribution feeders: contributions to the evaluation of the low frequency spectrum," *Power Delivery, IEEE Transactions on*, vol. 5, no. 2, pp. 676–686, 1990.

[128] L. U. Iurinic, A. R. Herrera-Orozco, R. G. Ferraz, and A. S. Bretas, "Distribution systems high-impedance fault location: A parameter estimation approach," *IEEE Transactions on Power Delivery*, vol. 31, no. 4, pp. 1806–1814, Aug 2016.

[129] M. Kizilcay and T. Pniok, "Digital simulation of fault arcs in power systems," *European Transactions on Electrical Power*, vol. 1, no. 1, pp. 55–60, 1991.

[130] W. Zhang, Y. Jing, and X. Xiao, "Model-based general arcing fault detection in medium-voltage distribution lines," *IEEE Transactions on Power Delivery*, vol. 31, no. 5, pp. 2231–2241, Oct 2016.

[131] N. I. Elkalashy, M. Lehtonen, H. A. Darwish, M. A. Izzularab, and I. T. Abdel-maksoud, "Modeling and experimental verification of high impedance arcing fault in medium voltage networks," *IEEE Transactions on Dielectrics and Electrical Insulation*, vol. 14, no. 2, pp. 375–383, 2007.

[132] A. Sultan, G. Swift, and D. Fedirchuk, "Detecting arcing downed-wires using fault current flicker and half-cycle asymmetry," *IEEE Transactions on Power Delivery*, vol. 9, no. 1, pp. 461–470, 1994.

[133] K. El-Arroudi and G. Joos, "Data mining approach to threshold settings of islanding relays in distributed generation," *IEEE Transactions on power systems*, vol. 22, no. 3, pp. 1112–1119, 2007.

[134] L. Yang, "Protective relay with improved DFT function," Jun. 1 1999, US Patent 5909656.

[135] H. C. Wood, N. G. Johnson, and M. S. Sachdev, "Kalman filtering applied to power system measurements relaying," *IEEE Transactions on Power Apparatus and Systems*, vol. PAS-104, no. 12, pp. 3565–3573, Dec 1985.

[136] I. Kamwa, S. Samantaray, and G. Joos, "Wide frequency range adaptive phasor and frequency pmu algorithms," *IEEE Transactions on Smart Grid*, vol. 5, no. 2, pp. 569–579, 2014.

[137] N. V. Chawla, K. W. Bowyer, L. O. Hall, and W. P. Kegelmeyer, "Smote: synthetic minority over-sampling technique," *Journal of artificial intelligence research*, vol. 16, pp. 321–357, 2002.

[138] M. Hall, E. Frank, G. Holmes, B. Pfahringer, P. Reutemann, and I. H. Witten, "The weka data mining software: an update," *ACM SIGKDD explorations newsletter*, vol. 11, no. 1, pp. 10–18, 2009.

[139] J. L. Blackburn and T. J. Domin, *Protective relaying: principles and applications*. CRC press, 2006.

[140] M. O. Faruque, T. Strasser, G. Lauss, V. Jalili-Marandi, P. Forsyth, C. Dufour, V. Dinavahi, A. Monti, P. Kotsampopoulos, J. A. Martinez *et al.*, "Real-time simulation technologies for power systems design, testing, and analysis," *IEEE Power and Energy Technology Systems Journal*, vol. 2, no. 2, pp. 63–73, 2015.

[141] J. Belanger, P. Venne, and J. Paquin, "The what, where and why of real-time simulation," *Planet RT*, vol. 1, no. 0, p. 1, 2010.

[142] SEL-421. (2016) Protection, automation, and control system. [Online]. Available: https://www.selinc.com/SEL-421/

[143] A. Q. D. I. Manual, "Schweitzer engineering laboratories inc," *Pullman, WA*, 2006.

[144] M. Ross, C. Abbey, Y. Brissette, and G. Joos, "Photovoltaic inverter characterization testing on a physical distribution system," in *Power and Energy Society General Meeting, 2012 IEEE*. IEEE, 2012, pp. 1–7.

[145] S. Raza, H. Mokhlis, H. Arof, J. Laghari, and H. Mohamad, "A sensitivity analysis of different power system parameters on islanding detection," *IEEE Transactions on Sustainable Energy*, vol. 7, no. 2, pp. 461–470, 2016.

[146] "IEEE guide for conducting distribution impact studies for distributed resource interconnection," *IEEE Std 1547.7-2013*, pp. 1–137, Feb 2014.

[147] D. Zhuang, "Real time testing of intelligent relays for synchronous distributed generation islanding detection," Master's thesis, McGill University, December 2012.

[148] J. R. Quinlan, *C4.5: programs for machine learning*. Elsevier, 2014.

[149] I. Kononenko, "On biases in estimating multi-valued attributes," in *IJCAI'95 Proceedings of the 14th international joint conference on Artificial intelligence*, vol. 2, 1995, pp. 1034–1040.

[150] L. Ming and P. Vitányi, *An introduction to Kolmogorov complexity and its applications*. Springer Heidelberg, 1997.